

STATUS OF THESIS

Title of thesis

A NEW ROLL, PITCH AND BUOYANCY CONTROL MECHANISM
FOR AN UNDERWATER GLIDER

I KESAVAN PANJAVARNAM

hereby allow my thesis to be placed at the Information Resource Center (IRC) of Universiti Teknologi PETRONAS (UTP) with the following conditions:

1. The thesis becomes the property of UTP
2. The IRC of UTP may make copies of the thesis for academic purposes only.
3. This thesis is classified as

☐

Confidential

☒

Non-confidential

If this thesis is confidential, please state the reason:

The contents of the thesis will remain confidential for _____ years.

Remarks on disclosure:

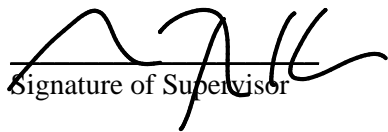


Signature of Author

Permanent address: Jalan Anggerik,
Kota Kemuning, 40460,
Shah Alam, Selangor.

Date : 3/Feb/2022

Endorsed by



Signature of Supervisor

Name of Supervisor
Dr. Mark Ovinis

Date: 3/Feb/2022

UNIVERSITI TEKNOLOGI PETRONAS

A NEW ROLL, PITCH AND BUOYANCY CONTROL MECHANISM FOR AN

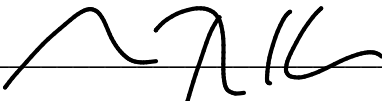
UNDERWATER GLIDER

by

KESAVAN PANJAVARNAM

The undersigned certify that they have read and recommend to the Postgraduate Studies Programme for acceptance this thesis for the fulfillment of the requirements for the degree stated.

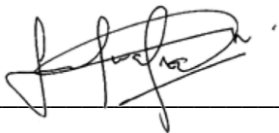
Signature:



Main Supervisor:

Dr. Mark Ovinis

Signature:



Co-Supervisor:

Assoc. Prof. Dr Saravanan Karupanan

Signature:



Head of Department:

Assoc. Prof. Dr Masdi bin Muhammad

Date:

8/02/2022

A NEW ROLL, PITCH AND BUOYANCY CONTROL MECHANISM FOR AN
UNDERWATER GLIDER

by

KESAVAN PANJAVARNAM

A Thesis

Submitted to the Postgraduate Studies Programme

as a Requirement for the Degree of

MASTER OF SCIENCE

DEPARTMENT OF MECHANICAL ENGINEERING

UNIVERSITI TEKNOLOGI PETRONAS

BANDAR SERI ISKANDAR,

PERAK

FEBRUARY 2022

DECLARATION OF THESIS

Title of thesis

A NEW ROLL, PITCH AND BUOYANCY CONTROL MECHANISM
FOR AN UNDERWATER GLIDER

I KESAVAN PANJAVARNAM

hereby declare that the thesis is based on my original work except for quotations and citations which have been duly acknowledged. I also declare that it has not been previously or concurrently submitted for any other degree at UTP or other institutions.

Witnessed by



Signature of Author



Signature of Supervisor

Permanent address: Jalan Anggerik,
Kota Kemuning, 40460,
Shah Alam, Selangor.

Name of Supervisor
Dr. Mark Ovinis

Date : 3/02/2022

Date : 3/02/2022

DEDICATION

To my beloved father, Panjavarnam, and my family members for their continuous support.

ACKNOWLEDGEMENTS

First and foremost, praises to the supreme power the almighty God who is the one as always guided me to work on the right path of life. I believe without his grace this research & thesis could not become reality. Next to him are my parents, whom I'm greatly indebted for me brought up with love and encouragement to who am I today. I'm highly obliged in taking the opportunity to sincerely express my thanks to Dr. Mark Ovinis for giving me the opportunity to do research and providing invaluable guidance throughout this research. His dynamism, vision, sincerity and motivation have deeply inspired me. He has taught me the methodology to carry out the research and to present the research works as clearly as possible. It was a great privilege and honor to work and study under his guidance. He always pushed me and gave me the chance to grow professionally and kept commenting on my papers and even helped me to clarify the doubts I had. I am also thankful to Universiti Teknologi Petronas for providing me an opportunity to utilize the labs all the time.

ABSTRACT

Underwater gliders are able to travel autonomously with the aid of separate pitch and roll control mechanisms. Nevertheless, it is significant to consider the hull load and mass of the glider to improve the gliding efficiency in the water. Therefore, in this study, a single pitch and buoyancy as well as roll control mechanism for an underwater glider are discussed. This mechanism controlled the pitch and roll of the glider without using the conventional buoyancy engine and rotational mass. It consisted of four sets of water bladders located in the front, rear, left and right of the glider and two high-flow rate water pumps that shifted water from these water bladders. By shifting water between the left and right water bladders, the roll moment was induced. Similarly, the pitch was achieved by shifting water between the front and rear water bladders. The system dynamics and the glider parameters were derived and simulated as well as validated experimentally. Four different pump rates (2.5, 5, 7.5 and 10 LPM) were simulated with pitch and roll rates increasing with increasing pump rate. Furthermore, during the field test, the glider was able to maneuver in a sawtooth pattern with a maximum pitch angle of 46.3° , a pitch rate of $2.70\text{E-}01$ rad/s, and a maximum roll angle of 42.3° . The results demonstrated better performance compared to the existing control mechanism of the UTP glider, with pitch and roll angle variations of 2.8% and 29.1%, respectively. Thus, the new roll and pitch control mechanisms can replace the dedicated mechanisms for pitch and roll motions.

ABSTRAK

Peluncur bawah laut dapat melakukan perjalanan secara autonomi dengan bantuan mekanisme kawalan pitch and gulungan yang berasingan. Namun begitu, adalah penting untuk mempertimbangkan beban badan kapal peluncur dan jisim peluncur untuk meningkatkan kecekapan meluncur di dalam air. Oleh itu, dalam kajian ini, pitch dan daya apung tunggal, serta mekanisme kawalan gulungan untuk peluncur bawah air dibincangkan. Mekanisme ini mengawal pitch dan gulungan peluncur tanpa menggunakan enjin daya apung konvensional dan jisim bergerak. Ia terdiri dari empat set kantung air yang terletak di hadapan, belakang, kiri dan kanan peluncur, dan dua pam air dengan kadar aliran tinggi yang mengalihkan air daripada kantung air ini. Dengan mengalihkan air di antara kantung air kiri dan kanan, momen penggulung dihasilkan. Begitu juga, pitch dicapai dengan mengalihkan air antara kantung air hadapan dan belakang. Dinamika sistem dan parameter peluncur diperoleh dan disimulasikan, serta disahkan secara eksperimen. Empat kadar pam yang berbeza (2.5, 5, 7.5 dan 10 LPM) disimulasikan dengan kadar pitch dan gulungan yang meningkat dengan peningkatan kadar pam. Selanjutnya, semasa ujian lapangan, peluncur dapat bergerak dalam corak bergerigi dengan sudut pitch maksimum 46.3° , kadar pitch $2.70\text{E}-01$ rad/s, dan sudut gulungan maksimum 42.3° . Hasil kajian menunjukkan prestasi yang lebih baik berbanding dengan mekanisme kawalan sedia ada peluncur UTP, dengan variasi sudut pitch dan gulungan masing-masing adalah 2.8% dan 29.1%. Oleh itu, mekanisme kawalan gulungan dan pitch yang baharu dapat menggantikan mekanisme khusus untuk pergerakan pitch dan gulungan.

In compliance with the terms of the Copyright Act 1987 and the IP Policy of the university, the copyright of this thesis has been reassigned by the author to the legal entity of the university,

Institute of Technology PETRONAS Sdn Bhd.

Due acknowledgement shall always be made of the use of any material contained in, or derived from, this thesis.

© Kesavan, 2022

Institute of Technology PETRONAS Sdn Bhd

All rights reserved.

TABLE OF CONTENTS

ABSTRACT.....	VII
ABSTRAK.....	VIII
LIST OF FIGURES	XII
LIST OF TABLES	XV
LIST OF SYMBOLS	XVI
LIST OF ABBREVIATIONS.....	XIX
CHAPTER 1 INTRODUCTION	1
1.1 Chapter Overview	1
1.2 Research Background and Motivation	1
1.3 Problem Statement	6
1.4 Research Objectives	6
1.5 Research Scope	7
1.6 Brief Thesis Overview	7
CHAPTER 2 LITERATURE REVIEW	9
2.1 Chapter Overview	9
2.2 Overview of the Existing Underwater Gliders	9
2.3 Pitch, Roll and Buoyancy Control Mechanisms	16
2.4 Hydrodynamic Model	30
2.4.1 CFD and Towing Tank Simulation.....	31
2.5 Overview of the Simulink Model.....	34
2.6 Summary	35
CHAPTER 3 METHODOLOGY	36
3.1 Chapter Overview	36
3.2 Flow Chart of Research Methodology	36
3.3 Mathematical Model	38
3.3.1 Six DOF Equations	39
3.3.2 Mass Distribution Equations.....	40
3.3.3 Moment Equations.....	41

3.3.4	Dynamics Equations of Motion	42
3.3.4.1	Buoyancy Equations	45
3.3.4.2	Kinematics Equation of Motions	46
3.3.5	Hydrodynamic Model	48
3.4	Simulink Model	49
3.5	Design Overview	50
3.6	Experimental Setup and Application of Control Modules	51
3.6.1	Key Components	52
3.6.2	Pitch Control Module	56
3.6.3	Roll Control Module	58
3.6.4	Processing Module	59
3.6.5	Experimental Test with the Control Architecture	59
3.7	Summary	61
CHAPTER 4 RESULTS AND DISCUSSION		62
4.1	Chapter Overview	62
4.2	Motion of Glider During Experimental Test	62
4.3	Pitch and Roll Angle	65
4.4	Relationship Between Pitch Rate and Pump Flow Rate	69
4.5	Relationship Between Roll Rate and Pump Flow Rate	71
4.6	Relationship of Pitch and Roll and Pump Flow Rate	73
4.7	Summary	74
CHAPTER 5 CONCLUSIONS AND RECOMMENDATIONS		76
5.1	Chapter Overview	76
5.2	Conclusions	76
5.3	Recommendations for Future Works	77
REFERENCES		78
LIST OF PUBLICATIONS		87
APPENDIX A		88

LIST OF FIGURES

Figure 1.1: Overview of the underwater glider [44]	2
Figure 1.2: Conventional pitch and buoyancy control mechanism [32]	3
Figure 1.3: Rotational roll control mechanism [47].....	4
Figure 1.4: An overview of the existing buoyancy engine and roll control mechanism on UTP glider [32].....	5
Figure 2.1: Slocum glider [3].....	10
Figure 2.2: Overview of Spray glider [10].....	11
Figure 2.3: Seaglider [8]	12
Figure 2.4: ROUGHIE glider [9]	12
Figure 2.5: Gliding in sawtooth pattern [23]	16
Figure 2.6: Roll motion and acting forces [54].....	17
Figure 2.7: Internal configuration of Slocum glider [54]	18
Figure 2.8: Internal configuration of Spray glider [7]	19
Figure 2.9: Internal configuration of Seaglider [8].....	20
Figure 2.10: Internal configuration of ROUGHIE glider [9].....	21
Figure 2.11: ROUGHIE's roll module [9].....	21
Figure 2.12: Internal configuration of Hybrid Underwater Glider (HUG) [11]	22
Figure 2.13: Buoyancy engine of the South Korea _Underwater Glider [15]	23
Figure 2.14: Petrel II HUG [16].....	23
Figure 2.15: Internal configuration of the USM Hybrid-Driven underwater glider [22]	24
Figure 2.16: Internal configuration of the USM underwater glider [22]	25
Figure 2.17: Internal configuration of Grace glider [23]	26
Figure 2.18: Grace tested in lab tank [23].....	26
Figure 2.19: Internal configuration of the STARFISH [29]	27
Figure 2.20: Roll control mechanism of the STARFISH underwater glider [28]	27
Figure 2.21: Internal configuration of the disk type underwater glider [37]	28
Figure 2.22: Internal configuration of the Mk.III underwater glider [47]	29

Figure 2.23: Internal configuration of the Unmanned Underwater Glider [59]	30
Figure 2.24: Fluid domain simulation around the glider [73].....	32
Figure 2.25: Towing tank test	33
Figure 2.26: Simulink model for the motion of the underwater glider [81]	34
Figure 3.1: Flow chart of research methodology	37
Figure 3.2: References coordinate frame of the underwater glider	39
Figure 3.3: Internal mass distribution frame.....	40
Figure 3.4: References frame for the forces and moments on the glider body [32]	44
Figure 3.5: Front view of the UTP glider	47
Figure 3.6: Simulink model to simulate the pitch and roll performances for a given pump flow rate	50
Figure 3.7: CAD model of the UTP underwater glider	51
Figure 3.8: Experimental setup of the UTP glider	51
Figure 3.9: Overview of the UTP underwater glider	52
Figure 3.10: Water pump_ DQB415-SB	53
Figure 3.11: Water Bladder.....	53
Figure 3.12: FEELBACH solenoid valve	54
Figure 3.13: Microcontroller_Arduino Mega 2560	54
Figure 3.14: Honeywell pressure sensor	55
Figure 3.15: MPU6050 IMU.....	55
Figure 3.16: Motor driver_MD-L298	56
Figure 3.17: Schematic diagram of the internal configuration for the pitch control module	57
Figure 3.18: Gliding trajectory with four dept limits.....	57
Figure 3.19: Schematic diagram of the internal configuration for the roll control module	58
Figure 3.20: Illustration of control architecture operation.....	59
Figure 4.1: Pitch motion during the experimental test.....	64
Figure 4.2: Roll motion during the experimental test	64
Figure 4.3: Pitch angle (degree) against time (second).....	66

Figure 4.4: Roll angle (degree) against time (second)	67
Figure 4.5: Comparison of experimental and simulation results for pitch angle	68
Figure 4.6: Comparison of experimental and simulation results for roll angle	69
Figure 4.7: Pitch rate simulation for pump flow rates of 2.5, 5, 7.5, and 10 LPM	70
Figure 4.8: Comparison of experimental and the simulation results for pitch rate	71
Figure 4.9: Roll rate simulation for pump rates of 2.5, 5, 7.5, and 10 LPM	72
Figure 4.10: Maximum pitch and roll rates with the corresponding pump rates	74

LIST OF TABLES

Table 2.1: Several list of existing underwater gliders.....	13
Table 2.2: Hydrodynamic Coefficients [65]	31
Table 2.3: Drag Force against Froude Numbers [73]	34
Table 3.1: Parameters of the UTP Glider.....	48
Table 3.2: Water pump specifications	53
Table 3.3: Pump rotations on various digital signals (INn) of the motor driver.....	61
Table 4.1: Pump rate against pitch rate.....	70
Table 4.2: Pump rate against roll rate	72

LIST OF SYMBOLS

F	Total external forces acting on the glider
Fr	Fraud numbers
J	Moment of inertia
J_{xx}	Moment of Inertia 'x' axis
J_{yy}	Moment of Inertia 'y' axis
V_f	Fluid's velocity
h	Distance from the free water surface
g	Gravitational force
D_f	The top width of the fluid surface
V_{inlet}	Inlet velocity
q_f	Angular velocity of flow
R	Radius
o	Geometric center of glider
E_0	Origin for earth frame
m_{total}	Total glider mass
m_b	Ballast mass
m_w	Point mass
m_h	Hull mass
m_o	Additional mass
m_t	Trim mass
$[x \ y \ z]$	The body fixed frame of reference
$[u, v, w]$	Translational Speed
$[p, q, r]$	Angular Speed
p	Roll angular velocity/Rate
q	Pitch rate
M	Rigid body mass
M_f	Added mass

V	Velocity vector
D	Drag force
L	Lift force
α	Angle of attack
β	Side slip angle
$P_p = (P_{px} \quad 0 \quad P_{pz})$	Momentum property on the vertical plane
$\bar{u} = (u_x \quad 0 \quad u_z)$	Control forces acting on point masses
$k\text{-}\varepsilon$	K-epsilon
$[X, Y, Z]$	External force
$[K, M, N]$	External moments
J	Moment of inertia
τ	Torque
τ_{hydro}	Hydrostatic moment
τ_{drag}	Rolling drag
τ_{AM}	Rolling added mass
$K_{\dot{p}}$	Rolling added mass coefficient
$K_{\dot{p}\dot{p}}$	Rolling quadratic drag coefficient
\dot{p}	Roll angular acceleration
θ	Pitch angle
\emptyset	Roll angle
γ	Yaw angle
θ_g	Gliding angle
\bar{u}	Control forces acting on point masses
u_4	Control input
α_a	Angular acceleration
pt	Trim weight inertia
R_{EB}	Rotational matrix
R_{\emptyset}	Rotational matrix (Roll)

R_θ	Rotational matrix (Pitch)
R_γ	Rotational matrix (yaw)
$[K_{q1}, K_{q2}]$	Hydrodynamic coefficients
$[K_{D0}, K_D]$	Coefficients of drag force
$[K_{L0}, K_L]$	Coefficients of left force
$[K_{m0}, K_m]$	Coefficients of moment force
P	Pressure
d	Depth
ρ	Density
ΔP	Pressure difference
M_{DL1}	Added Roll Moment Inertia
M_{DL2}	Added Pitch Moment Inertia
v	Linear velocity
ω	Angular velocity

LIST OF ABBREVIATIONS

AUG	Autonomous Underwater Glider
AUV	Autonomous Underwater Vehicle
CB	Center of Buoyancy
CG	Center of Gravity
ROV	Remote Operative Vehicle
LPM	Liter/Minute
DC	Direct Current
ALU	Aluminum
PID	Proportional Integral Derivative
HUG	Hybrid Underwater Glider
UTP	Universiti Teknologi Petronas
PCB	Printed Circuit Board
CAD	Computer-Aided Design
NACA	National Advisory Committee for Aeronautics
SST	Shear Stress Transport
IMU	Inertial Measuring Unit
USM	Universiti Sains Malaysia
RF	Radio Frequency
GPS	Global Positioning System
CW	Clockwise
CCW	Counter-Clockwise
CFD	Computational Fluid Dynamics
AH	Amp Hour
ITTC	International Towing Tank Conference
VDC	Volts of Direct Current
PVC	Polyvinyl Chloride Plastic
NC	Normally Close
MPU	Motion Processing Unit

MD	Motor Driver
INn	Input Signals
DOF	Degree of Freedom

CHAPTER 1

INTRODUCTION

1.1 Chapter Overview

This chapter presents new pitch, roll and buoyancy control mechanisms for an underwater glider. Six sub-sections describe the background of existing pitch, roll and buoyancy control mechanisms, new mechanism and key factors that inspired this research.

The remainder sub-sections in this chapter are organized as follows: in Section 1.2, the underwater gliders are reviewed, in particular their pitch, roll and buoyancy control mechanisms. This is followed by the key factors and motivations for conducting this study. Subsequently, the gap between the current and desired conditions is explained in the problem statement. The objectives of the research are presented in Section 1.4, while the scope of this study is explained in sub-section 1.5. Finally, Section 1.6 presents the overview of this thesis.

1.2 Research Background and Motivation

An AUV is an underwater robot equipped with an advanced control system that allows it to travel independently using a GPS navigation system to a predetermined depth [1], [2]. Oceanographers often use these gliders to collect physicochemical data on the seafloor such as salinity, temperature and oxygen level [3], as there are limitations for human divers to dive into the ultra-deepwater. Furthermore, it is also used to monitor sea currents, underwater pipeline constructions, and marine resources as well as for

military missions [4]. Data recorded from sensors on the glider are stored in internal memory and transmitted to the base station via satellite connections.

The first concept for a fleet of floats was presented in 1989 by Henry Stommel, who inspired the development of the Slocum glider. Slocum, Spray and Sea Glider are well-known legacy gliders [6], which in turn inspired the development of other glider models such as ROUGHIE [9], ALBAC [10], Hybrid Underwater Glider (HUG) [11], South Korea_Underwater Glider [15], Petrel-II [16], [18], USM Underwater Glider [22], Grace [23], Starfish [27], Alex [31], UTP glider [32], Miniature Underwater Glider [34], Disk type Underwater Glider [37], GUPPIE [38] and Underwater Glider Mk. III [47], each with design and configuration differences.

Glider as watercraft are mostly designed in the form of torpedoes or ellipsoids for better hydrodynamics. A conventional glider design has wings, a rudder fin, cylindrical hull, buoyancy engine, movable masses, rotational mechanisms, batteries or power pack, and communication devices.

Fundamentally, the conventional glider model has cylindrical hull surface, fixed wings, and rudder/tail fin as shown in Figure 1.1 [35]. The hull is built to accommodate control mechanisms such as buoyancy engine and pitch, and roll control mechanisms.

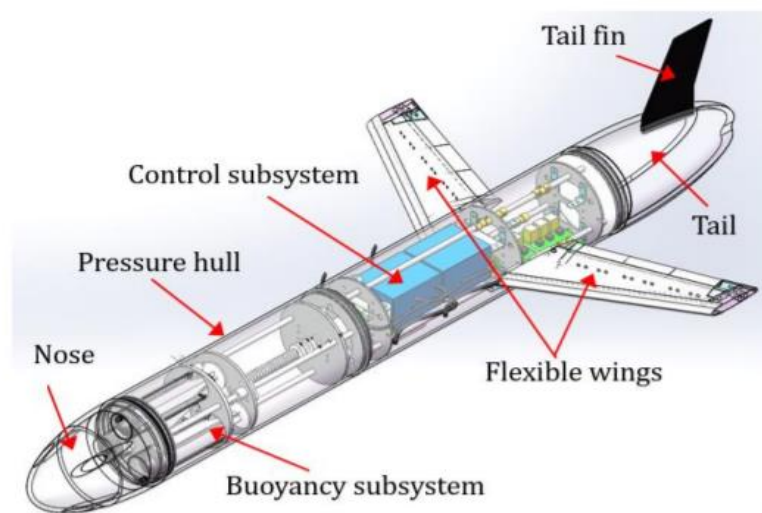


Figure 1.1: Overview of the underwater glider [44]

Gliders move in underwater by controlling the amount of pitch, roll and buoyancy. Initially, the glider is in neutrally buoyant mode. A signal is received by the navigation module which activates the internal configuration of the glider. Figure 1.2 shows a conventional buoyancy engine consisting of a piston driven by a DC motor to control the fluid flow in the ballast tank and a sliding mass to shift the center of gravity. The pitch is achieved by shifting the center of gravity of the glider and shifting the movable mass linearly with the amount of buoyancy controlled by the ballast tank. The piston in the ballast tank is used to control the amount of fluid. The glider pitches downwards when the gravity force is greater than the buoyancy force, which is a negative buoyancy state, with a positive buoyancy state being when the buoyancy force is greater than the force due to gravity.

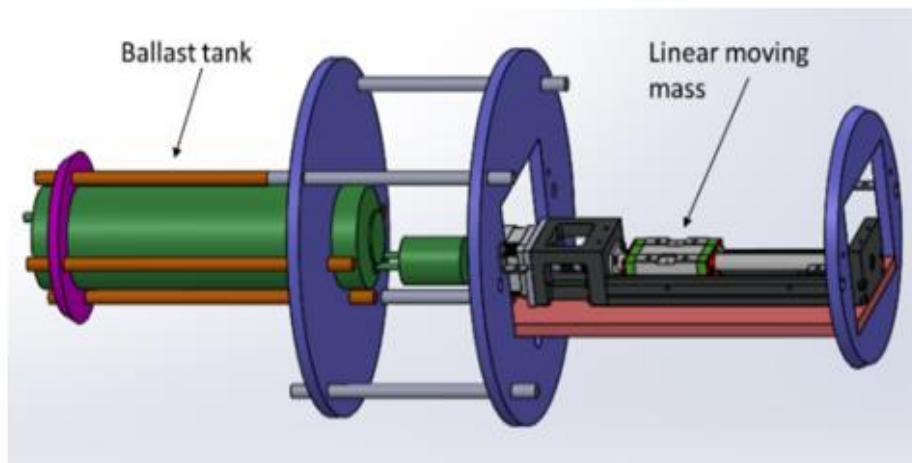


Figure 1.2: Conventional pitch and buoyancy control mechanism [32]

During the descent motion, the battery mass is displaced linearly towards the nose of the underwater glider and the piston is retracted to allow fluids to enter the ballast tank. After the predetermined depth is reached, the ascent begins by shifting the battery mass towards the tail of the glider and the piston is extended to expel fluid from the tank. This sequence is repeated until the end of the mission.

The glider induces roll motion by shifting the center of gravity from left to right or vice versa [9], [45]. Therefore, the underwater gliders use a movable mass to shift the CG along the swaying axis.

As shown in Figure 1.3, the hull is equipped with a rotational mass and the roll is achieved by rotating the rotational mass in a clockwise or counter-clockwise direction.

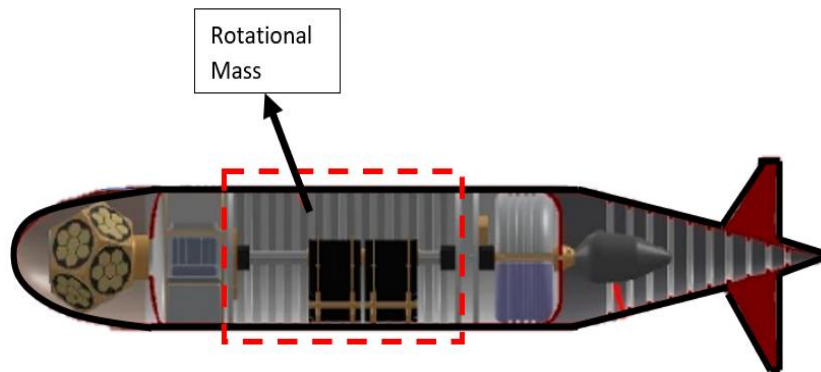


Figure 1.3: Rotational roll control mechanism [47]

Control signals are executed by a processing module to control the maneuvering of the underwater glider, while pitch and roll performances are tracked by a gyroscope module. The processing module is integrated with the navigation system and communication devices of the glider. A data logger is used to record data over time and a hard drive is used to store information.

The material used to construct the glider is another consideration for sustaining the performance of the glider. For example, fiberglass and carbon fiber materials have better seakeeping abilities and stability. The glider's structural shape, wings, rudder, and related dimensions play a key role in enhancing the maneuverability of the glider. The consideration of structural geometry, such as overall size, weight and hull diameter, is significant for glider modeling to accommodate control mechanisms [47], [51]. Therefore, the hull size and load of the glider are subjective to the volume and mass of the control mechanisms. It also affects the performance of underwater glider [51]. For example, by reducing the size of the hull, a minimum displacement of the center of gravity can be achieved by pitch and roll [34], [47]. Lightweight glider such as 'Grace' can produce lower resistance in the water and thus improve gliding efficiency.

As shown in Figure 1.4, the UTP glider built with a conventional buoyancy engine consists of a ballast tank and movable masses. The total mass of the glider with full ballast is 42.1 kg. The trajectory of the sawtooth is achieved by controlling the pitch angle to 45° and the amount of buoyancy on the glider. For the pitch control, the CG is altered by 0.38 kg, 20 cm linear actuator with NEMA 17 servo motor which displaces 2.3 kg of movable mass for 18 cm. The Tmax ballast tank integrated with 12V DC motor is used to control the gliding depth of the glider. Thus, the glider is negatively buoyant when the ballast tank is filled with water and changes to a positive buoyant state when water is expelled from the ballast tank. Both the linear actuator and ballast tank are attached to the internal frame, adding 8.58 kg to the hull mass. The roll is induced by shifting the water mass via the Prolux water pump in between the left and right rolling tanks. The glider can accomplish an optimum roll angle of 30° [32], [54].

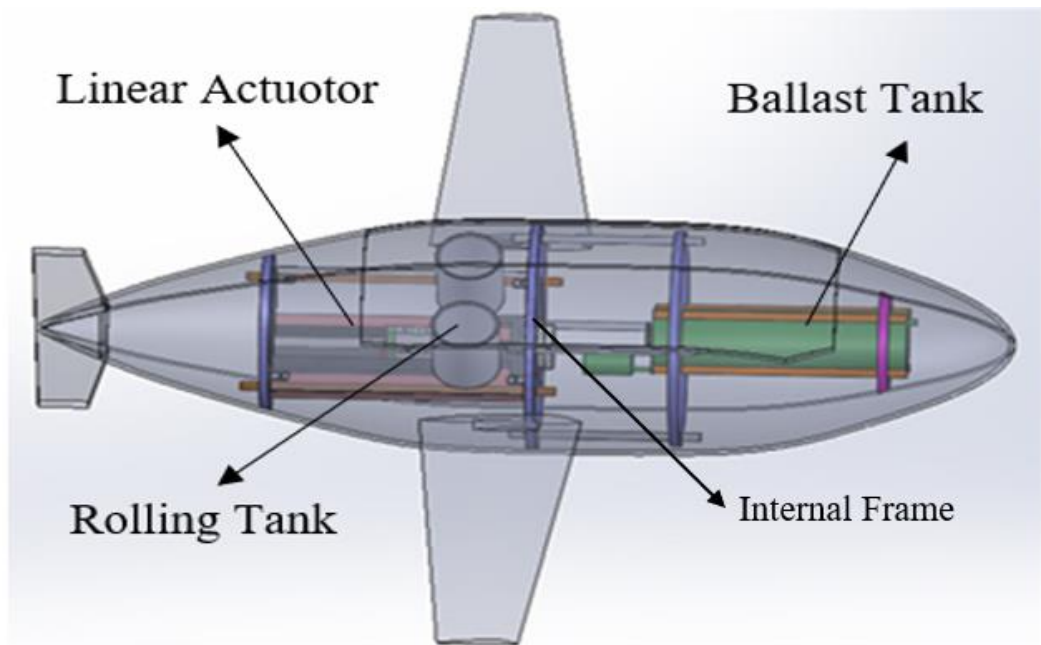


Figure 1.4: An overview of the existing buoyancy engine and roll control mechanism on UTP glider [32]

Previously, the use of a water pump with rolling tank for roll control was proposed for the UTP glider. In this study, the use of a water pump with water bladders was not only for roll control but also proposed for pitch and buoyancy control as well.

1.3 Problem Statement

To improve the efficiency of the underwater glider, an in-depth analysis of the hull load and mass of the glider as well as the competency of its control mechanisms is significant [51]. Similarly, gliders with minimum load can produce better pitch and roll performance [32], [34]. Thus, the performance of the UTP glider can be improved by allowing a reduction in the internal hull mass of the glider.

By referring to [32], [54]; the existing design of the UTP glider was developed without considering the effect of body mass and the use of various control mechanisms that increase the hull load and affect the performance of the glider in the water. The pitch control module is employed with a conventional coupled control mechanism to alter the pitch and buoyancy amount. As discussed earlier, a linear actuator is used to control the pitch and buoyancy amount by a ballast tank with a 12V DC motor, where the buoyancy engine with a coupled control mechanism complicates the control of the glider motion. As a roll control module, a water pump with a low volume of rolling tanks is integrated on the hull surface. To reduce the need for a conventional buoyancy engine, the use of a single control mechanism for pitch and buoyancy as well as roll control is proposed in this study. This will ultimately reduce the internal hull mass and high potential to improve the pitch and roll performance of the UTP glider.

1.4 Research Objectives

In this study, a single mechanism was developed for the pitch, roll and buoyancy control modules to regulate the amount of buoyancy, pitch and roll of the glider. The control modules were tested to evaluate the pitch and roll performance of the glider. The objectives are as follows:

- i. To develop a single mechanism that controls pitch and buoyancy as well as roll control.
- ii. To determine the correlation between the pitch and roll response of the glider with the control mechanisms.

- iii. To derive the relevant mathematical equations based on a single mechanism for the pitching and rolling motions.

1.5 Research Scope

The scope of this study is to further develop a single mechanism for pitch and depth as well as roll control of the underwater glider. The goal is to eliminate the use of a dedicated mechanism for pitch and roll control as well as separate buoyancy engine.

This study focuses on the development of pitch, roll and buoyancy control mechanisms that use water as trim mass. Both pitch and roll control modules are equipped with an individual water pump to displace water from the water bladders which are located at the front, rear, left, and right of the glider. The pitch is achieved by shifting water between the front and rear water bladders. The amount of water in the water bladders directly influences the center of gravity and buoyancy amount of the underwater glider, causing the glider motion in the water. The roll is induced by shifting water from the left and right water bladders through the water pump system.

A simulation model is used to evaluate the pitch and roll performance at various pump flow rates. The developed control mechanisms are physically tested to determine the pitch and roll motion of the UTP glider. Thus, the data obtained from the Simulink model are validated with the field test results.

This study is limited only to the performance of the proposed pitch and roll control mechanisms. Noise test and control algorithms are excluded. Data are collected from a geographic region and then are analyzed.

1.6 Brief Thesis Overview

This thesis consists of five chapters as outlined below.

In chapter 1, an overview of the underwater glider is presented emphasizing on pitch, roll and buoyancy control mechanisms. The constraints of existing models and

the purposes of this research are also discussed. The proposed methods for improving the control mechanism of the underwater glider are explicitly explained.

The configurations and limitations of the existing underwater gliders, in particular pitch, roll and buoyancy control mechanisms are elaborated in Chapter 2. The techniques used to determine the hydrodynamic effects on the motion of the underwater glider are also included.

Chapter 3 describes a comprehensive methodology and the flow of this research. It also includes dynamic modeling, working principle, design of pitch and roll control modules and techniques to determine the pitch and roll motions of the underwater glider.

In chapter 4, the results of the performance of underwater glider are discussed. The simulation and experimental validation of the developed control mechanisms are thoroughly explained.

Chapter 5 concludes this research by describing the goals achieved. In addition, the recommendations for future underwater glider development are also included.

CHAPTER 2

LITERATURE REVIEW

2.1 Chapter Overview

This chapter reviews the existing gliders, specifically their pitch and roll control mechanisms. This chapter is divided into six sections. Section 2.2 provides an overview of the existing underwater gliders. Section 2.3 describes the internal configuration of existing underwater gliders, focusing on pitch and roll control mechanisms. Section 2.4 outlines the hydrodynamic characteristics and methods applicable to evaluate the hydrodynamic parameters, such as CFD and Towing Tank Simulations. Section 2.5 describes the use of Simulink model to evaluate the motion of the glider. Finally, Section 2.6 summarizes pitch and roll control techniques as well as the limitation of the existing underwater gliders.

2.2 Overview of the Existing Underwater Gliders

As shown in Figure 2.1, the Slocum glider is torpedo-shaped with a diameter of 0.21 m, length of 1.8 m and weight of 52 kg. Slocum can travel underwater using a buoyancy mechanism and its wings. It can reach a maximum depth of 200 m and the vehicle communicates with the base station through an RF modem or Iridium device. According to Oscar Schofield et al. [3], the glider can travel up to 24 km per day using alkaline batteries. The battery lasts about 25 to 50 days and needs replacement to continue traveling. The vertical travel distance is predetermined in the program [35].



Figure 2.1: Slocum glider [3]

Jeff Sherman et al. [7] developed a glider named Spray for long-distance travel to acquire oceanographic data. As depicted in Figure 2.2, it has an ellipsoid-shaped hull 2 m length, 1.2 m width, and 0.2m diameter and 50 kg weight. The wings and stabilizer have thicknesses of 4 mm and 3.2 mm, and control vertical motion.

The hull of the glider was divided into three sections and a hydraulic system at the rear section acted as a ballast engine, which achieved pitch and roll by shifting the battery mass. The glider wing was equipped with an ORBCOMM communication system to connect with the vessel control room, while GPS navigation system directed the glider to the targeted coordinates. The glider's depth level was pre-programmed to prevent any loss of communication with the glider throughout its ocean mission [7], [35].



Figure 2.2: Overview of Spray glider [10]

Seaglider was developed in 2001 by Erikson et al. [8], and its design complied with a one-year duration for ocean-basin range exploration. Figure 2.3 depicts a torpedo-shaped glider with 1.8 m length, 0.3 m hull diameter and 52 kg weight. For better seakeeping, Seaglider used fiberglass material, and the hull portions were made of ALU T6. The 1m-long wing generated a hydrodynamic lift force, controlling the forward velocity of the vehicle [8], [35].

A buoyancy engine with a hydraulic system was used to control the buoyancy amount, while a gear system was used to displace the center of gravity and control pitch and roll motion of the Seaglider. There was a fixed rudder with a GPS antenna to communicate with the base station [8].

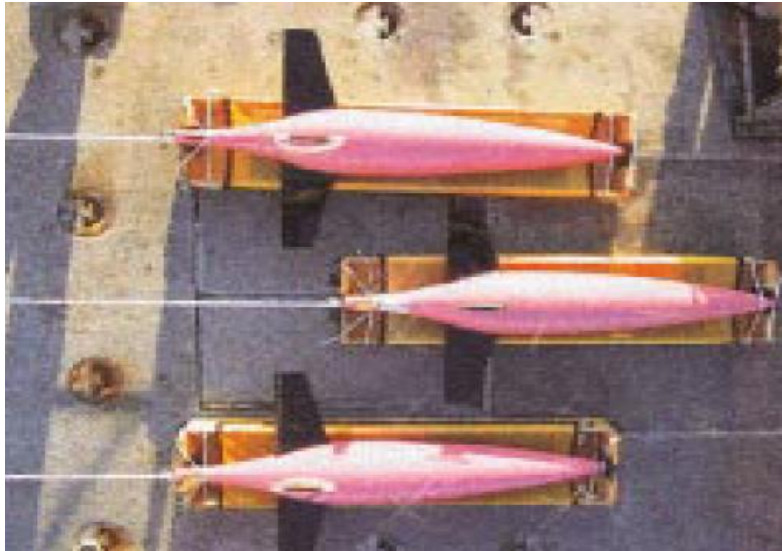


Figure 2.3: Seaglider [8]

The ROUGHIE glider was developed as a portable underwater glider with a length of 1.2 m and weighed 12.8 kg. As displayed in Figure 2.4, the glider has a torpedo shape with two hulls made of acrylic and aluminum to adapt to different pressure levels.

The ROUGHIE glider controlled its pitch and roll by shifting the battery mass linearly. Its buoyancy was controlled by a buoyancy engine with a rolling mechanism integrated with hull surface consisting of 90% of the glider's internal mass. The roll was induced by shifting the center of the gravity of the vehicle along the y-axis. The ROUGHIE was associated with Arduino mega as a central processing unit to compute all the control signals. It has rear wings to sustain the ascent and descent motions and it can be used for shallow-water gliding, under depths of less than 3 m [9].



Figure 2.4: ROUGHIE glider [9]

Table 2.1 lists several types of underwater gliders with distinct shapes, dimensions and functions for research and commercial purposes as well as described the research gaps or limitations of each of the glider models.

Table 2.1: Several list of existing underwater gliders

Glider Name/Type	Design Overview	Research Gap/Limitation
Hybrid Underwater Glider (HUG) [11]	<p>Glider structured with a cylindrical hull with elliptical-shaped bow and stern as well as wings, rudder and thruster.</p> <p>The glider was 1.97 m in length with a hull diameter of 0.22 m and weight of 50.5 kg.</p> <p>The glider could control pitching motion by displacing the internal battery mass linearly and controlling the amount of fluid in the ballast tank. It could achieve an average pitch angle of 38.6°.</p>	<p>The use of the conventional mechanism caused the hull load/mass to increase which affected the performance of the glider. It was designed without roll control module.</p>
South Korea_ Underwater Glider [15]	<p>Designed in torpedo shape and equipped with a thruster propulsion system.</p> <p>It was 1.3 m in length with a hull diameter of 0.22 m and weight of 60 kg.</p> <p>Able to control pitch and buoyancy by altering the 10 kg of movable mass linearly and operating the hydraulic pump. It achieved a maximum pitch angle of 35°.</p>	<p>It could only control pitch and buoyancy.</p> <p>When conventional mechanism was utilized, the hull load/mass increased, affecting the glider's performance.</p>

Table 2.1: Several list of existing underwater gliders (Cont.)

Petrel-II [16]	<p>The glider was torpedo-shaped and employed with hybrid - driven mode consisting of propeller thruster.</p> <p>The glider was 2.3 m in length (excluded antenna), diameter was 0.22 m and weighed 70 kg.</p> <p>A coupled control mechanism was used for pitch and rotational mass for rolling motions. The optimal pitch angle was 35.5°.</p>	<p>The use of multiple control mechanism affected the mass of the glider and complicated the motion control of the Petrel-II glider.</p>
USM Hybrid-Driven Underwater Glider [22]	<p>The glider was in cylindrical-shaped with controllable wings, rudder and propeller.</p> <p>It was 1.65 m in length, 0.17 m in diameter and weighed 30.95 kg.</p> <p>The glider was equipped with conventional coupled control mechanism as pitch control module and controllable wings and rudder for roll control. It achieved optimal pitch angle of 46.03° and it produced higher error rate when experimental and simulation data were compared.</p>	<p>The use of multiple control mechanism consumed more space and affected the size of the glider. Higher error rate was generated between experimental and simulation data.</p>
Grace [23]	<p>Modeled as robotic fish. It has a fish-like shape and the wings were trapezoidal for better maneuverability.</p> <p>Its total length was 0.9 m including the tail, width of 0.75 m including wings and weighed 9kg.</p> <p>Multiple control mechanisms were used to control pitch and roll motions. The maximum roll angle achieved was less than 15° and an optimal pitch angle was achieved at 40°.</p>	<p>The use of multiple control mechanisms complicated the motion control and has an impact on the roll performance of the glider.</p>

Table 2.1: Several list of existing underwater gliders (Cont.)

STARFISH [27]- [29]	<p>Torpedo-shaped with two rudder fins and two elevator fins.</p> <p>The glider has length of 2m with a hull diameter of 0.2 m and weighed 50 kg.</p> <p>It was implemented with conventional pitch and buoyancy control mechanisms, with a pitch angle of 5°. The roll was achieved by rotational mass with an optimal roll angle of 25°.</p>	<p>The use of conventional coupled pitch control mechanism and rotational mass caused the hull mass to increase and thus affected the pitch and roll performance of the glider.</p>
Disk type Underwater Glider [37]	<p>The glider is designed in axisymmetric and without any appendage such as wings, rudder and propeller.</p> <p>It was designed with movable mass and ballast actuator with the maximum pitch angle of $\pm 34^\circ$.</p>	<p>Without wings and rudder, it was difficult to convert the vertical motion into horizontal and complicated the motion control of the glider. No physical test data available.</p>
Mk.III Underwater Glider [47]	<p>The glider developed in torpedo shape with fix wings and rudder.</p> <p>The pitch and buoyancy were controlled by the movable mass and hydraulic oil pump system accordingly. The rotational battery mass used to control the roll motion. The control mechanism was not tested through experiments or graphics to obtain pitch and roll data.</p>	<p>The use of multiple control mechanisms complicated the gliding motion. Pitch and roll data were not sufficient for comparison.</p>
Unmanned Underwater Glider [59]	<p>The glider was designed in a torpedo shape with the stern rudder located at the tail.</p> <p>It was 3.1 m in length, 0.2 m in diameter and weighed 58 kg.</p> <p>The pitch and buoyancy amount can only be controlled using conventional coupled control mechanism.</p>	<p>The design was limited to pitching motion only.</p> <p>The conventional pitch control mechanism caused the glider mass to increase.</p>

2.3 Pitch, Roll and Buoyancy Control Mechanisms

The physical trajectory of most underwater gliders is in a sawtooth pattern as illustrated in Figure 2.5. Glider has a buoyancy engine and movable masses as the pitch control module and wings convert vertical movement to a horizontal plane, enabling the glider to achieve its intended destination [23].

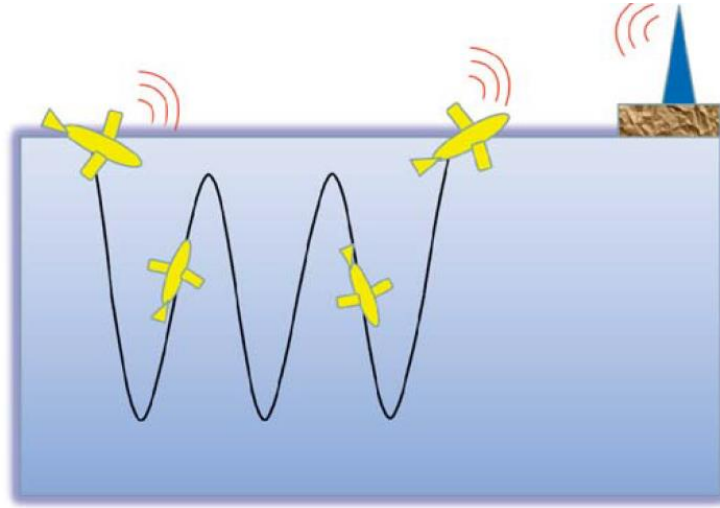


Figure 2.5: Gliding in sawtooth pattern [23]

A pressure sensor is used to detect the predetermined depth level and produce a signal to alter the gliding motion accordingly. The signal from the sensor is received by the processing module, which then triggers the pitch controller module.

Underwater gliders can turn either to right or left side by shifting its center of gravity towards the left and right sides of the wings [7]. As shown in Figure 2.6, the glider rolls in a circular path while accelerating towards the circle's center, where ' m_l ' and ' m_r ' are the left and right ballast mass, respectively, and the glider mass respective to the gravitational force is denoted as ' mg '. According to Newton's second law, the centripetal force acting on the glider during the roll motion has the same direction as the acceleration. Lift force ' L ' acts as a centripetal force, causing the glider to roll in a circular pattern [54].

According to Hong You [28], the meta-centric height of the underwater glider needs to be considered for better roll stability to prevent undesired roll motions due to

unexpected disturbance in the aquatic environment. Hence, the undesired roll motions affect the performance of the glider by diverting it from achieving the desired coordinates [23], [28].

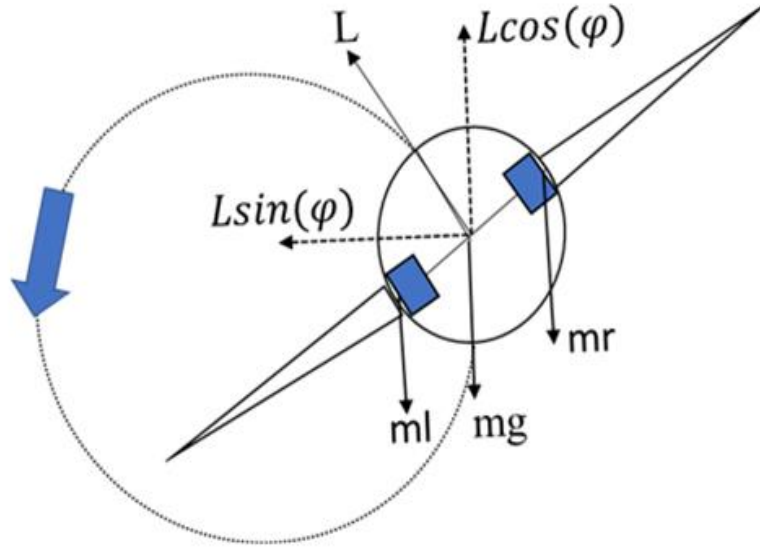


Figure 2.6: Roll motion and acting forces [54]

The Slocum [3], Spray [7], Sea Glider [8], ROUGHIE [9], Hybrid Underwater Glider (HUG) [11], Petrel II [16], [18], USM Underwater Glider [22], Grace [23], STARFISH [27]-[29], Miniature Underwater Glider [34], Disk type Underwater Glider [37], Underwater Glider Mk.III [47] and Unmanned underwater Glider [59], are among the underwater gliders that employ with a buoyancy engine and moveable mass to control the depth, pitch and roll.

The layout of the Slocum glider can be divided into three sections (Figure 2.7): two wet sections and a science payload bay. The front wet section consists of a single-stroke buoyancy pump and battery mass, and the rear wet section includes a steering fin, inflatable bladder, antenna and oxygen sensor. The amount of buoyancy is controlled by the buoyancy pump and the tail fin rudder alters the forward propulsion. The glider is negatively buoyant into the water by inflating the rear bladder which allows the tails to lift. Then, the configuration signals from the scientific bay trigger the battery mass to move towards the bow, and the descent occurs by retracting the piston allowing the fluid flow into the ballast tank. When the glider reaches the predetermined depth level,

the ascent is achieved with the battery mass being shifted to the tail of the glider and the piston being extended to release the fluid from the tank. As the gliding depth is preprogrammed, the ascent and decent motions are determined by using a pressure sensor. Thus, the motion is repeated and causes the glider to move in a sawtooth pattern [3], [35].

It can travel at a forward speed of 0.2 – 0.3m/s and a gliding angle of 35°. By the way, the science payload bay is integrated with these electronics devices such as optical sensors, the main processing module, GPS receiver, attitude sensor, and the battery pack [3].

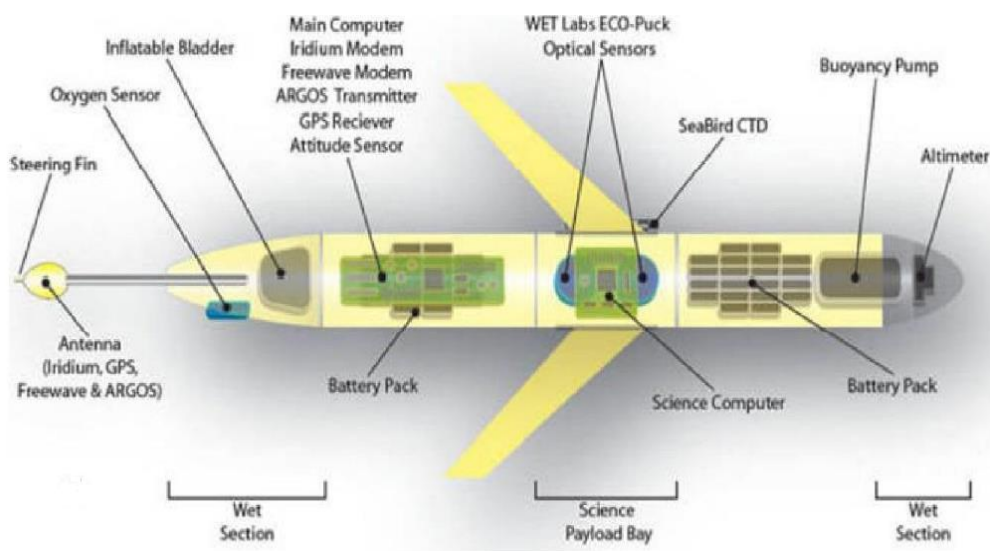


Figure 2.7: Internal configuration of Slocum glider [54]

In contrast, the Spray glider has three internal sections (Figure 2.8). Pitch is achieved by displacing the ‘Pitch Battery Pack’ linearly. There is a rack and pinion mechanism integrated with DC motors to move the battery pack up to 10 cm. At the rear section, there is a hydraulic system that consists of hydraulic components to control the gliding motion for a pitch angle of 16.6° and a vertical speed of -0.08 to 0.09 m/s [7]. When the battery pack moves forward, the CG of the glider is displaced about 17 mm, which creates a negative pitch angle. Prior to reaching the predetermined depth, the hydraulic pump activates to make the glider glides upward and prevents the glider from exceeding the predetermined depth level. The hydraulic pump and valve are used

to control the flow of hydraulic oil in between the internal and external bladders. The gliding motion is controlled using a compass, altimeter and pressure gauge.

The internal weight of the Spray glider is carried by a battery mass, which is rotated 360 degrees around the axial column to achieve the roll motion. The glider is integrated with multiple sensors to sense essential information and store the data in memory [7], [35].

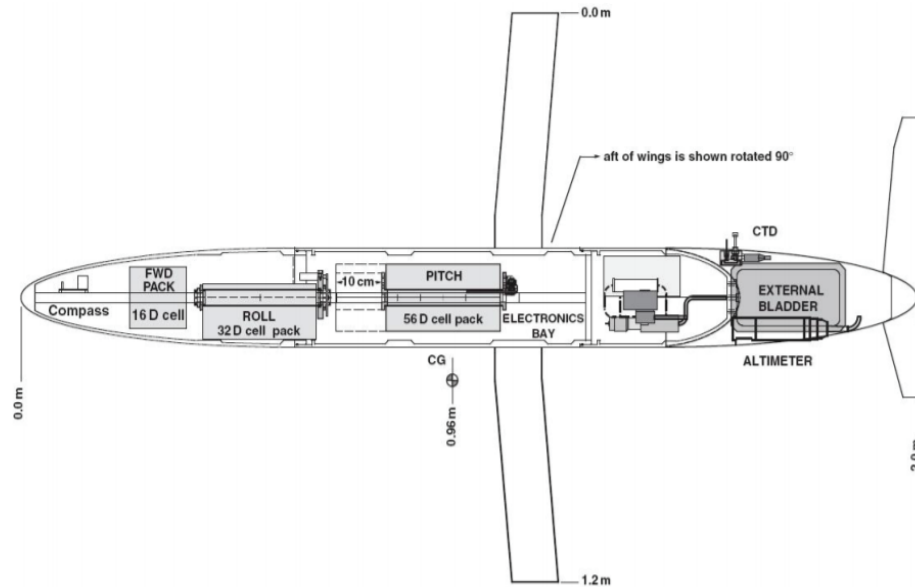


Figure 2.8: Internal configuration of Spray glider [7]

The Seaglider is divided into four sections (A-D) as shown in Figure 2.9. The glider's linear actuator is driven by 16-mm Maxon neodymium magnet motors, which are combined with a planetary gear system, spur gear and worm drive mechanisms to displace the CG by shifting the battery pack linearly, resulting in a maximum pitch angle of 45° . In addition, the gear system is used to rotate the battery pack left or right to achieve the maximum roll angle of 30° [8].

The variable buoyancy system in Section D consists of a hydraulic system to displace the oil in between the inner and outer reservoir. The solenoid valve is used to control the flow of the oil shifted. A boost pump is used to supply high pressure to the hydraulic piston pump [35], [8].

According to Erikson et al. [8], check valves can be utilized to increase the pumping rate up to 50% with a zero increase in power consumption. The gliding speed of Seaglider is 0.25 m/s and the pitch is measured by an attitude sensor module.

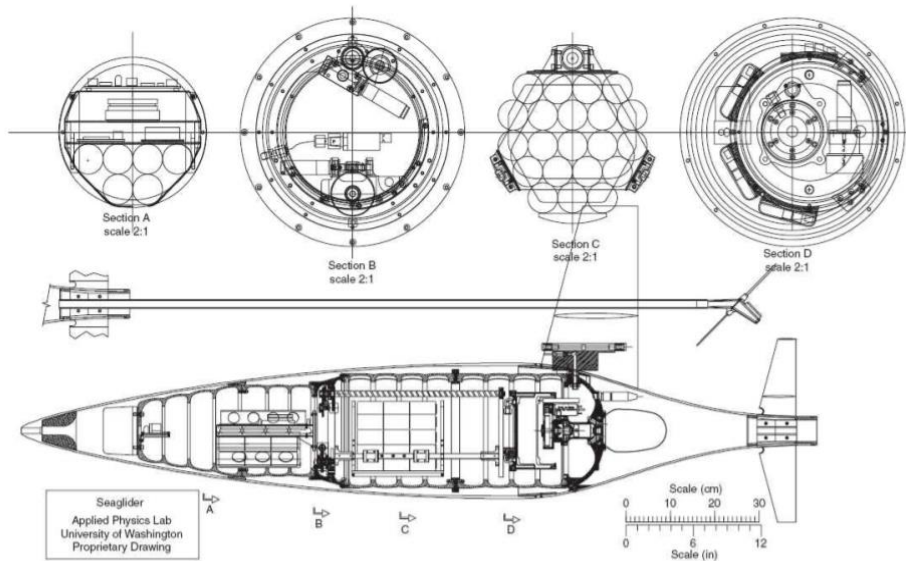


Figure 2.9: Internal configuration of Seaglider [8]

The ROUGHIE is suitable for shallow water applications. As depicted in Figure 2.10, the pitch control module of the ROUGHIE glider is equipped with movable mass and buoyancy-driven mechanisms. The ROUGHIE achieves the desired pitch angle $\pm 20^\circ$ by moving linearly the battery mass of 2.2 kg about 0.85 m. To control the buoyancy amount of the glider, a water pump with a normally closed solenoid valve is used to control the presence of water in the ballast tank. The pressure sensor is used to calculate the gliding depth level.

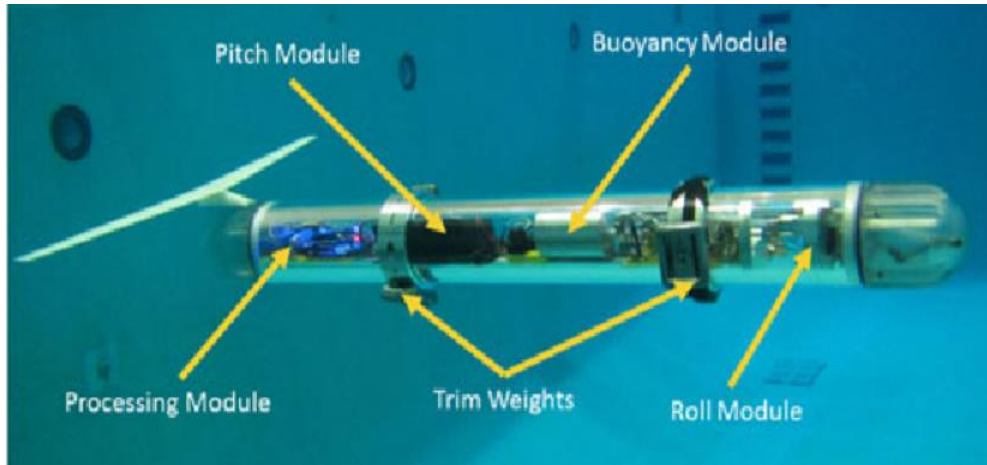


Figure 2.10: Internal configuration of ROUGHIE glider [9]

Furthermore, the ROUGHIE glider is equipped with a switching control system. Figure 2.11 shows the ROUGHIE's roll module including an aluminum ring attached to an internal hull surface, which is driven by a servo motor. The rolling motion of the vehicle is induced by spinning along the common rail, which carries 90% of the vehicle's internal mass. This glider is capable of a maximum roll angle of 60° . An Arduino Mega processor is attached to the rear of the glider [9].

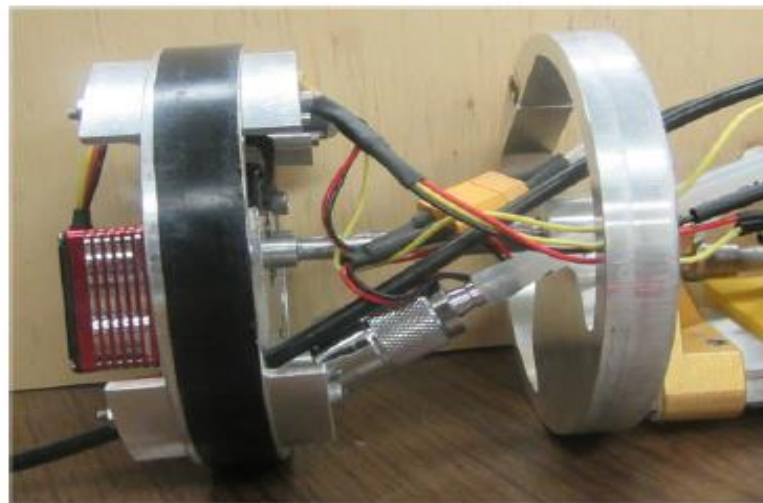


Figure 2.11: ROUGHIE's roll module [9]

In 2018, Dae-Hyeong Ji et al. [11] introduced the Hybrid Underwater Glider (HUG) as shown in Figure 2.12. The glider consisted of key components such as altimeter, attitude controller, buoyancy engine, battery pack, rudder fin, thruster and external antenna. The pitching motion was controlled by a conventional coupled control

mechanism. The CG of the glider was shifted by changing the battery mass linearly, which caused the glider to pitch negatively, with a buoyancy engine activated to control the flow of water in the ballast tank via a motor with a belt and pulley mechanism. A thruster was used to enhance the gliding speed. Wings and a rudder fin stabilized the gliding motion in high sea currents.

Field tests showed that the HUG glider can achieve an average pitch angle of 38.6° . Using only buoyancy engine, the velocity of the vehicle was 0.77 m/s. When using only propeller, the velocity was 0.46 m/s, and the combination of both buoyancy engine and propeller resulted in 1.2 m/s velocity [11].

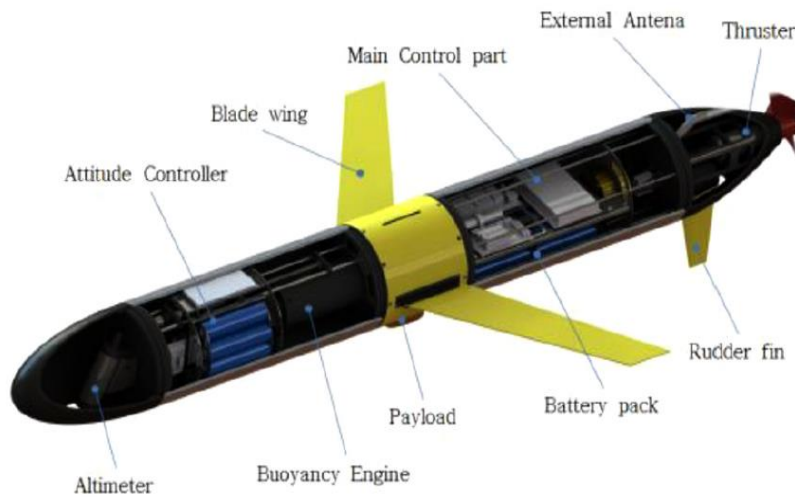


Figure 2.12: Internal configuration of Hybrid Underwater Glider (HUG) [11]

In 2018, Sung-Min Hong et al. [15] developed an underwater glider integrated with a buoyancy engine and thruster. The glider was equipped with a hydraulic pump and movable mass to control the pitch motion. The Pitch angle was adjusted by displacing an internal 10 kg battery mass linearly up to 15 cm to achieve maximum pitch angle of 35° .

As shown in Figure 2.13, the hydraulic buoyancy engine was designed to control the flow of hydraulic oil and pressure, which changed the buoyancy amount. The motor and solenoid valve were used to control the flow of hydraulic oil from the oil reservoir to extend and retract the piston. The pressure accumulator was used to apply a pressure up to 25 bar when the piston moved forward. By activating the solenoid valve, the

piston retracted backward due to vacuum pressure. The optimal gliding velocity of the glider was 0.62 m/s. However, the thruster was activated in the specific ocean environment and current conditions [15].

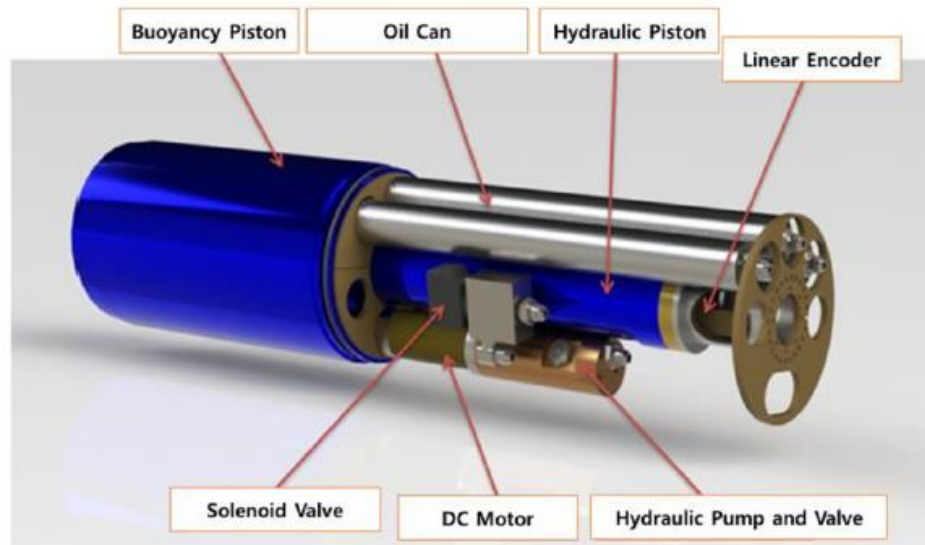


Figure 2.13: Buoyancy engine of the South Korea _Underwater Glider [15]

Similar to the conventional underwater gliders, Petrel II glider used a ballast pump to control the fluid flow into the oil reservoir and the buoyancy amount. The roll and pitch were achieved by rotating and displacing the battery pack for 40 mm to control the center of gravity of the glider. By referring to the data, the optimal gliding angle was 35.5° . Pressure sensor was used to determine the depth level. During the hybrid-driven mode, the propeller was actuated to improve the gliding speed [16], [18].

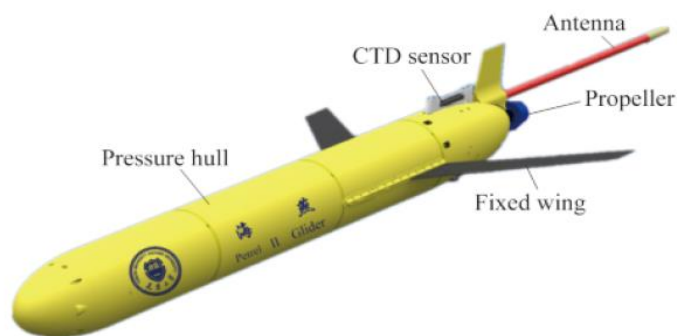


Figure 2.14: Petrel II HUG [16]

According to Khalid Isa et al. [22], the interior configuration of the USM glider was divided into three hull sections. Typically, the pitch module was a conventional coupled system with an optimal pitch angle of 46.03° by shifting the sliding mass linearly, while the ballast pump regulated the amount of buoyancy of the glider. However, the pitch rate has an error of 81.5% between the experimental and simulation data as the dynamics of the glider were affected by the environmental disturbances.

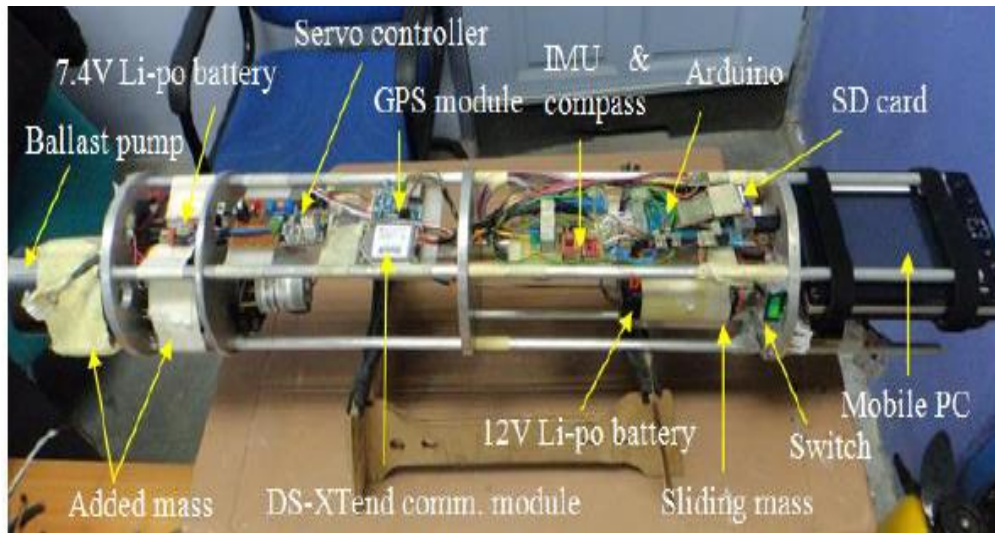


Figure 2.15: Internal configuration of the USM Hybrid-Driven underwater glider [22]

The USM underwater glider (Figure 2.16) was designed with controllable wings and a rudder for roll control. The rotation plane of wings and rudder determined the vehicle's rolling direction. The center of gravity was shifted along the sway axis by rotating both wings and rudder. A maximum roll angle error of 24% with a roll rate error of more than 5 deg/s was reported.

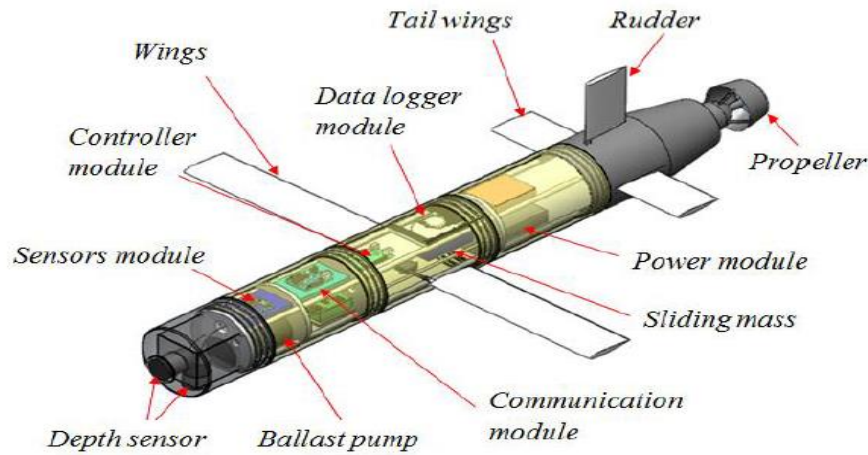


Figure 2.16: Internal configuration of the USM underwater glider [22]

Zhang et al. [23] developed a hybrid robotic fish underwater glider known as Grace. It can travel in two different motions with three actuation systems as depicted in Figure 2.17. These actuation systems were the buoyancy adjustment system, center-of-gravity (CG) control system, and tail control system. The pitch motion was controlled by the CG control mechanism, which consisted of linear actuator to displace the battery mass. A water pump in the buoyancy adjustment system was used to pump water in and out to the water tank. A pressure sensor was used to detect the depth level and send the appropriate signals to enable a heavy-duty linear actuator, which then operated the water pump.

The buoyancy of the glider depends on water mass. Descent occurs when water is pumped into the tank and ascend occurs when water is pumped out from the tank. Energy was only consumed during these motion transitions. During field testing, Grace achieved an optimal pitch angle of 40° with a terminal velocity of 0.2 m/s. Grace was outfitted with two processing units, namely a control PCB and a driver PCB. Each PCB serves a unique purpose in the motion control system. The pitch angle was computed using the accelerometer sensor [23], [60].

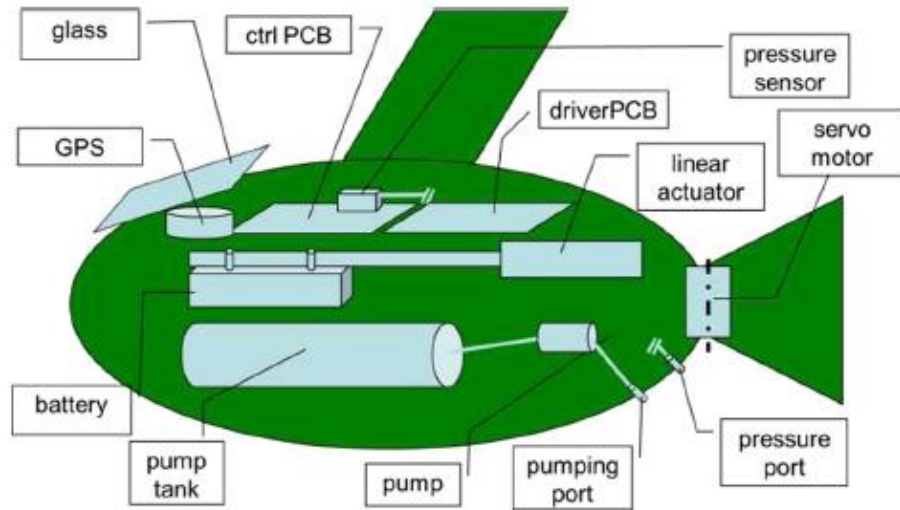


Figure 2.17: Internal configuration of Grace glider [23]

Grace used a tail control mechanism to achieve a turning motion. As shown in Figure 2.18, the glider has a fish-like tail that flapped using a DC servo motor via a chain transmission, which produced a steering moment. The vehicle has a 1-m turning radius and a maximum roll angle of less than -15 degrees.

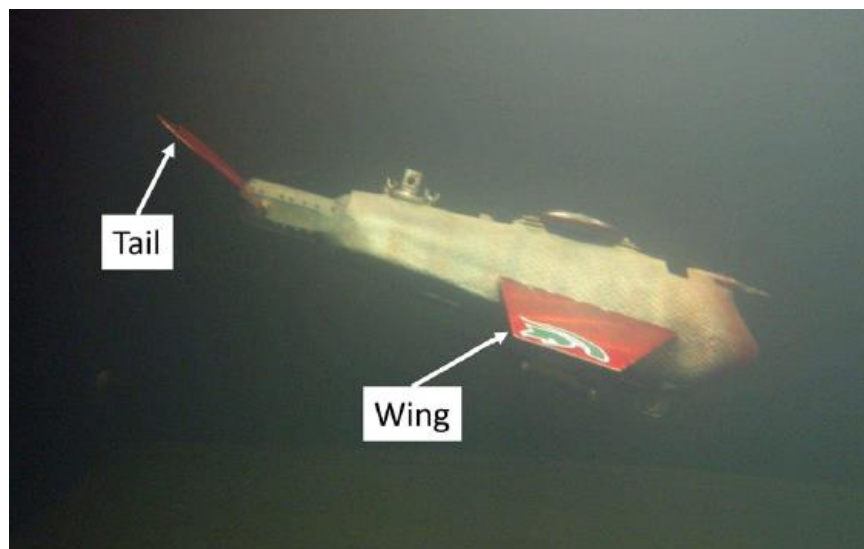


Figure 2.18: Grace tested in lab tank [23]

On the other hand, the STARFISH underwater glider as displayed in Figure 2.19 dived to a predetermined depth level with an optimal pitch angle of less than 20° and maintained 2 m depth with the pitch angle of 5° . The nose of the glider was equipped

with two tubes coupled to a buoyancy engine to control the flow of fluid into the reservoir. The servo motor drove the thruster fins, which produced 10 kg of thrust force to enable the glider to maneuver. The pitch of the glider was determined via the microcontroller and IMU device [27]-[29].

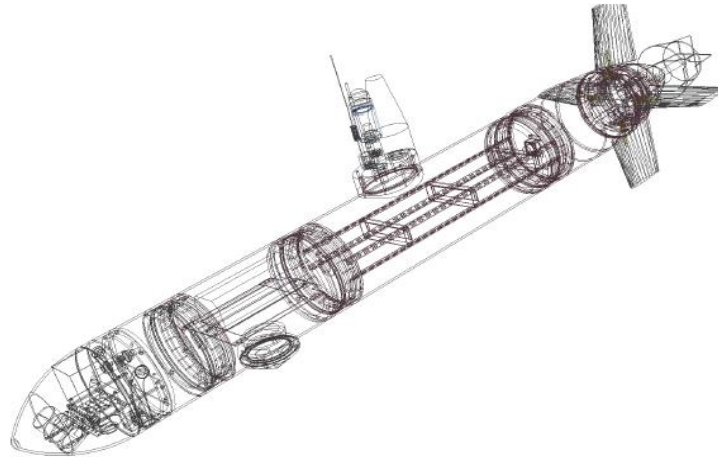


Figure 2.19: Internal configuration of the STARFISH [29]

Hong You et al. [28] developed the STARFISH underwater glider with roll control mechanisms as demonstrated in Figure 2.20. Roll was induced by shifting the CG along the y -axis with a rotating mass. A servo motor actuated at a maximum speed of 6.16 rad/s to drive two timing belt pulleys and to produce an output torque. The torque was transferred via coupling pins and rotated the tail tray located in the hull of the glider. Experimental data showed that the glider can achieve an optimal roll angle of 25° .

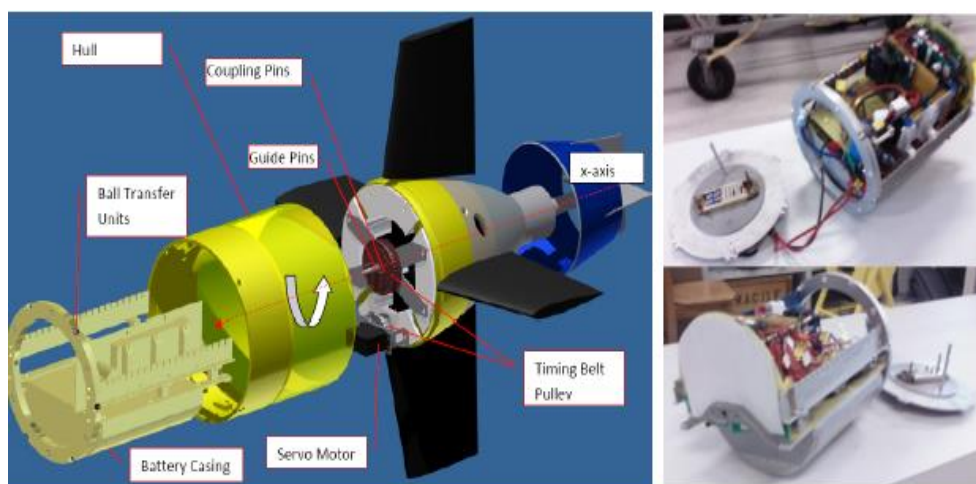


Figure 2.20: Roll control mechanism of the STARFISH underwater glider [28]

In 2017, Pengyao Yu et al. [37] developed a disk type underwater glider. As shown in Figure 2.21, the pitch control mechanism of the glider consisted of movable masses (Block P1 and Block P2) and a buoyancy adjustment system. The glider moved in a sawtooth pattern with a pitch angle of $\pm 34^\circ$ and a gliding velocity of 0.285 m/s. Pitch was induced by shifting the center of gravity by moving the movable masses along with the circular path located on the upper and lower structures of the underwater glider. To adjust the buoyancy condition of the underwater glider, the ballast actuator was used to control the ballast mass which influenced the glider mass.

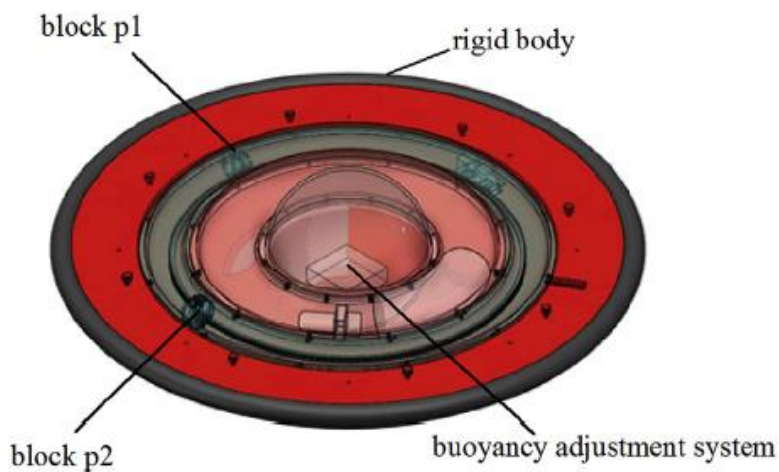
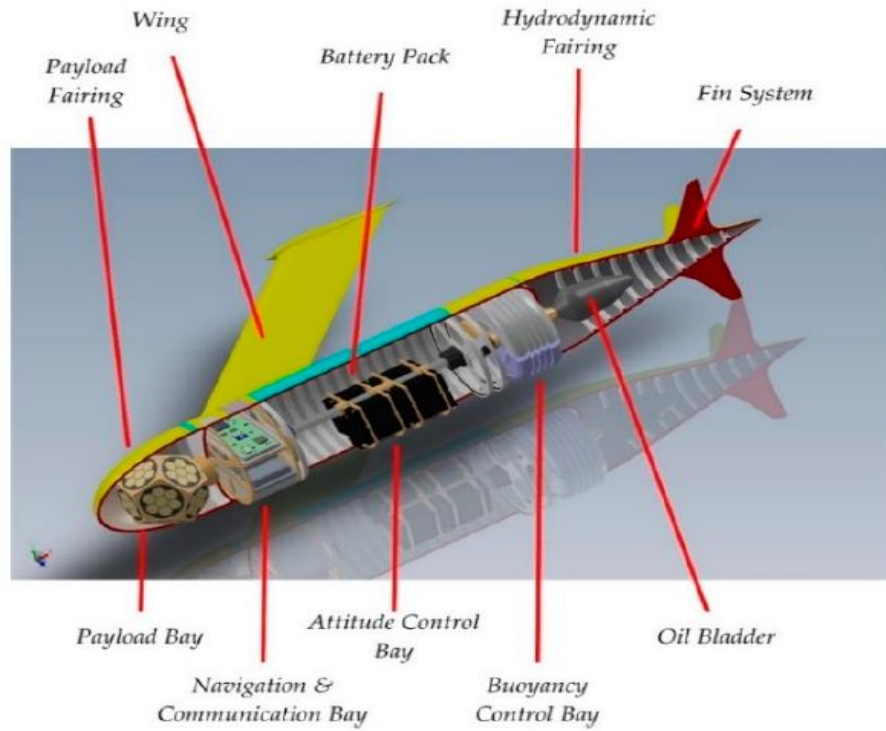
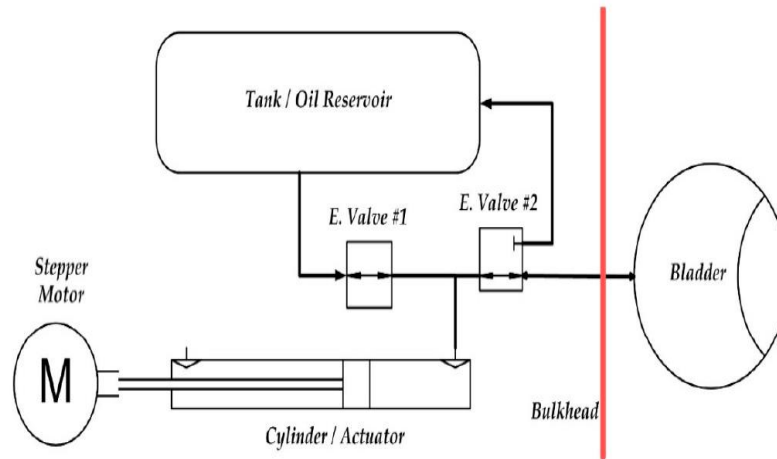


Figure 2.21: Internal configuration of the disk type underwater glider [37]

Figure 2.22 depicts the design configuration of Mk.III underwater glider. Initially, the glider was in the neutrally buoyant state, which has an equal density with the seawater. During the pitch, the CG of the glider was displaced by moving the battery pack linearly. The ascent and descent of the underwater glider were regulated by the bladder volume. The glider was propelled downwards by triggering the hydraulic pump, which then transferred oil from the inflatable bladder to the oil reservoir via the solenoid valve. While the glider ascending, the hydraulic oil from the tank shifted to the inflatable bladder, thus reducing the density of the bladder. The roll was accomplished by rotating the battery mass along the longitudinal axis which shifted the center of gravity from left to right or vice versa [47].



(a) Cross section view of the Mk.III underwater glider



(b) Buoyancy system

Figure 2.22: Internal configuration of the Mk.III underwater glider [47]

Sang-Ki Jeong et al. [59] developed an unmanned underwater glider with a conventional coupled pitch control mechanism. As shown in Figure 2.23, the internal structure of the glider was divided into three sections such as prow section, control section and aft section. The pitch of the glider was controlled by shifting the battery

mass linearly and a hydraulic buoyancy engine was used to regulate the flow of seawater into the prow section to control the buoyancy amount of the glider with the maximum speed of 1.2 m/s [59].

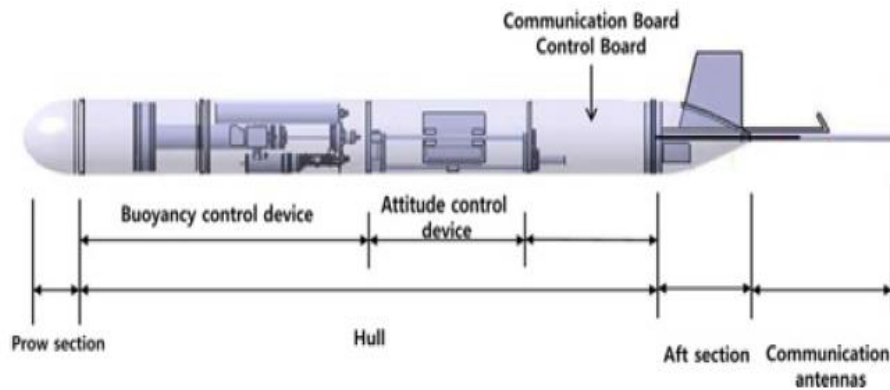


Figure 2.23: Internal configuration of the Unmanned Underwater Glider [59]

2.4 Hydrodynamic Model

Hydrodynamic effect cannot be ignored as it is significant in the dynamics of an underwater glider [64]. The hydrodynamics on the underwater glider are similar to the aerodynamics of an aircraft [65], [68]. As the relative density of water is higher than the air, the hydrodynamic forces play a major role in the velocity of the glider and gliding motion. The hydrodynamic coefficients are a function of the angle of attack, i.e., the angle between the velocity vector and the body axis along with the bow of the underwater glider [72]. There are three hydrodynamic coefficients, namely drag coefficients, lift coefficients and moment coefficients as summarized in Table 2.2 [65]. The hydrodynamic coefficients are influenced by the structure of the wings and rudder.

Table 2.2: Hydrodynamic Coefficients [65]

Parameters	Description
K_{D0}	Drag Coefficient
K_D	
K_{L0}	Lift Coefficient
K_L	
K_{M0}	Moment Coefficient
K_M	

A few techniques are available to evaluate hydrodynamic coefficients such as Computational Fluid Dynamics (CFD) simulation, wind tunnel test, towing tank test and parametric model. CFD simulation is widely used to identify the hydrodynamic coefficients at various angles of attack. In CFD, the CAD model of an underwater glider with appropriate boundary values is used to determine the fluid flow and pressure circulation around the glider body [31], [68]. Yogang Singh et al. [31] compared towing tank experimental data with CFD simulation data at various towing speeds and angles of attack, and found that the experimental results were almost identical to the simulation data.

2.4.1 CFD and Towing Tank Simulation

The UTP glider was simulated using Ansys Fluent software to analyze the fluid phenomena with the $k-\varepsilon$ SST turbulence model along with Reynolds number in the range of 1×10^5 to 1×10^6 . The grid size ranged from 4×10^6 - 4.5×10^6 was fixed to establish the hydrodynamic parameters [73]. The drag and lift forces were evaluated with various Fraude numbers (Fr).

The fluid property ‘Fraude numbers (Fr)’ are the function of the top width of the fluid surface ‘ D_f ’, distance from plain water surface level ‘ h ’, ‘ g ’ is gravity force as shown by Equation 2.1, where ‘ V_f ’ is fluid’s velocity [78].

$$Fr = V_f / \sqrt{(gh/D_f)} \quad (2.1)$$

The rotational motion of the vehicle can be simulated by altering the flow of inlet velocity ‘ V_{inlet} ’ to achieve the appropriate circumferential velocity in specified radius ‘ R ’ as expressed in Equation 2.2, where ‘ q_f ’ is the angular velocity of the flow [73].

$$q_f = V_{inlet}/R \quad (2.2)$$

A tow tank test was conducted to evaluate the CFD simulation results. The fluid domain size (2 L_{inlet} x 4 L_{outlet} x 8 D side-wall) was defined by referring to the International Towing Tank Conference (ITTC) specifications as shown in Figure 2.24.

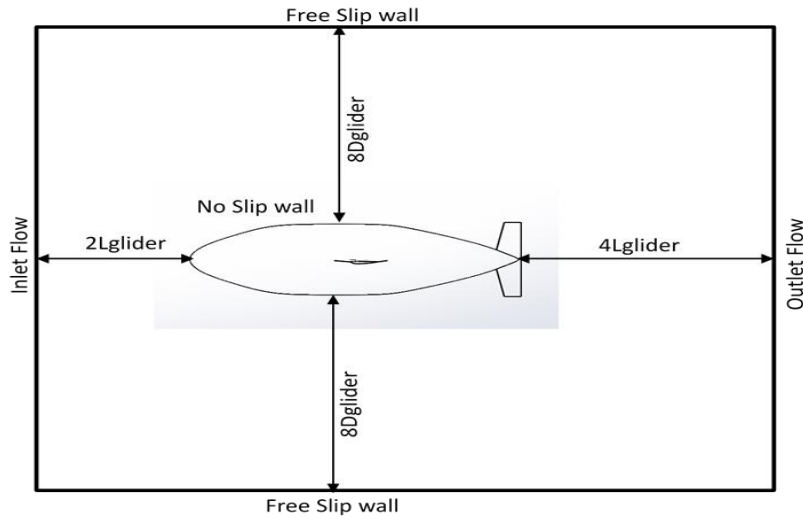
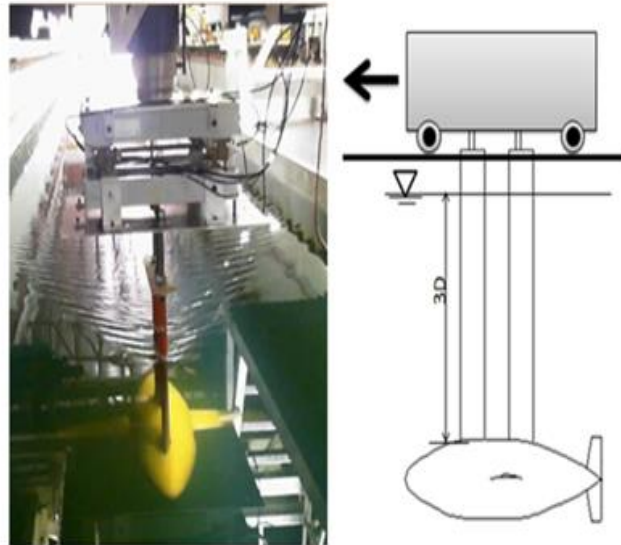


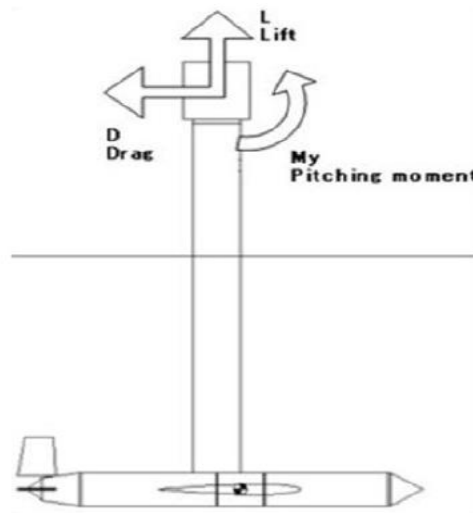
Figure 2.24: Fluid domain simulation around the glider [73]

The hydrodynamic data were acquired while the carriage towed the glider in water as shown in Figure 2.25. During the test, the drag force ‘ D ’ was opposite to the resistance force of the glider in the horizontal plane. The lift force ‘ L ’ acted opposite to the gravitational force in the vertical plane.

By referring to data obtained by Javaid [73], towing tank test produced less than 10% of drag and lift forces error compared to the CFD simulation. Moreover, the drag force increases by increasing the Fraude numbers (Fr) as shown in Table 2.3.



(a) Towing tank test and schematic of the UTP glider [73]



(b) Direction of hydrodynamic force and moment [31]

Figure 2.25: Towing tank test

Table 2.3: Drag Force against Froude Numbers [73]

Fr	CFD	Experimental	Error
0.33	0.577494	0.563013	2.50
0.55	1.393193	1.315216	5.59
0.77	2.617866	2.471175	5.60
1.10	4.962295	5.305635	6.91

2.5 Overview of the Simulink Model

Referring to Zhou [81], the glider's motions can be simulated through the Simulink model as shown in Figure 2.26. It is used to determine the glider's roll angle and roll rate to evaluate the performance of the roll control mechanism. The roll is achieved by shifting the 1 kg trim mass, which displaces the CG from the left and right along the 'y' axis direction.

The integrator and constant gain are applied to simulate the roll performance. The constant gain is substituted with the corresponding kinematic coefficients which derive the roll motion of the glider. The model produces output over a specified time.

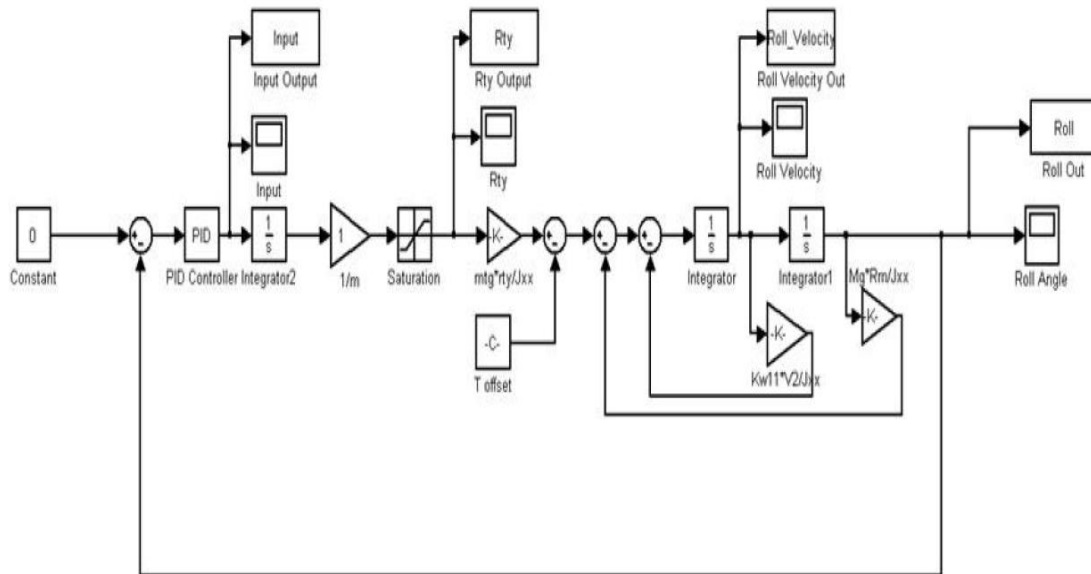


Figure 2.26: Simulink model for the motion of the underwater glider [81]

2.6 Summary

This section summarizes the existing pitch and roll control mechanisms of the underwater gliders. In addition, the shape, total size, weight and relevant configurations of the glider are elaborated.

Gliders move in a saw tooth motion by controlling their pitch angle. The pitch angle is achieved by shifting the center of gravity of the glider and by moving an internal mass linearly. When the glider reaches a predetermined depth, the glider pitches upwards by pumping water out from the ballast tank and shifting the internal moving mass toward the tail of the glider [59]. Underwater gliders, therefore, use a buoyancy engine and moveable mass as a coupled mechanism in the pitch control module. It can make a right or left turning motion or rotational movements along with sway axis by shifting the center of gravity from left to right or vice versa [7]. Roll motion is achieved by shifting the movable mass with the glider body rotating accordingly. CFD simulation and towing tank experiments were previously performed to determine the hydrodynamic behavior of the underwater glider. The hydrodynamic data obtained were used for pitch and roll moment analysis. In addition, the Simulink model was built by referring to the mathematical equation to evaluate the motion of the glider. However, it was found that there were constraint to the existing glider models as follows:

- The design of the glider with multiple control mechanisms caused its size and mass to increase which could affect the performance of the underwater glider in the water.
- Conventional coupled control mechanism as a buoyancy engine complicated the gliding motions.
- Glider without a roll control module was restricted to pitching motion only.
- Previous studies on the comparison between simulation and experimental data to evaluate the performance of the underwater glider are scarce.

CHAPTER 3

METHODOLOGY

3.1 Chapter Overview

This chapter describes the approach used to conduct this research. The process flow of this study is presented in Section 3.2. The mathematical equations which represented the dynamics and the motion of the underwater glider are derived in Section 3.3, and the underwater glider's pitch and roll responses were determined through the Simulink model as shown in Section 3.4. Section 3.5 presents the overview and the exterior design of the UTP underwater glider. Section 3.6 describes the experimental setup and testing details such as key components, control modules, processing module and control architecture. Finally, Section 3.7 is a summary of this chapter.

3.2 Flow Chart of Research Methodology

The glider's pitch and roll motions were controlled by the water pump system. Figure 3.1 depicts the process flow of this research, along with the adopted methods to validate the developed control mechanisms.

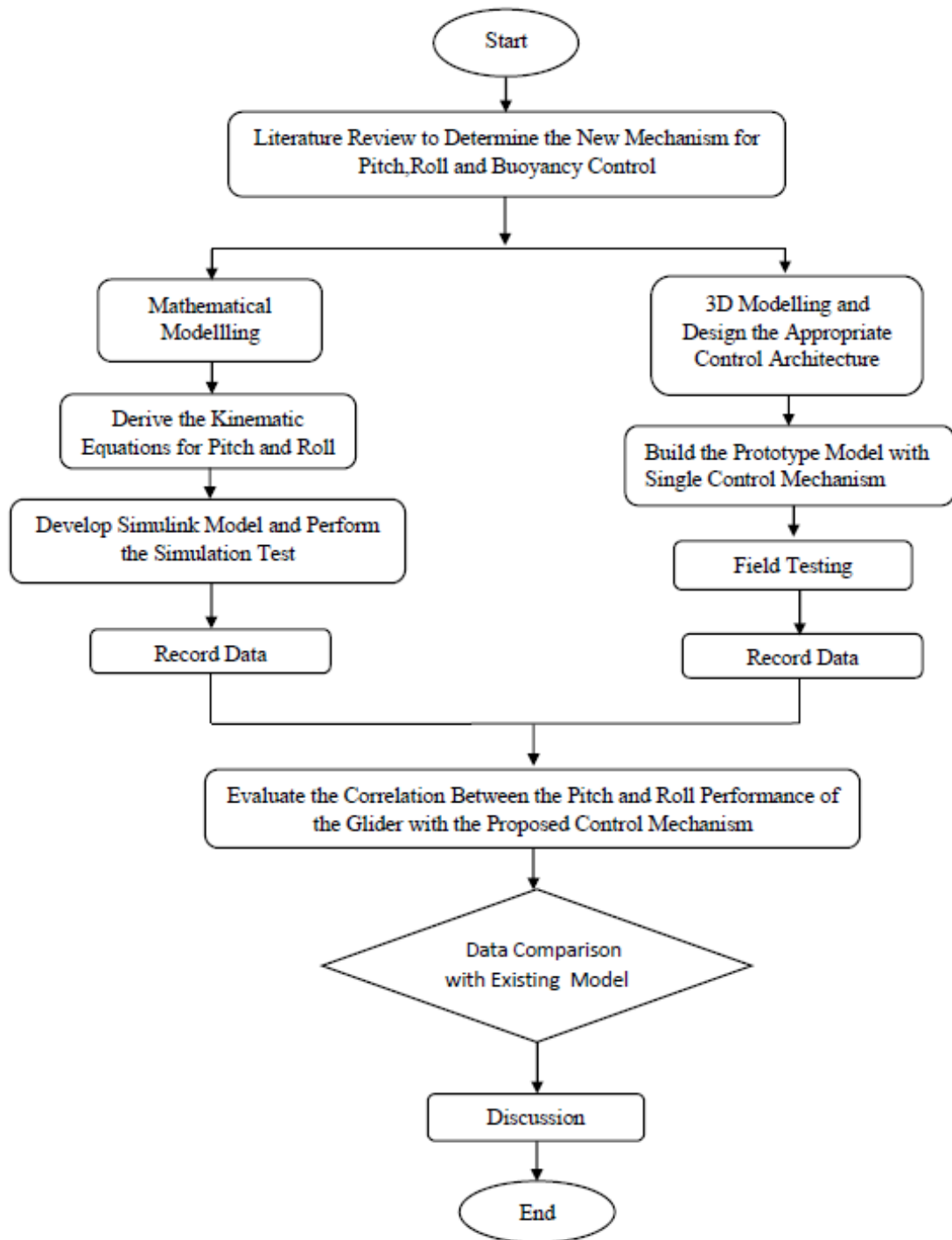


Figure 3.1: Flow chart of research methodology

3.3 Mathematical Model

A mathematical model was used to model the dynamic characteristics of the glider based on its structure. Graver et al. derived the dynamic equations of an autonomous underwater glider based on a nonlinear controller to regulate its motion [57]. Dynamic equations were applied to describe the nonlinear coupling between the vehicle and the internal actuators. The pitch and roll control systems were designed by considering the glider's six degree of freedom (DOF) equations, mass distribution and moment equations, dynamics equations and hydrodynamic terms.

It is essential to determine the appropriate coordinate system prior to constructing these dynamic equations to determine the working principle of the applied force and moments. There are three coordinate systems, namely the Earth Fixed coordinate system, Body Fixed coordinate system and Stream coordinate system. The origin for earth frame (X, Y, Z) is denoted as E_0 . The body frame 'o' is fixed on the geometric center of the glider, while 'x' is in the forward direction of the vehicle, 'y' axis points towards the wings and the direction of the 'z' axis is determined by the right-hand rule and points downwards towards the gravitational force as shown by Figure 3.2. The stream coordinate systems consist of hydrodynamic forces and torques.

An underwater glider can move independently in water through translational movement in the forward/backward direction along the x -axis (surge), in the up/down direction along the z -axis (heave), and along left/right y -axis direction (sway) as well as the rotational movement of yaw, pitch, and roll motions as shown in Figure 3.2.

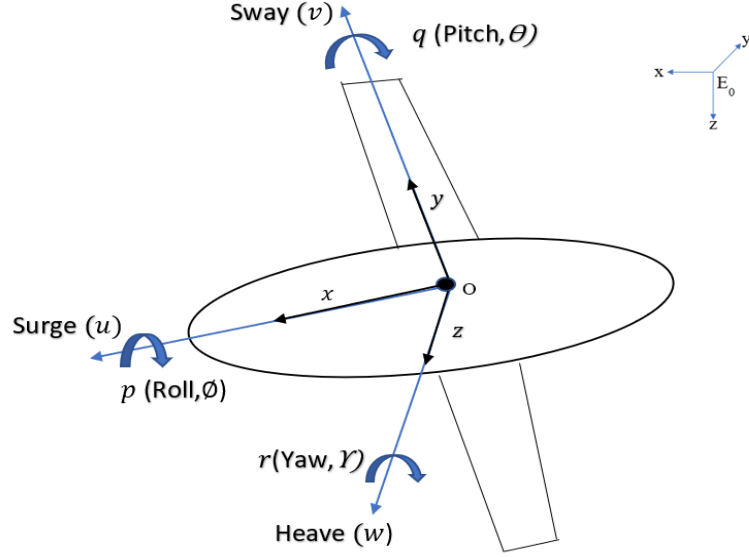


Figure 3.2: References coordinate frame of the underwater glider

3.3.1 Six DOF Equations

These translational and rotational motions were derived through the six DOF equations by referring to the glider's body fixed coordinate system. In Equation 3.1, u, v, w and p, q, r are the respective linear and angular speed components along the x, y, z axes. X, Y, Z and K, M, N are the external forces and moments on the glider, respectively [59], [83].

$$m\dot{u} - vr + wq - x_G(q^2 + r^2) + y_G(pq + \dot{r}) + z_G(pr + \dot{q}) = X$$

$$m\dot{v} - wq + ur - y_G(r^2 + p^2) + z_G(qr + \dot{p}) + x_G(pq + \dot{r}) = Y$$

$$m\dot{w} - uq + vp - z_G(p^2 + q^2) + x_G(pr + \dot{q}) + y_G(qr + \dot{p}) = Z$$

$$J_{xx}\dot{p} + (J_{zz} - J_{yy})qr - J_{yz}(q^2 - r^2) + J_{xy}(pr - \dot{q}) - J_{zx}(pq + \dot{r}) + m[y_G(\dot{w} - uq + vp) - z_G(\dot{v} - wp + ur)] = K$$

$$J_{yy}\dot{q} + (J_{xx} - J_{zz})pr - J_{zx}(r^2 - p^2) + J_{yz}(pq - \dot{r}) - J_{xy}(qr + \dot{p}) + m[z_G(\dot{u} - vr + wq) - x_G(\dot{w} - uq + vp)] = M$$

$$J_{zz}\dot{r} + (J_{yy} - J_{xx})pq - J_{xy}(p^2 - q^2) + J_{zy}(qr - \dot{p}) - J_{yz}(pr + \dot{p}) + m[x_G(\dot{v} - wp + ur) - y_G(\dot{u} - vr + wq)] = N \quad (3.1)$$

3.3.2 Mass Distribution Equations

Figure 3.3 illustrates the mass distribution of the glider. In Equation 3.2, m_{total} is the total glider mass, where m_h is the glider hull mass, m_w is the point mass to the fixed centre of gravity and buoyancy and m_b is the variable ballast mass with respect to geometry center (CG). Furthermore, m_o is the additional mass after eliminating the displaced water mass/trim mass m_t as shown in Equation 3.3. These mass equations are significant to define the buoyancy condition of the glider; where if m_o is positive, the glider is in neutrally buoyant state and vice versa [32], [86].

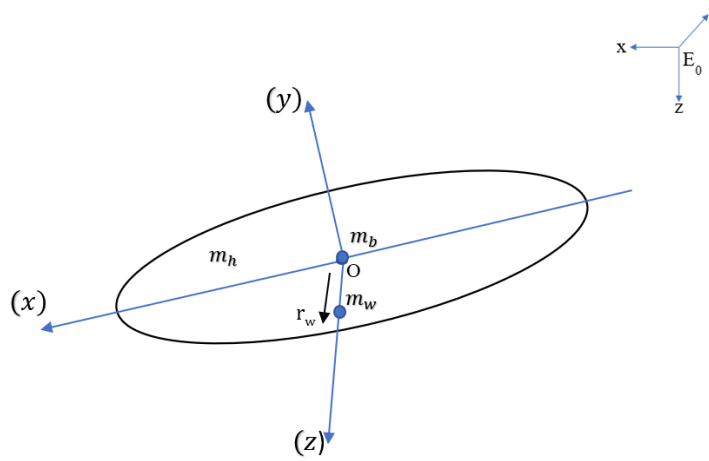


Figure 3.3: Internal mass distribution frame

$$m_{total} = m_h + m_w + m_b \quad (3.2)$$

$$m_o = m_{total} - m_t \quad (3.3)$$

The glider's linear displacement can be derived by referring to Newton's second law as shown in Equation 3.4; where, M is the sum of glider's mass including total glider mass (m_{total}) and added mass (M_A) matrix [65].

$$F = \frac{dMv_i}{dt} = M \frac{dv_b}{dt} + \omega_b \times Mv_b \quad (3.4)$$

$$M = m_{total} + M_A \quad (3.5)$$

3.3.3 Moment Equations

The hydrostatic righting moment defines the influence of the glider's weight on its pitch and roll moments. Thus, the glider's Center of Gravity (CG) and Center of Buoyancy (CB) are not coinciding in the 'Z' axis, torque is produced and causes the glider to make the corresponding righting moments [28]. Equation 3.6 shows the torque equation, referred to Newton's 2nd law of motion ($F = ma$); where, τ is torque, J is the moment of inertia and α_a is the angular acceleration of the underwater glider.

$$\tau = J\alpha_a \quad (3.6)$$

The total pitch/roll moments were obtained by summing up the hydrostatic moment, added mass and drag coefficients as given in Equation 3.7 [81]. A hydrostatic moment τ_{hydro} is generated by the buoyancy force and total weight of the glider [28]. The wings and fins result in a rolling drag τ_{drag} and the rolling added mass τ_{AM} is the mass of the displaced water. The added mass can be obtained from the multiplication of the rolling added mass coefficient $K_{\dot{p}}$ and the roll angular acceleration, \dot{p} . In Equation 3.10, K_{pp} is the rolling quadratic drag coefficient and p is the roll angular velocity [28].

$$\Sigma\tau = (\tau_{hydro} + \tau_{AM} + \tau_{drag}) \quad (3.7)$$

$$\tau_{hydro} = m_t \cdot g \cdot r_{ty} \cos \phi - m_t \cdot g \cdot r_{tz} \sin \phi - (m_{total} - m_t) \cdot g \cdot r_z \sin \phi \quad (3.8)$$

$$\tau_{AM} = K_{\dot{p}} \dot{p} \quad (3.9)$$

$$\tau_{drag} = K_{pp} p |p| \quad (3.10)$$

3.3.4 Dynamics Equations of Motion

According to Zhou [81], the geometric relationship between the earth fixed coordinate (E-frame) and body fixed coordinate (B-frame) can be obtained by the rotational matrix R_{EB} . The rotational matrix R_{EB} can be obtained by multiplying rotation matrices, R_ϕ (roll), R_θ (pitch), and R_γ (yaw).

$$R_\phi = \begin{bmatrix} 1 & 0 & 0 \\ 0 & \cos \phi & \sin \phi \\ 0 & -\sin \phi & \cos \phi \end{bmatrix} \quad (3.11)$$

$$R_\theta = \begin{bmatrix} \cos \theta & 0 & -\sin \theta \\ 0 & 1 & 0 \\ \sin \theta & 0 & \cos \theta \end{bmatrix} \quad (3.12)$$

$$R_\gamma = \begin{bmatrix} \cos \gamma & \sin \gamma & 0 \\ -\sin \gamma & \cos \gamma & 0 \\ 0 & 0 & 1 \end{bmatrix} \quad (3.13)$$

$$R_{EB} = \begin{bmatrix} \cos \gamma \cos \theta & \sin \gamma \cos \theta & -\sin \theta \\ -\sin \gamma \cos \theta + \cos \gamma \sin \phi \sin \theta & \cos \gamma \cos \theta + \sin \phi \sin \theta \sin \gamma & \cos \theta \sin \phi \\ \sin \gamma \sin \phi + \cos \gamma \cos \phi \sin \theta & -\cos \gamma \sin \phi + \sin \theta \sin \gamma \cos \phi & \cos \theta \cos \phi \end{bmatrix} \quad (3.14)$$

The linear displacement and angular velocity of the glider with respect to the Earth Fixed Coordinate system is denoted as $v_e = [x, y, z]^T$ and $\omega_e = [\dot{\phi}, \dot{\theta}, \dot{\gamma}]^T$ as well as linear velocity and angular velocity of the glider with respect to the Body Fixed Coordinate is denoted as $v = [v_x, v_y, v_z]^T$ and $\omega = [\omega_x, \omega_y, \omega_z]^T$ [32], [86]. The glider's velocity given in vector form 'V' is shown in Equation 3.15. The linear velocity ' v_b ' and angular velocity ' ω_b ' of the glider with respect to the body frame in vertical planes are defined as in Equation 3.16-3.17 [32].

The mathematical expression of the motion of the glider with respect to the earth fixed coordinate system and body fixed coordinate system is shown in Equation 3.18.

The summation of body fixed coordinate and earth fixed coordinate systems gives linear velocity as shown in Equation 3.19 as well as Equation 3.20 for angular velocity of the glider.

$$V = [v \quad \omega] \quad (3.15)$$

$$v_b = [v_x \quad 0 \quad v_z] \quad (3.16)$$

$$\omega_b = [0 \quad \omega_y \quad 0] \quad (3.17)$$

$$\dot{V}_e = R_{EB}^T \cdot v_b \quad (3.18)$$

$$\begin{bmatrix} \dot{x} \\ \dot{y} \\ \dot{z} \end{bmatrix} = R_{EB}^T \cdot \begin{bmatrix} v_x \\ 0 \\ v_z \end{bmatrix} \quad (3.19)$$

$$\omega_e = \begin{bmatrix} \dot{\phi} \\ \dot{\theta} \\ \dot{\gamma} \end{bmatrix} = \begin{bmatrix} 1 & 0 & -\sin \theta \\ 0 & \cos \phi & \cos \theta \sin \theta \\ 0 & -\sin \phi & \cos \theta \cos \phi \end{bmatrix}^{-1} \begin{bmatrix} 0 \\ \omega_y \\ 0 \end{bmatrix} \quad (3.20)$$

According to Zhang et al. [34], the dynamic model and the external forces acting on the glider can be simplified by modifying it to the motion along the longitudinal plane. Figure 3.4 illustrates the forces and moments acting on the glider body. The drag force ' D ' acting in the opposite direction of the velocity vector ' V ' and lift force ' L ' is perpendicular to the velocity vector ' V ' [32], [68]; where, ' α ' is the angle of attack and ' θ_g ' is the gliding angle. The pitch angle ' θ ' can be obtained by adding both gliding and attack angles as in Equation 3.22. The sideslip angle ' β ' is shown in Equation 3.23.

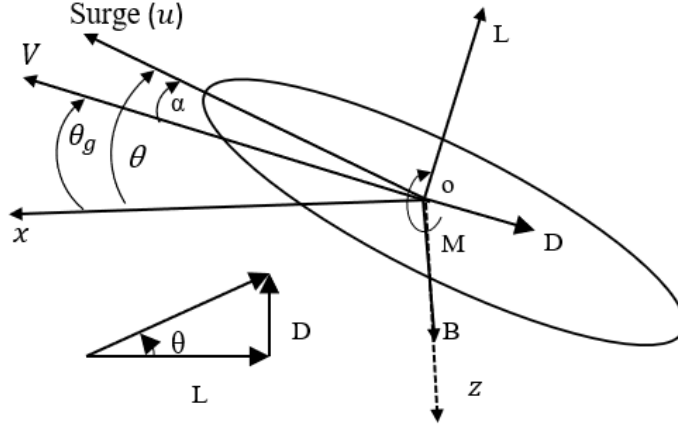


Figure 3.4: References frame for the forces and moments on the glider body [32]

$$\alpha = \tan^{-1}\left(\frac{v_z}{v_x}\right) \quad (3.21)$$

$$\theta = \theta_g + \alpha \quad (3.22)$$

$$\beta = \sin^{-1}\left(\frac{v_y}{v}\right) \quad (3.23)$$

During the pitch motion analysis, the momentum principles along the vertical plane must be taken into account. These applied momentum properties and control forces acting on point masses in the vertical plane are derived as shown in Equations 3.24-3.27. Both forces are zero in 'y' axes, as there is no action in a particular direction [32], [72]. Javaid et al. [32] described that the flow rate of fluid to the ballast tank depends on the control input u_4 shown in Equation 3.28.

$$P_p = (P_{px} \quad 0 \quad P_{pz}) \quad (3.24)$$

$$\bar{u} = (u_x \quad 0 \quad u_z) \quad (3.25)$$

$$\dot{P}_{px} = u_x \quad (3.26)$$

$$\dot{P}_{pz} = u_z \quad (3.27)$$

$$\dot{m}_b = u_4 \quad (3.28)$$

The simplified motion equations along the longitudinal plane re-written from [65] are shown in Equations 3.29-3.30. Equations 3.31 and 3.32 represent the glider's velocity along 'x' axes and 'y' axes, respectively

$$\dot{x} = v_x \cos \theta + v_z \sin \theta \quad (3.29)$$

$$\dot{z} = -v_x \sin \theta + v_z \cos \theta \quad (3.30)$$

$$\dot{\theta} = \omega_y \quad (3.31)$$

$$v_x = \frac{1}{m_t} (-m_t \cdot v_z \cdot \omega_y - m_o g \sin \theta + L \sin \alpha - D \cos \alpha) \quad (3.32)$$

$$v_z = \frac{1}{m_t} (-m_t \cdot v_x \cdot \omega_y - m_o g \cos \theta - L \cos \alpha - D \sin \alpha) \quad (3.33)$$

$$\omega_y = \frac{1}{J_y} (M - m_w \cdot g r_w \sin \theta \cdot \omega_y) \quad (3.34)$$

3.3.4.1 Buoyancy Equations

Buoyancy can be derived by the motion equations [91] in polar coordinates as shown by the nonlinear dynamics Equations 3.35-3.38. 'V' represents the total velocity vector of the glider with respect to gliding angle ' θ_g '. The total inertia generated in the y-axis is ' J_y '. Equations 3.39-3.44 reflect the equilibrium condition of underwater glider [72].

$$\dot{V} = -\frac{1}{m} (m_o g \sin \theta_g + D) \quad (3.35)$$

$$\dot{\theta}_g = \frac{1}{mV} (-m_o g \cos \theta_g + L) \quad (3.36)$$

$$\dot{\alpha} = \omega_y - \dot{\theta}_g \quad (3.37)$$

$$\dot{\omega}_y = \frac{1}{J_y} (K_{M0} + K_M \alpha + K_{q2} \omega_y) V^2 \quad (3.38)$$

$$\dot{\theta}_e = \tan^{-1} \left(\frac{-K_{De}}{K_{Le}} \right) \quad (3.39)$$

$$\dot{\alpha}_e = \tan^{-1}\left(\frac{-K_{Mo}}{K_M}\right) \quad (3.40)$$

$$\dot{\omega}_{ye} = 0 \quad (3.41)$$

$$V_e = \left(\frac{m_o g}{\sqrt{(K_{De}^2 + K_{Le}^2)}}\right)^{1/2} \quad (3.42)$$

$$K_{De} = (K_{D0} + K_D \alpha_e^2) \quad (3.43)$$

$$K_{Le} = (K_{L0} + K_L \alpha_e) \quad (3.44)$$

3.3.4.2 Kinematics Equation of Motions

In this study, the kinematic equations were derived to determine the pitch and roll performance of the UTP glider through a Simulink model. The pitch and roll angle is zero when the glider is in equilibrium condition. Zhou [81] stated that the pitch and roll motions can be determined by referring to the conservation law of angular momentum [81].

By referring to the roll characteristics, these roll angle and rate were the key factors to evaluate the roll performance of the underwater glider. Figure 3.5 shows the acting forces on the glider during the roll motion, and the roll angle ' \emptyset ' is defined as in Equation 3.45. Furthermore, the roll rate ' p ' can be determined by integrating four terms in Equation 3.47 [81]. The hydrodynamic non-linear terms in the steady state equation can be linearized as $\cos \emptyset = 1$, $\sin \emptyset = \emptyset$, $\arctan(r_{mz} / r_{my}) = r_{mz} / r_{my}$ and $M_{DL1} = K_{q1} p V^2$ [81]; where, the velocity vector ' V ' was assumed as 0.55 m/s to solve the pitch and roll motions of the glider. The trim weight can be determined by integrating the division of trim weight inertia ' pt ' and trim mass ' m_t ' as shown in Equation 3.48, where ' pt ' can be determined by integrating the input of the mechanism ' u ' as shown in Equation 3.49.

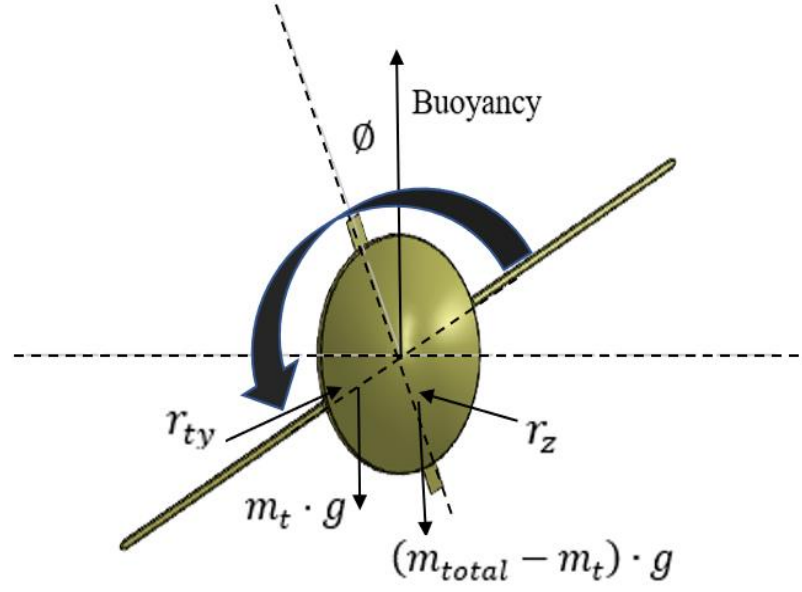


Figure 3.5: Front view of the UTP glider

$$\dot{\phi} = p \quad (3.45)$$

$$J_{xx}\dot{p} = m_t \cdot g \cdot r_{ty} \cos \phi - (m_{total} - m_t) \cdot g \cdot r_z \sin \phi + D_e + M_{DL1} \quad (3.46)$$

$$\dot{p} = 1/J_{xx} (m_t \cdot g \cdot r_{ty} - (m_{total} - m_t) \cdot g \cdot r_z \cdot \phi + D_e + K_{q1}pV^2) \quad (3.47)$$

$$\dot{r}_{ty} = p_t/m_t \quad (3.48)$$

$$\dot{p}_t = u \quad (3.49)$$

The same kinematic equation can be used for pitch rate ‘ q ’ determination by referring to the pitch components where the parameters were the same, except for the added pitch moment inertia (M_{DL2}) and moment of inertia (J_{yy}). Table 4.1 show, the parameters of the UTP underwater glider obtained through the CAD model simulation and these hydrodynamic coefficients were determined via CFD simulation.

Table 3.1: Parameters of the UTP Glider

Parameters	Description	Values
m_{total}	Total Glider Mass	37.7 kg
J_{xx}	Moment of Inertia 'x' axis	0.7026 kg·m ²
J_{yy}	Moment of Inertia 'y' axis	4.507 kg·m ²
m_t	Trim Mass	4.8 kg
g	Gravity	9.81
r_z	CG respect to CB	-10 mm
K_{q1}	Hydrodynamic Coefficient	-20 kg.s/rad ²
K_{q2}	Hydrodynamic Coefficient	-60 kg.s/rad ²
M_{DL1}	Added Roll Moment Inertia	-6.05
M_{DL2}	Added Pitch Moment Inertia	-18.15

3.3.5 Hydrodynamic Model

Hydrodynamic impact on the underwater glider must be considered to evaluate the performance of the glider in water. It can be affected by the gliding speed and the gliding path. The hydrodynamic equations are derived based on Computational Fluid Dynamics (CFD) simulation to determine the hydrodynamic properties of the underwater glider used in the dynamic simulation [31], [73]. The drag and lift forces are modeled as in Equations 3.50 and 3.51, which is the function of the angle of attack and gliding velocity of the glider [72]. Where hydrodynamic drag coefficients are denoted as ' K_{D0} ' and ' K_D '. By the way, ' K_{L0} ' and ' K_L ' are related to the lift forces and ' V ' as the magnitude of the velocity referred to the body frame [72], [65].

$$L = (K_{L0} + K_L \alpha) V^2 \quad (3.50)$$

$$D = (K_{D0} + K_D \alpha^2) V^2 \quad (3.51)$$

By referring to Zhou [81], the added roll moment inertia (M_{DL1}) and the added pitch moment inertia (M_{DL2}) are described in Equations 3.52-3.53. These ' K_{m0} ' and ' K_m ' are the moment coefficients with the magnitude of the velocity ' V ' as stated in the equation below.

$$M_{DL1} = (K_m\beta + K_{q1}p)V^2 \quad (3.52)$$

$$M_{DL2} = (K_{m0} + K_m\alpha + K_{q2}q)V^2 \quad (3.53)$$

The hydrodynamic coefficients, fluid force and pressure acting on the glider can be evaluated through CFD simulation [31]. Therefore, associated hydrodynamic coefficients for the UTP underwater glider were determined through the CFD simulation modeling and validated with towing tank tests [73].

3.4 Simulink Model

Referring to [81], the Simulink model as shown in Figure 3.6 was developed to solve the dynamic of the UTP glider. The kinematics (Equations 3.45-3.47) were used to determine both pitch and roll performances (angle and rate of change). The PID control gain was applied to the Simulink model to determine the appropriate pump flow rate to achieve the desired pitch and roll rates.

In this study, four different pump rates (2.5LPM, 5LPM, 7.5LPM and 10LPM) were considered to evaluate the pitch and roll performances of the glider. These pump rates, in multiples of the base pump rate, were chosen to compare the performance with the base pump.

The developed pitch and roll control modules use water as trim mass. The total glider's mass includes trim mass signified as ' m_{total} ' which is significant to obtain the desired pitch and roll angles during the simulation test. The water ratios in the front/rear and left/right water bladders were pre-set to 1.2:1.2 liters for the neutrally buoyant state

as the imbalance conditions of the water ratios could affect the equilibrium conditions of the glider. The ratios were validated through the experimental test to evaluate the function of the developed Simulink model.

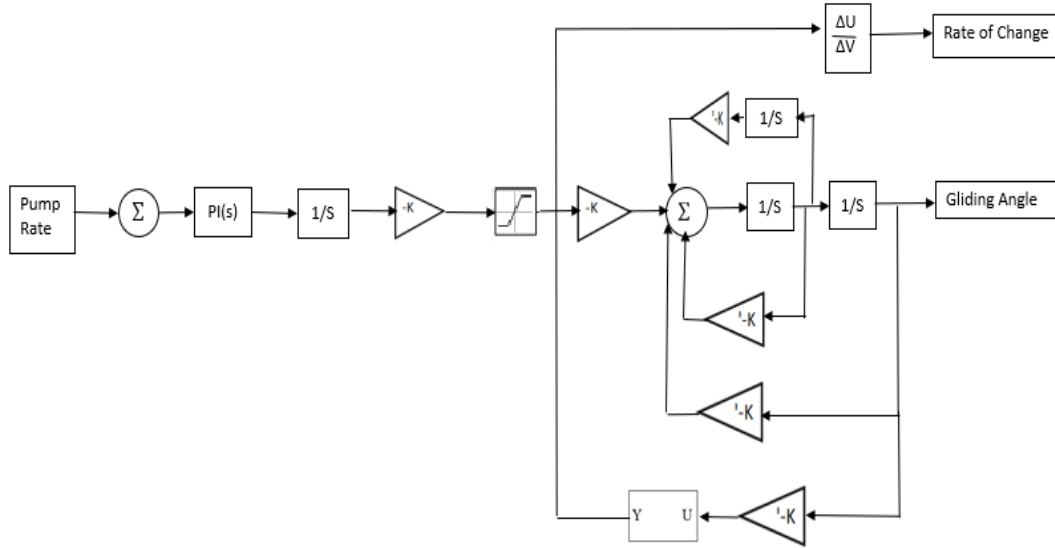


Figure 3.6: Simulink model to simulate the pitch and roll performances for a given pump flow rate

3.5 Design Overview

The 3D CAD model of the UTP glider was designed through Solidworks software as shown in Figure 3.7. The prototype was built using fiberglass, which has better seakeeping capability. It was 1.04 m in length and has an internal hull in an elliptical shape with a diameter of 0.2 m and weight of 26.7 kg. The total mass after assembly was 37.7 kg. The glider has NACA0012 wing profile and a rudder to stabilize the gliding motion as well as to convert vertical movement to horizontal motion [86].

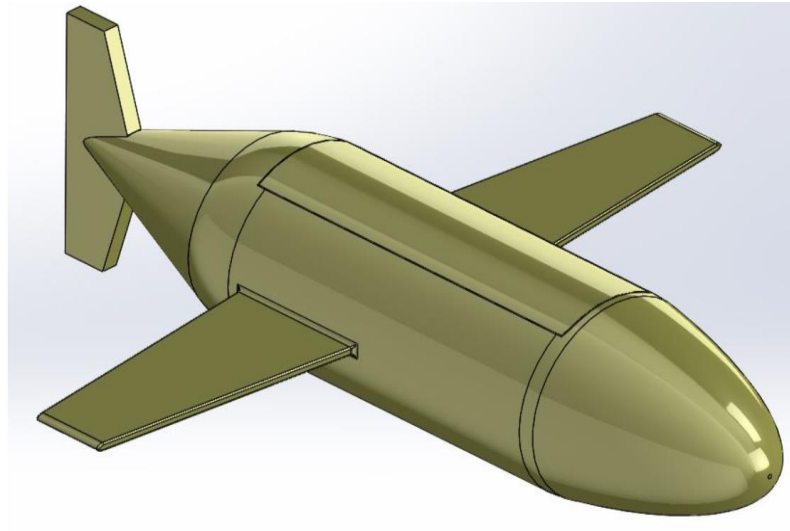


Figure 3.7: CAD model of the UTP underwater glider

3.6 Experimental Setup and Application of Control Modules

The assembly of the UTP glider is shown in Figure 3.8. The fabrication and standard components were used to build the glider with a single actuation system and water bladders instead of a ballast tank and linear actuator, to control pitch and buoyancy as well as roll individually.

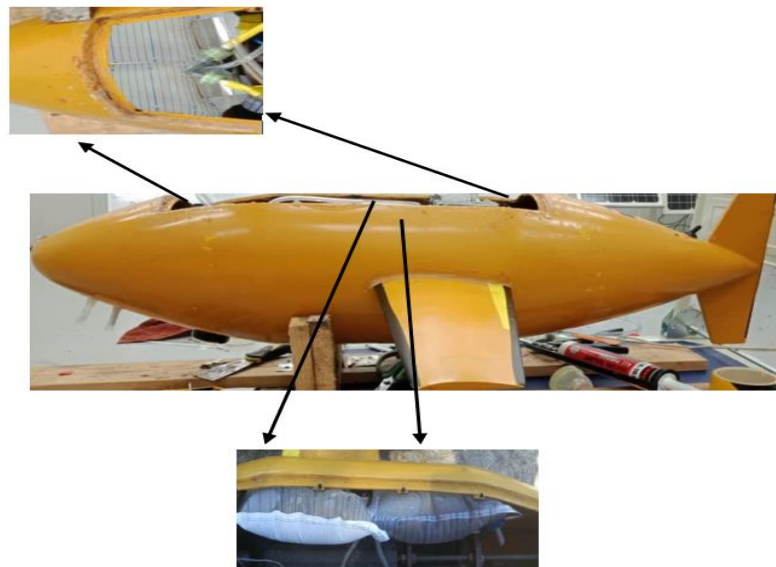


Figure 3.8: Experimental setup of the UTP glider

The control mechanisms and related electronic components were assembled in the hull of the glider as shown in Figure 3.9. Three different control modules were employed, such as pitch control, roll control and a processing module. Each control module was developed with individual components. Both pitch and roll control modules were connected to the processing module.

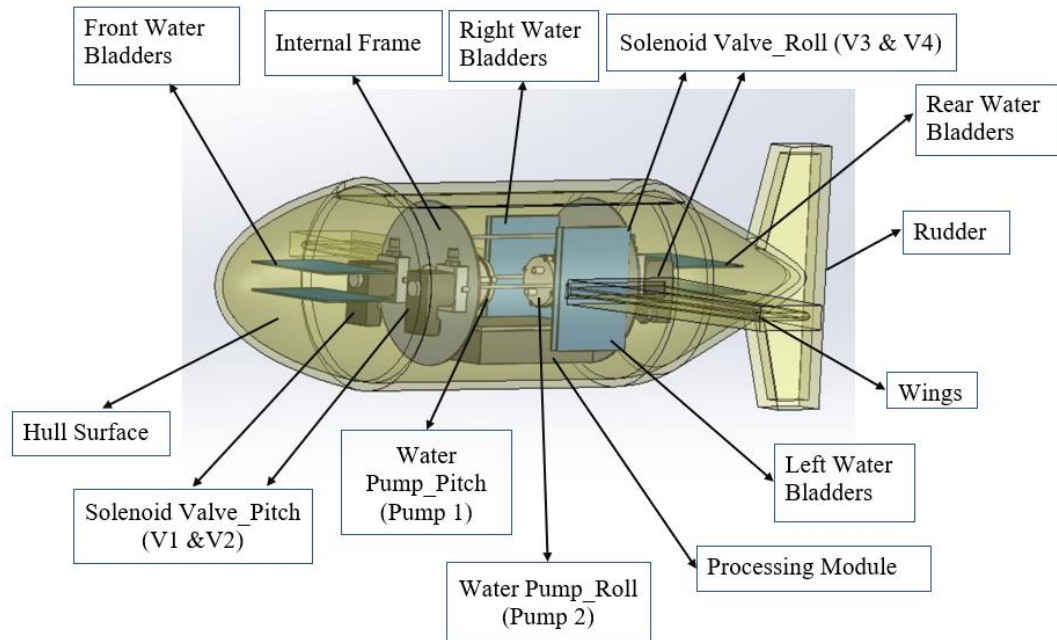


Figure 3.9: Overview of the UTP underwater glider

3.6.1 Key Components

Both Pump 1 and 2 (Figure 3.9) were the same model of DQB415-SB liquid pump as depicted in Figure 3.10. The pump was small in size and mounted on the internal frame. It was powered by a 12V DC power supply and can transfer fluids up to 2.5 LPM. The pump rotated alternately between clockwise (CW) or counter-clockwise (CCW) by changing the motor driver signal accordingly.



Figure 3.10: Water pump_ DQB415-SB

Table 3.2: Water pump specifications

Specification	
Length	90.7 ± 1.0 mm
Width	39.3 ± 0.5 mm
Weight	100g
Rated Voltage	12VDC
Flow Rate	2.5 LPM
Transfer Medium	Water
Environment	5°C - 95°C

In this study, water bladders were used instead of a ballast tank. The water bladder (Figure 3.11) was PVC type which can accommodate up to 2 L of water. It weighed 66g and flexible to be located on the hull surface.



Figure 3.11: Water Bladder

FEELBACH K222 solenoid valves weighing 0.21 kg were applied to control the amount of water in the water bladders. Initially, the solenoid valve was in a normally closed (NC) state and required 12 VDC to trigger the internal plunger enabling the flow of water with maximum pressure of 20 bar.



Figure 3.12: FEELBACH solenoid valve

Figure 3.13 shows the Arduino Mega 2560 with an ATmega 2560 eight-bit microcontroller with 54 digital input/output pins. It is compact with the dimensions of 102 x 53 mm and powered by a 12V power supply. Arduino is used to communicating with other electronic devices such as pressure sensor, motor driver, IMU unit and shield data logger.

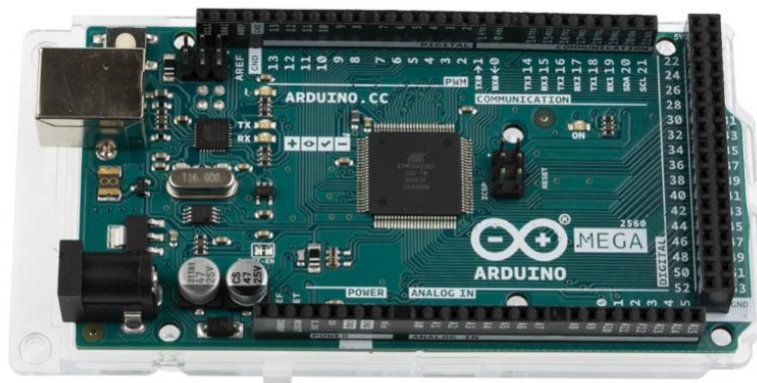


Figure 3.13: Microcontroller_Arduino Mega 2560

Figure 3.14 depicts the ‘Honeywell’ (PX2EF1XX030PAAAX) pressure sensor which can operate with an input voltage of 5 V. It is typically used to sense the pressure on the body of the submerged vehicle in the pressure range of 0 to 30 psi with an accuracy of $\pm 0.25\%$.



Figure 3.14: Honeywell pressure sensor

Meanwhile, the MPU6050 IMU shown in Figure 3.15 was used to detect the motion of the underwater glider with an input voltage of 3.3 V. The IMU was integrated with 3-axis of accelerometer and 3-axis gyroscope on a single chip. Gyroscope was used to measure the rotational velocity or rate of changes over time along the x, y, z axes, and the angular position can be calculated by integrating the rate of changes. An accelerometer was used to measure the gravitational acceleration along the x, y, z axes, and the corresponding angle can be calculated by applying trigonometric calculations.

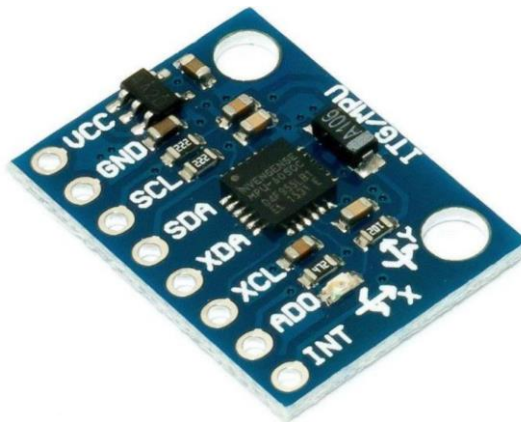


Figure 3.15: MPU6050 IMU

Figure 3.16 exhibits the MD-L298 motor driver which was programmed to communicate between Arduino control board and water pumps. The driver was powered by a 12 V power supply and was connected to the Arduino to transmit 12 V as an input voltage to the actuator. Furthermore, the pump rotation can be alternated by changing the input signals (INn).

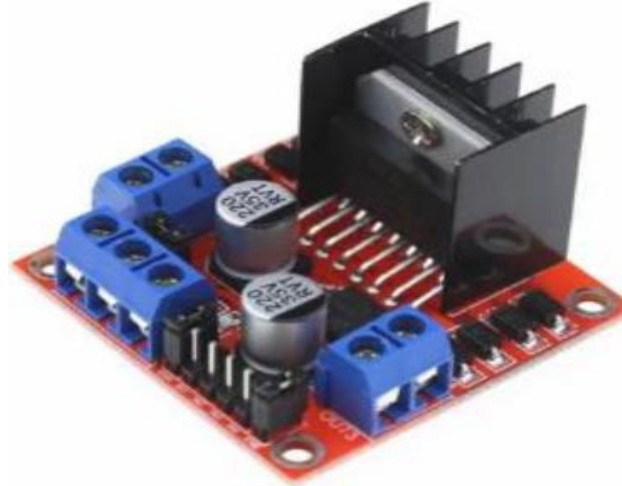


Figure 3.16: Motor driver_MD-L298

3.6.2 Pitch Control Module

The ascent and descent of the glider were controlled by adjusting the center of gravity and the buoyancy, respectively. The key components in the pitch control module were water bladders, solenoid valves (V1 and V2), water pump 1 and related hydraulic fittings. Each section of the front and rear hull was equipped with two water bladders and both sides were filled with an equal amount of water when neutrally buoyant. During the ascent and descent motions, 1.2 L of water was transferred between the front and rear water bladders. The glider was then negatively buoyant and pitched to predetermined depth when water was pumped from the rear to the front water bladders and pitched upward when water was displaced towards the rear water bladders. As shown in Figure 3.17, a water pump with two solenoid valves was applied to control the water flow. When pump 1 was enabled, its rotation was alternated between CW or CCW, according to the pressure differences at various depth levels.

Similarly, both solenoid valves (V1 and V2) were activated alternatively, and the triggering signal corresponded to the input signal of pump 1.

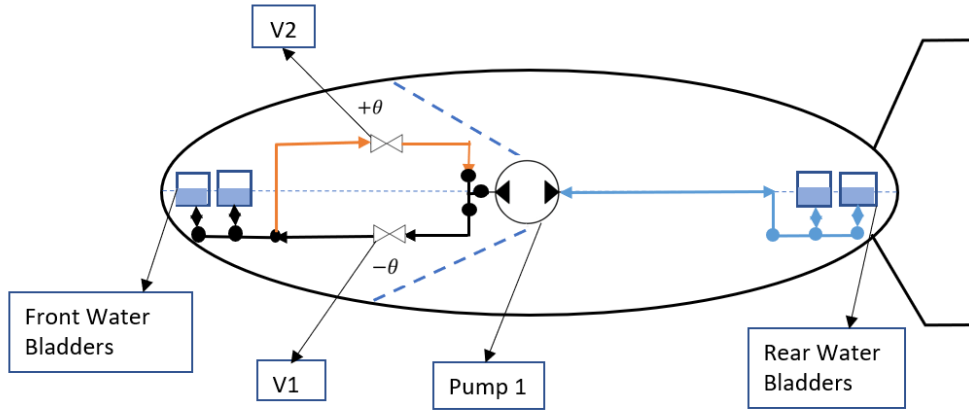


Figure 3.17: Schematic diagram of the internal configuration for the pitch control module

The glider trajectory was in sawtooth motion and divided into four depth levels, namely the upper limit, upper threshold, lower threshold and lower limit (Figure 3.18), which were detected by a pressure sensor. Changes in gliding motion required about 0.4 m prior to reaching the predetermined maximum depth limit. The pump was reversed CCW as it reached the lower threshold limit during descending motion, and then changed to CW when it reached the upper threshold limit during ascending motion. This sequence was repeated throughout the glider maneuvering in the water.

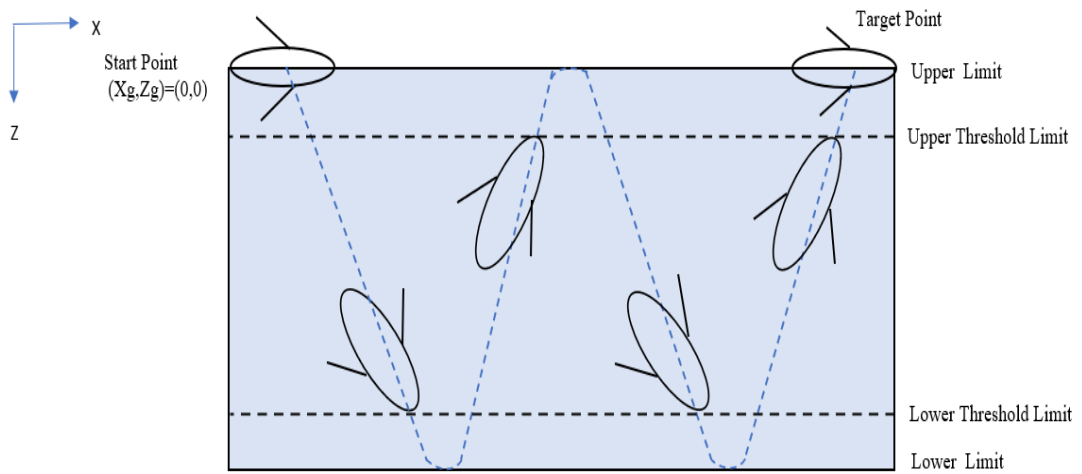


Figure 3.18: Gliding trajectory with four dept limits

The depth is calculated using Equation 3.55; where, P denotes pressure in Pascal (Pa), d is depth in meter (m), g is gravity in m/s^2 , ρ is density in kg/m^3 , and ΔP is a pressure difference between pressure at the water surface and pressure at a given depth.

$$P = d \cdot \rho \cdot g \quad (3.54)$$

$$D = \Delta P \times 100 / \rho g \quad (3.55)$$

3.6.3 Roll Control Module

The roll module controls the left and right rotational motion of the glider. The module consists of a water pump, two solenoid valves, with each left and right section equipped with two rolling tanks (water bladders) and related hydraulic fittings. The roll angle of the glider should remain at 0° when in equilibrium with an equal amount of water on both sides. Roll is induced by shifting 1.2 L of water from left to right side or vice versa, which results in the center of gravity of the glider shifting on the 'y' axis. In this case, pump 2 was activated to displace the water mass based on the IMU signals. Both solenoid valves (V3 and V4) were triggered alternatively, corresponding to pump 2 signals to control the flow of water between the water bladders as shown in Figure 3.19.

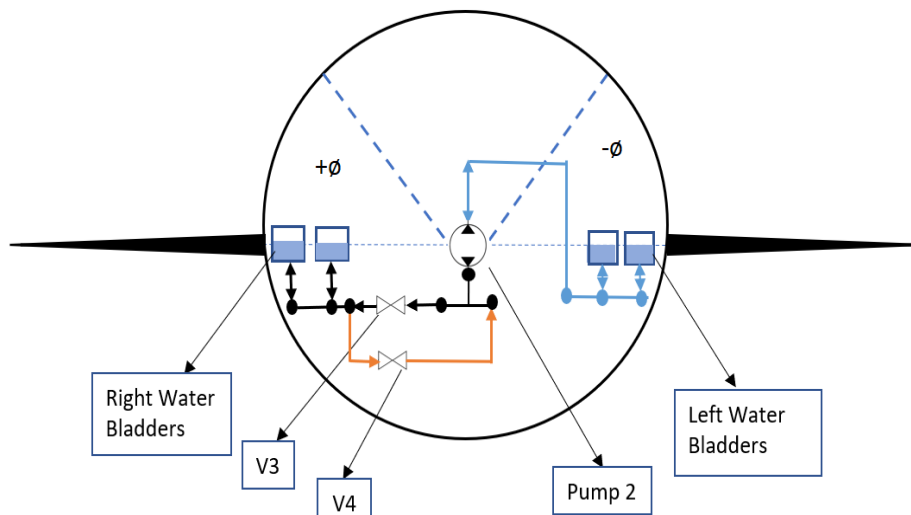


Figure 3.19: Schematic diagram of the internal configuration for the roll control module

3.6.4 Processing Module

The processing module with associated electronics components enables the glider to function by interpreting sensor signals and converting them to commands. The module employed was Arduino Mega 2560 microcontroller as the central processor to control the attitude of the glider with other subsystems such as MPU 6050 IMU, Honeywell pressure sensor, motor driver, Omron relay and a shield data logger. The system was powered by a 12 V,7.2 AH sealed lead acid battery (rechargeable).

3.6.5 Experimental Test with the Control Architecture

A pitch and roll tests were conducted in the UTP swimming pool with a depth of 3 m. Prior to the test, the edges of the body cover were sealed with silicone glue to prevent water leakage into the hull space equipped with electronic devices. Initially, the glider was in a neutrally buoyant state. The mission started when the glider dived into the water and operated based on the motion control architecture as shown by Figure 3.20.

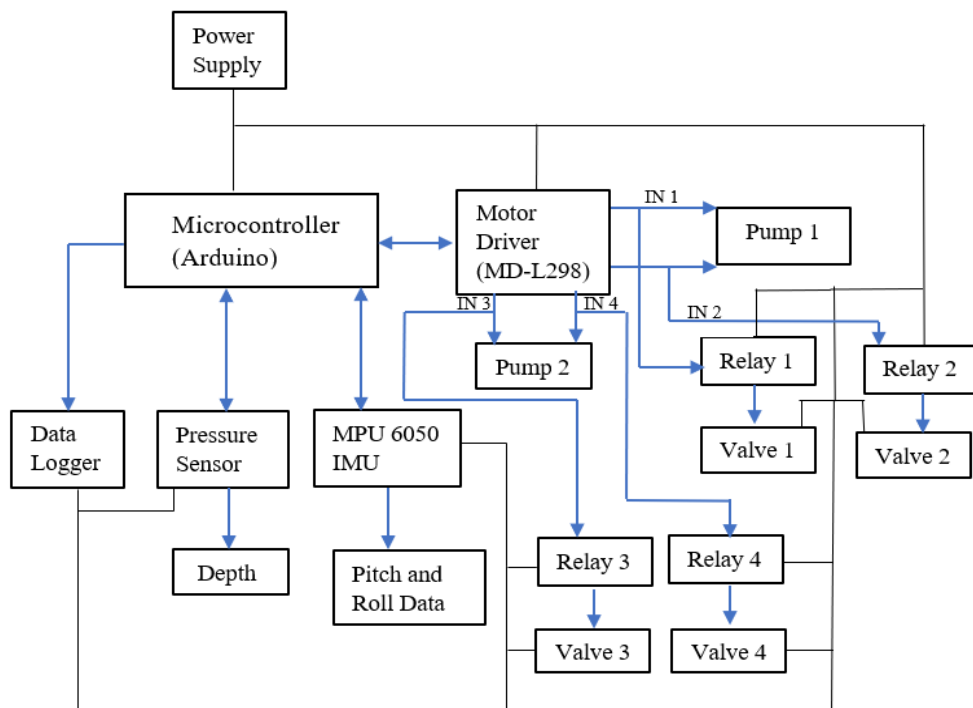


Figure 3.20: Illustration of control architecture operation

The Arduino microcontroller acts as a central processing unit that communicates among the subsystems to function accordingly. This device requires 3.3 V and 5 V as input voltage (V_{in}) powered by the microcontroller with respective 0V/-V terminal connected to the power supply directly. The microcontroller and the motor driver require 12 V as an input voltage (V_{in}) and are connected to a 12 V battery.

Honeywell pressure sensor is used to obtain pressure differences at various depth levels and measure the depths reached by the underwater glider. The predetermined lower threshold limit is -2.6 m, lower limit (bottom surface of the pool) is -3 m, upper threshold limit is +2.6 m and upper limit (upper water surface) is +3.0 m. The sensor calibration data shows that the voltage increases linearly when the depth increases [36].

The Arduino has a key role to determine the glider motion based on the sensor signals to achieve the predetermined depth level. It transmits digital signals to the motor driver to activate the water pump. For pitch control, pump 1 rotation was alternated by changing the IN1 and IN2 signals of the driver. For the roll control, pump 2 rotation was alternated by changing the IN3 and IN4 signals of the driver as summarized in Table 3.3. The single-pole relay was used to alternate the connectivity of the input voltage (V_{in}) to the solenoid valve, which controlled the amount of water in the water bladders. The coil/input voltage (V_{in}) of the relay is dependent on the digital signals (IN_n) of the motor driver. When Pump 1 rotated CW, Relay 1 was triggered to activate Valve 1, and when Pump 1 rotated CCW, Relay 2 was activated to trigger Valve 2. Similarly, for the roll control, Valve 3 and Valve 4 were activated alternatively according to Pump 2 rotations which corresponded to the IN3 and IN4 digital signals of the motor driver.

Table 3.3: Pump rotations on various digital signals (INn) of the motor driver

Rotation	Pump 1		Pump 2	
	IN1	IN2	IN3	IN4
Stop rotation	0	0	0	0
Clockwise (CW) rotation	0	1	0	1
Counter-clockwise (CCW) rotation	1	0	1	0
Stop rotation	1	1	1	1

The IMU unit was compatible with the Arduino microcontroller to acquire pitch and roll data while the glider moved in the water. Communication between the IMU unit and Arduino is significant to control the motion of the glider. The performance of the glider was observed during the field test and the data stored in the data logger were used to make comparisons with the simulation results.

3.7 Summary

This chapter describes the methodology applied to validate the performance of the UTP underwater glider. The glider was designed to travel in a sawtooth pattern and perform a roll motion when required. The pitch and roll control modules of the glider were employed by water pumps, water bladders, valves and related hydraulic fittings to displace water mass between water bladders. Mathematical equations based on 6 DOF, mass distribution, moment and dynamics were derived to solve the nonlinear dynamic model of the underwater glider. The Simulink model was developed to determine the pitch and roll performances on various pump rates.

The earth and body fixed coordinate systems were used as the reference frame for the translational and rotational motions of the glider. The processing module with associated electronics components was programmed to communicate with the pitch and roll module accordingly. The control architecture was built to identify the function of each control element and the schematic diagrams can be used during troubleshooting or for further modification process.

CHAPTER 4

RESULTS AND DISCUSSION

4.1 Chapter Overview

In this chapter, the results of single control mechanism developed are discussed. Section 4.2 presents the pitch, roll and buoyancy performance of UTP glider during field test. The simulation and experiment validation of the relationship between the pump rates and the pitch and roll motions of the glider are elaborated in Sections 4.3 - 4.6. Section 4.7 summarizes the results obtained in this study.

4.2 Motion of Glider During Experimental Test

The UTP glider prototype was tested in a 3 m deep swimming pool to evaluate the accuracy of the pitch and roll data obtained from the Simulink model. The pitch and roll performance were tested using a 2.5 LPM pump, where the pitch and roll data were measured using IMU and stored in a data logger. Meanwhile, the pressure sensor was used to determine the depth limit. Figures 4.1 and 4.2 show the UTP glider pitching and rolling achieved by shifting water between the water bladders.

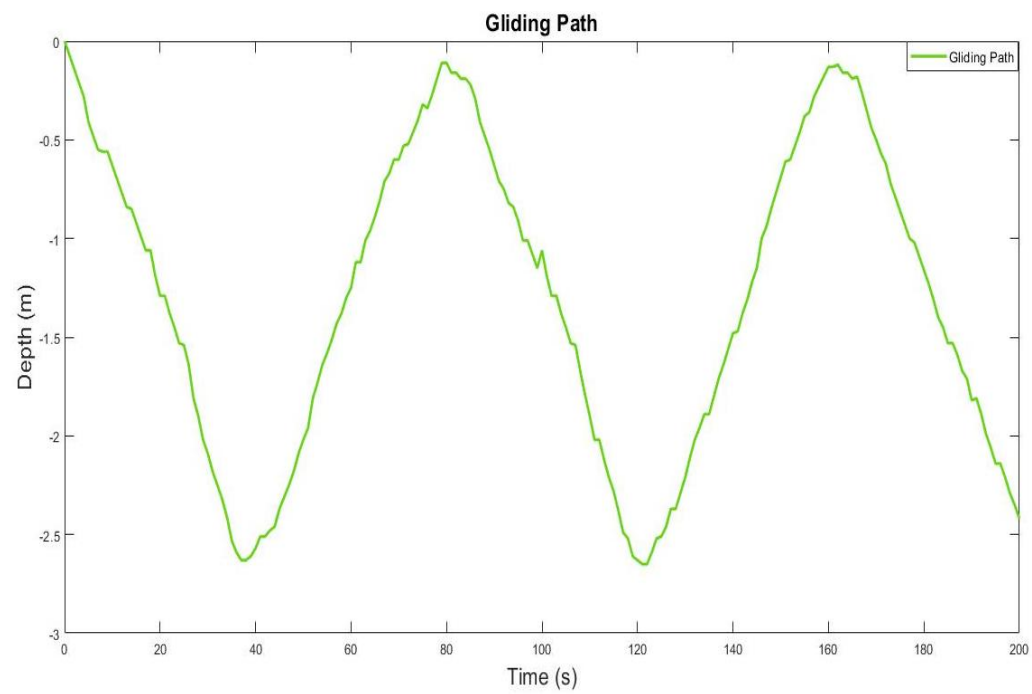
Initially, the UTP glider was in the neutrally buoyant state floating on the water surface. When the pitch control mechanism was activated, the glider was altered to a negative buoyant state. Prior to reaching the lower limit, the glider was switched to a positively buoyant state when it reached the predetermined depth level, resulting in the water mass being transferred to the rear water bladders allowing the glider to pitch upwards towards the water surface (upper limit). Figure 4.1(b) shows the response of the pitch control mechanism developed to the buoyancy control and the corresponding

gliding trajectory at water level depth of 3 m. The lower threshold limit is essential to prevent the glider from striking the bottom. Thus, the glider changed into a positively buoyant state at 2.63-2.65 m, followed by a transition to descent which occurred at 0.11-0.12 m. The results showed that without using a conventional coupled control mechanism, the UTP glider was able to travel in a sawtooth pattern and achieve the required horizontal and vertical distances. Each gliding cycle consumed an average of 37.3 s with an average vertical speed of 0.075 m/s, obtained from the relationship of expected depth and time. This indicated that the glider was free from leakage, which if occurs, it can interrupt the gliding trajectory and the pitch motion. The presence of fluctuations in the gliding path could be due to the water resistance on the glider.

Furthermore, for positive rolling motion as shown in Figure 4.2, the water mass shifted along with the center of gravity from the left to the right water bladders, and vice versa.



(a) Pitch control motion



(b) Gliding Path

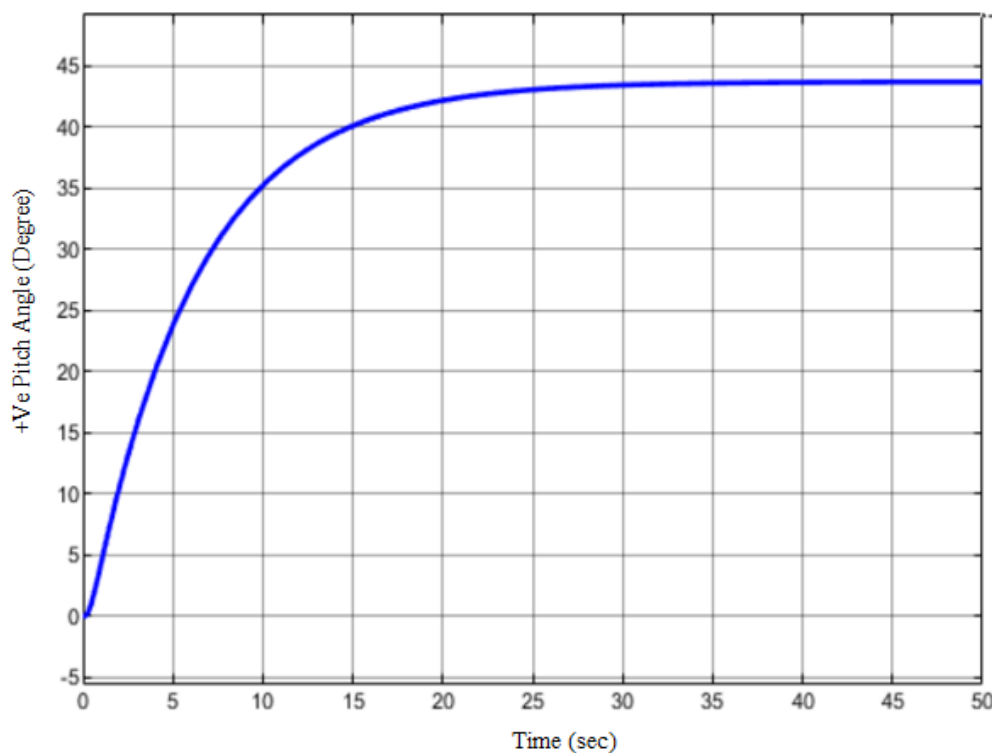
Figure 4.1: Pitch motion during the experimental test



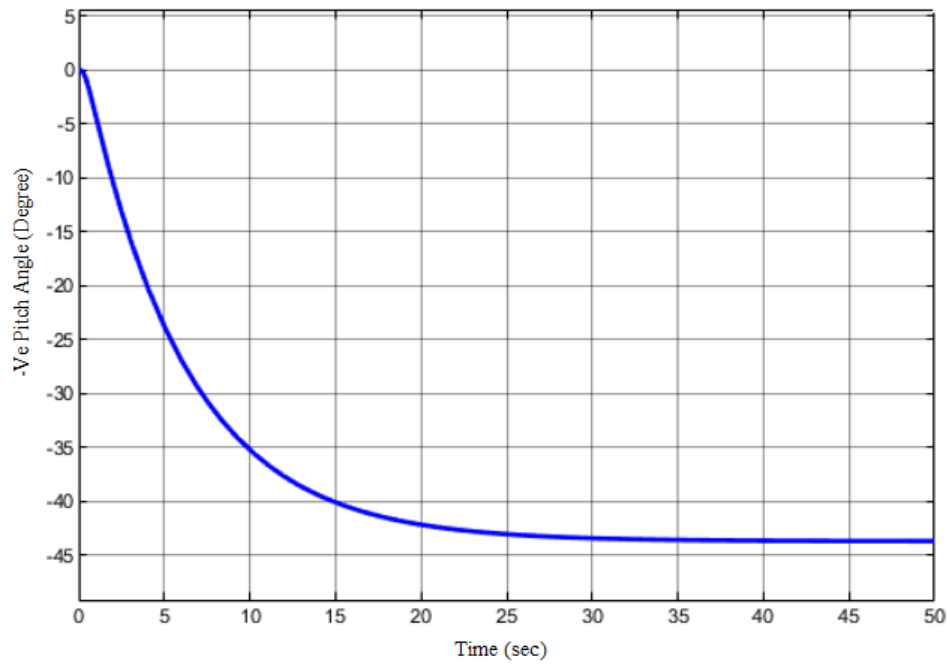
Figure 4.2: Roll motion during the experimental test

4.3 Pitch and Roll Angle

The simulation was performed and it was observed that the glider was capable of reaching a maximum pitch angle of 43.5° and a roll angle of 43.6° . The ascending and descending motions of the underwater glider were represented by the positive and negative pitch angles as shown in Figure 4.3. The right and left rolling motions were represented by positive and negative roll angles as depicted in Figure 4.4. The simulation results showed the glider with single control mechanism was able to achieve pitch and roll angle without the use of conventional buoyancy engine. It is significant in order to validate the performance of the developed pitch and roll control mechanism preceding to the field testing, which is not considered to the existing UTP glider design [54]. The distance between the water bladders is considerable in order to improve the time required to achieve the desired pitch and roll angles. It was reflected when the maximum roll angle was achieved in 15 s, approximately 16.5 s faster than the highest pitch angle.

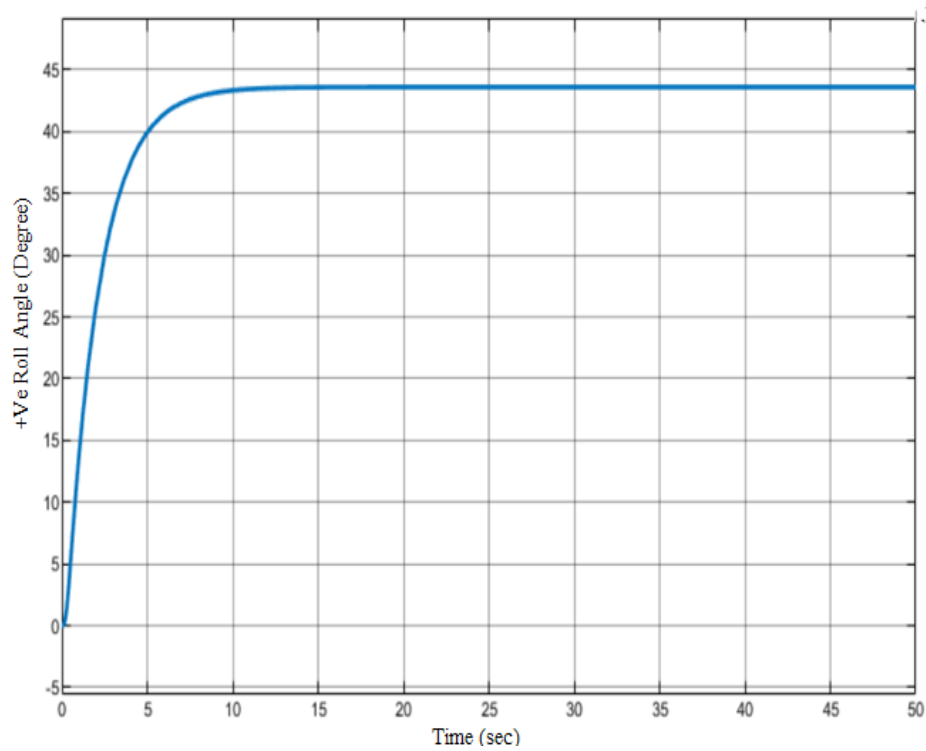


(a) Positive pitch angle (degree)

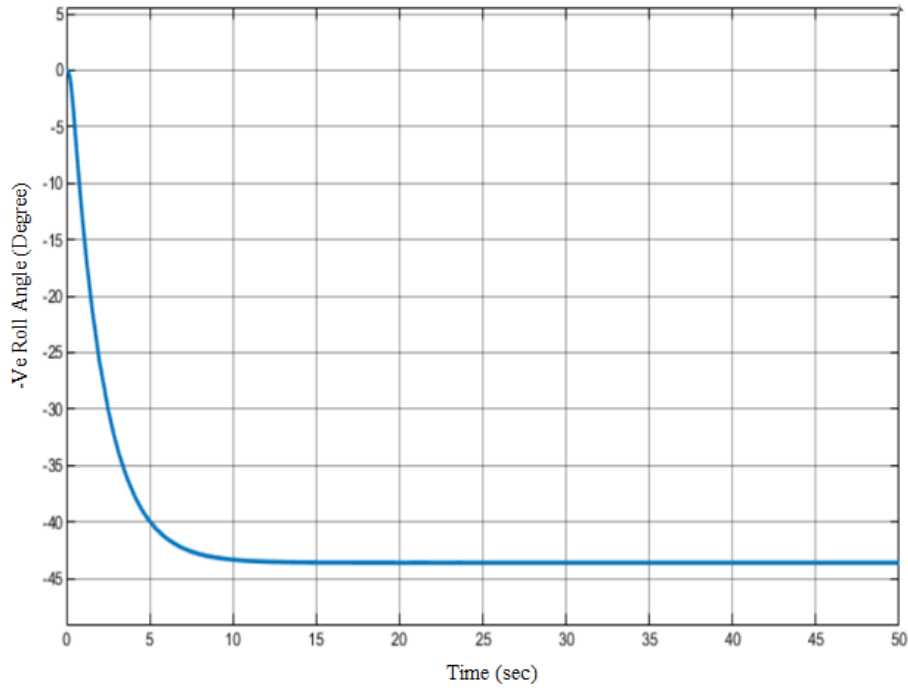


(a) Negative pitch angle (degree)

Figure 4.3: Pitch angle (degree) against time (second)



(a) Positive roll angle (degree)



(b) Negative roll angle (degree)

Figure 4.4: Roll angle (degree) against time (second)

To validate the pitch and roll angles from Simulink, a comparison with the experimental results are displayed in Figures 4.5 and 4.6, respectively. It was observed that the pitch and roll angles were dependent on the water mass. When the water bladder capacity was higher, the glider achieved the highest pitch and roll angles as opposed to lower water bladder capacity.

Experiments were conducted to determine the response between the developed pitch control mechanism and the desired pitch angle. Referring to Figure 4.5, the experimental data showed higher difference of 22.3% compared to the Simulink data obtained in the transient period. This trend was consistent with the experimental data. The maximum pitch angle was 46.3° , 6.04% higher than that of the Simulink model, whereas the UTP glider with a conventional pitch control mechanism (linear actuator with a movable mass) achieved a maximum pitch angle of 45° [54]. The results also showed a difference of 2.8% without using a conventional buoyancy engine which enabled a reduction in internal hull mass and improved the performance of the glider. Thus, the center of gravity could be changed by shifting the water mass from the nose

and tail inside the internal hull of the glider. External disturbances caused the pitch angle of the glider to fluctuate between 44.9 to 46.3° in the steady state condition.

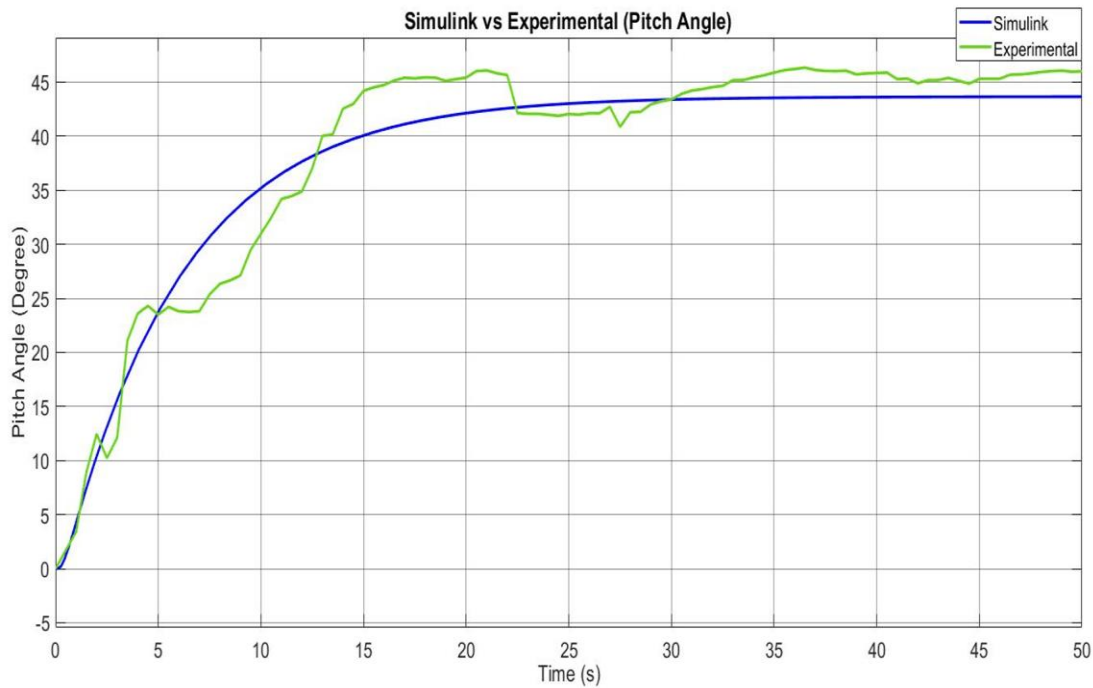


Figure 4.5: Comparison of experimental and simulation results for pitch angle

Roll control is substantial in preventing undesired roll motion which can affect the gliding trajectory. Referring to the experimental data, the glider achieved a maximum roll angle of 42.3° , which was 2.9% lower than that of the Simulink model. A comparison between Simulink and the experimental results demonstrated a roll angle error of less than 10%. This may be because the glider was not perfectly balanced in the water, while the simulation assumed perfect balance and symmetry.

Furthermore, the roll was achieved by shifting the water mass only, whereas several gliders relied on the rotational mass. Both existing and developed roll control modules of the UTP glider used water as the trim mass. However, the total capacity of the existing rolling tank was 50%, lower than the reservoir in proposed roll control module. Moreover, the roll control mechanism relied on the volume and number of water bladders employed to accommodate the water mass, which resulted in a better roll angle of 29.1% when compared to the existing modules. In fact, the existing roll control mechanism can only achieve a maximum roll angle of 30° [54].

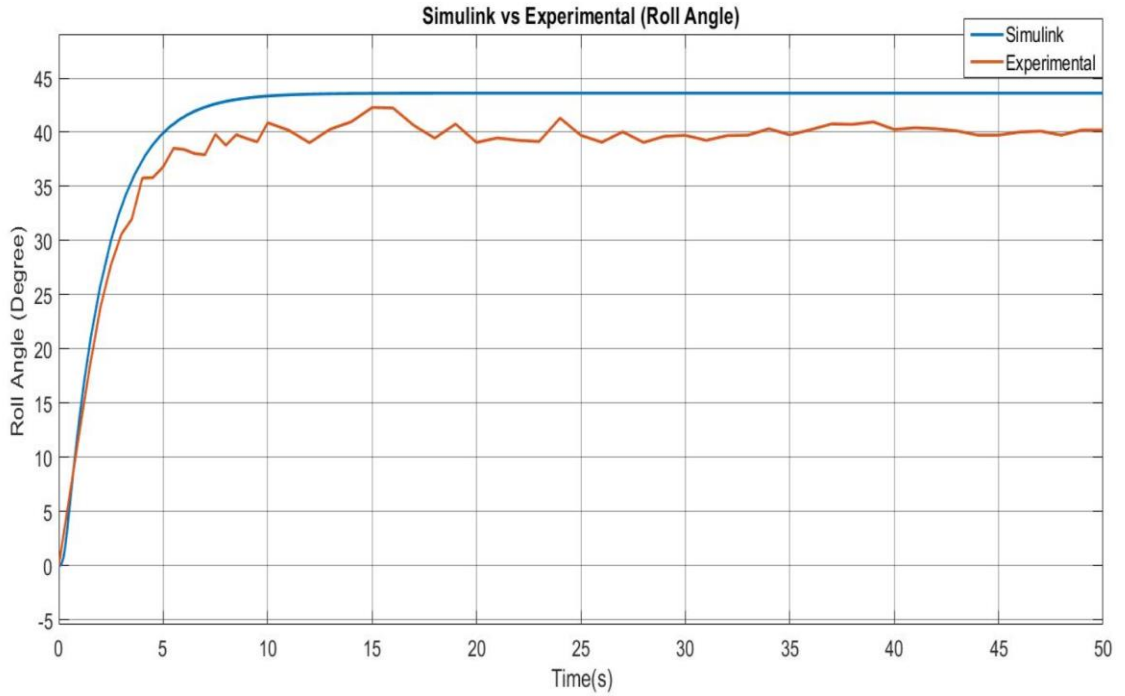


Figure 4.6: Comparison of experimental and simulation results for roll angle

4.4 Relationship Between Pitch Rate and Pump Flow Rate

Pitch rate was evaluated through the Simulink model by manipulating the pump rates. As previously mentioned, the applied pump rates were 2.5, 5, 7.5 and 10 LPM. All four pump rates were sampled simultaneously to determine the variation of the pitch rate. The results indicated that the pitch rate increased gradually with increasing pump rates. Moreover, the 2.5 LPM pump rate produced lower pitch rate ($2.64\text{E-}01$ rad/s) compared to the 10 LPM pump rate (1.07 rad/s). Based on Table 4.1, the 10 LPM pump rate achieved higher pitch rate of 73.3% compared to that of 2.5 LPM pump rate. As shown in Figure 4.7, although the rise time varied for different pump rates, the analysis showed that all four pump rates achieved steady state condition in 35 to 45 s. The optimum pitch angle was achieved in 35 s from the Simulink model.

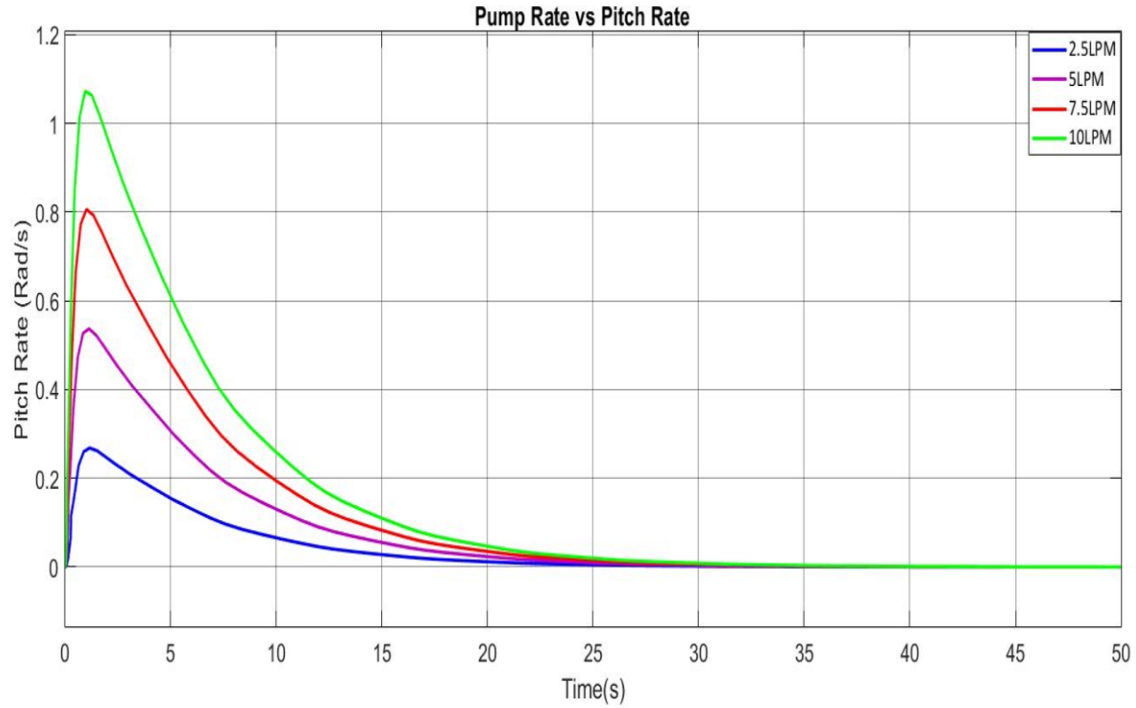


Figure 4.7: Pitch rate simulation for pump flow rates of 2.5, 5, 7.5, and 10 LPM

Table 4.1: Pump rate against pitch rate

Time (s)	Pump rate (LPM)			
	2.5	5	7.5	10
5	1.55E-01	3.07E-01	4.58E-01	6.10E-01
10	6.59E-02	1.30E-01	1.94E-01	2.59E-01
15	2.81E-02	5.54E-02	8.28E-02	1.10E-01
20	1.19E-02	2.35E-02	3.52E-02	4.68E-02
25	5.08E-03	1.00E-02	1.50E-02	1.99E-02
30	2.165E-03	4.23E-03	6.38E-03	8.44E-03
35	9.15E-04	1.77E-03	2.69E-03	3.55E-03
40	3.80E-04	7.19E-04	1.08E-03	1.39E-03
45	1.45E-04	2.57E-04	3.95E-04	4.87E-04

In this study, buoyancy and pitch were controlled by the water pump mechanism. Thus, the buoyancy of the glider was dependent on its pitch motion and proportional to the mass of the bladder. Figure 4.8 depicts the difference between the experimental and simulated pitch rates for 2.5 LPM pump flow rate.

The peaks for the experimental and simulated pitch rates achieved $2.70\text{E-}01$ rad/s and $2.67\text{E-}01$ rad/s, respectively. The experimental data were 1.1% higher than the Simulink data and it was achieved without using the conventional buoyancy engine. Comparison between experimental and simulation data is significant to determine the appropriate pump flow rate prior to physical test. The difference in pitch rate in the transient state indicated that the glider dynamics were asymmetric in the actual state as predicted in the Simulink model and it was affected by environmental disturbances.

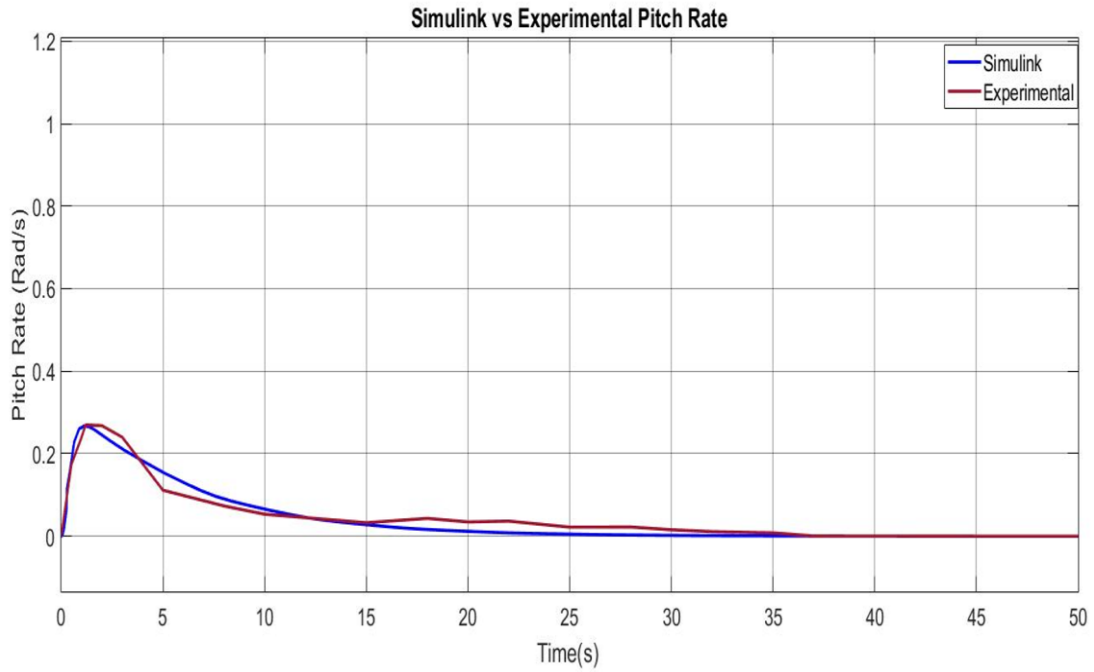


Figure 4.8: Comparison of experimental and the simulation results for pitch rate

4.5 Relationship Between Roll Rate and Pump Flow Rate

Roll rate is important to evaluate the rolling behavior of the underwater glider. The roll characteristics were evaluated through the roll rate of the vehicle as it rotated along its longitudinal axis. Similar to the pitch rate, the roll rate was proportional to the pump rate. Therefore, four pump rates of 2.5, 5, 7.5 and 10 LPM were simulated to determine the corresponding roll rate (rad/s) as shown in Figure 4.9. It was found that the pump rate of 10 LPM achieved the maximum roll rate of $6.77\text{E-}03\text{rad/s}$ and 2.5 LPM pump rate resulted in lower roll rate of 74.6%. Based on Table 4.2, the roll rate increased with

increasing pump rate. The variation in roll rate could be due to the water flow rate and the time consumed to displace the water mass between the water bladders. Thus, the roll rate increased while accelerating the water flow rate. An average of 74.7% roll rate difference was achieved compared to 10 and 2.5 LPM pump rates. The pump rates have an impact on the rise time, where the rise time fluctuated for different pump rates. The glider reached steady state within 10-15 s and also achieved optimum roll angle after 15 s during the field test. It exhibited that the roll responses were consistent between the experimental and simulation results.

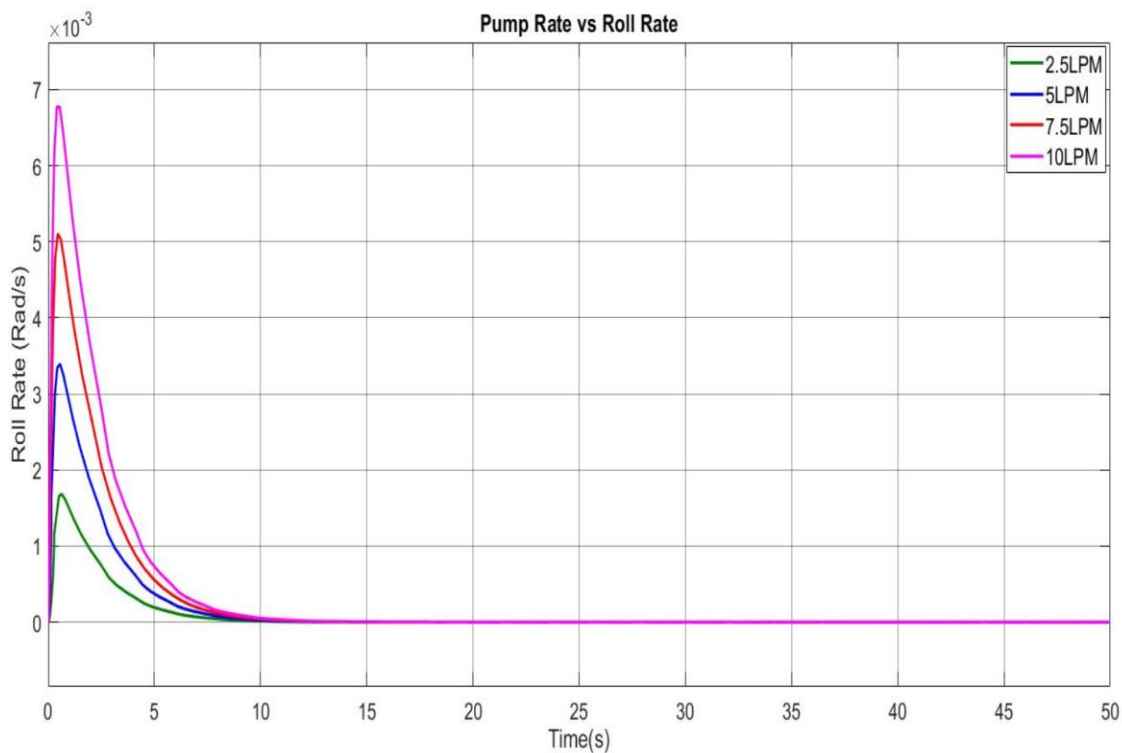


Figure 4.9: Roll rate simulation for pump rates of 2.5, 5, 7.5, and 10 LPM

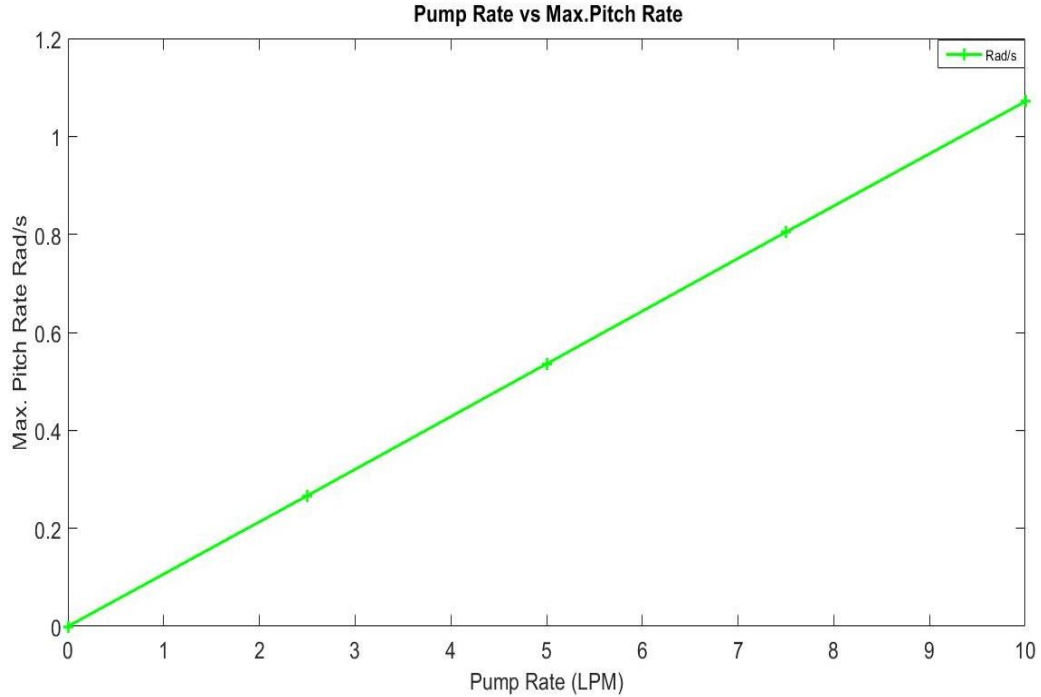
Table 4.2: Pump rate against roll rate

Time (s)	Pump rate (LPM)			
	2.5	5	7.5	10
5	1.93E-04	3.74E-04	5.54E-04	7.32E-04
10	1.46E-05	2.81E-05	4.08E-05	5.16E-05
15	9.40E-07	1.86E-06	3.04E-06	4.43E-06

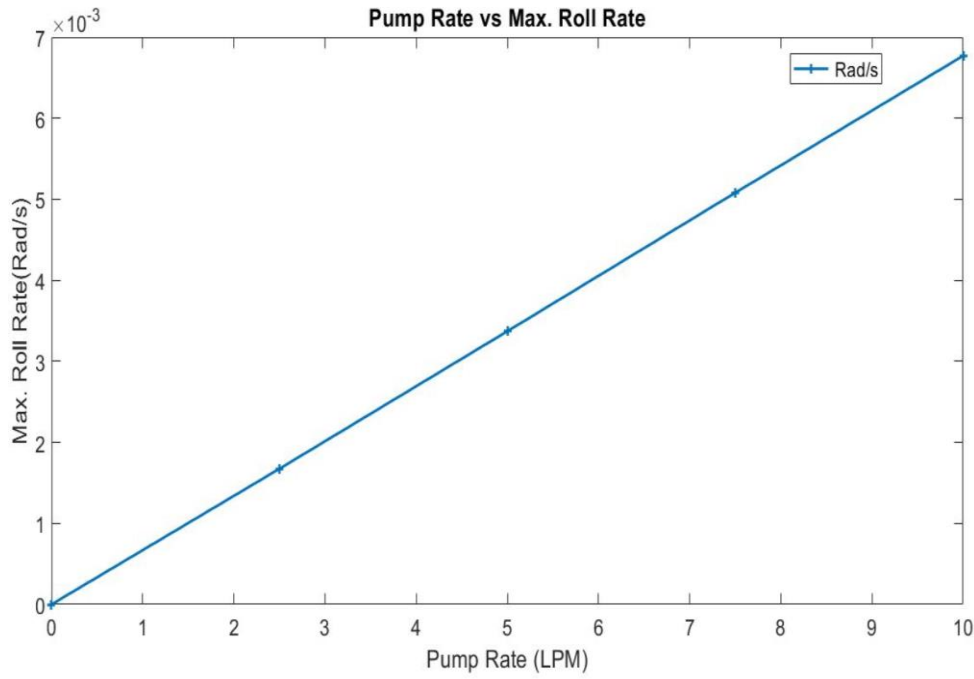
4.6 Relationship of Pitch and Roll and Pump Flow Rate

Figure 4.10 shows the maximum pitch and roll rate with the applied pump rate. The pitch and roll responses of the UTP glider to the pump rate signified positive results. Both the pitch and roll rates were directly proportional to the pump rate, where the pitch and roll rates increased as the pump rate increased. The performance of the glider could be improved by increasing the amount of water transferred, which minimized the time consumed on pitch, roll and buoyancy control.

The proposed control mechanism (water pump system) was comparable to the existing conventional buoyancy engine (ballast tank and movable masses) of the UTP glider. Furthermore, the results of pitch and roll angles of the UTP glider with single control mechanism were more reliable from the experimental and simulation data compared to the USM Hybrid-Driven Glider [22] which has an error rate of 81.5%. Steady state durations for roll and pitch were achieved in 15 s and 37 s, respectively, during the field test, indicating the consistency of the experimental and simulation data.



(a) Maximum pitch rate (rad/s)



(b) Maximum roll rate (rad/s)

Figure 4.10: Maximum pitch and roll rates with the corresponding pump rates

4.7 Summary

In this study, the pitch, roll and buoyancy performance of the UTP glider with the developed control mechanism were evaluated by comparing the experimental results with the Simulink model. It was noted that there was less than 10% error for optimum pitch and roll angles compared to the simulation data. However, the differences in results between the experiment and Simulink model demonstrated the influence of dynamic and environmental factors on the performance of the glider.

Both pitch and roll rates could be altered by manipulating the pump rates. The highest pump rate has greater pitch and roll rates as opposed to the lowest pump rate. In this study, the differences in pitch and roll rate were 0.81 rad/s and 5.1 E-03 rad/s, respectively, for the highest (10 LPM) and lowest (2.5 LPM) pump rates.

The pitch and roll data obtained were used to compare with the performance of the multiple control mechanism of the existing UTP glider. The data showed 2.8% pitch angle and 29.1% roll angle variation were obtained when compared with the existing

control mechanism of the UTP glider. It was noted that the use of water pump mechanism could neglect the use of multiple control mechanisms for pitching and rolling motions.

On other hand, the use of single control mechanism produced better pitch and roll performance compared to the legacy gliders by minimizing glider mass. Thus, the highest pitch and roll angle differences were with the Spray glider [7] and Seaglider [8] which were 64.1% and 29.1% respectively.

CHAPTER 5

CONCLUSIONS AND RECOMMENDATIONS

5.1 Chapter Overview

In this chapter, the conclusion of this study is summarized in Section 5.2. Section 5.3 presents recommendations that could be of high potential for extending this research in the future.

5.2 Conclusions

In conclusion, a single mechanism to control pitch and buoyancy as well as roll was developed for UTP glider. The purpose is to reduce the hull mass which significantly affected the glider performance. The depth, pitch and roll of the glider were controlled using the water pump system instead of a conventional buoyancy engine with a ballast tank and movable masses. Instead of using a rotational mass, the roll of the glider was controlled with water pump to displace the center of gravity by shifting the water mass. During the pitch, water as a trim mass was displaced along the 'x' axis, while for roll, the water mass was shifted along the 'y' axis of the body fixed coordinate system.

In this study, the relationship between the pitch and roll response of the glider with the control mechanism was determined through Simulink model and experimental test. Four different pump rates were considered and as a result, the pitch and roll rates increased by 74-75% as the pump rate increased from 2.5 to 10 LPM. Both pitch and roll motions are the key factors in evaluating the performance of UTP glider. Therefore, the buoyancy, pitch and roll performance were tested experimentally, and it was observed that the glider could maneuver in a sawtooth pattern at predetermined depth

levels as well as the roll motion was achieved by displacing the water mass. The experimental results indicated that the glider model with single buoyancy, pitch and roll control mechanism is a viable alternative to the existing conventional coupled control methods.

Relevant mathematical equations were derived based on single mechanism for pitching and rolling motions. Six DOF and dynamics equations were used to derive the motion of the glider with respect to the acting forces and moments on its body. Meanwhile, the kinematic equations were derived based on the mass of the developed control mechanism and the respective moment of inertia of glider; and solved through the Simulink model in order to determine the pitch and roll performance of the UTP glider by manipulating the pump rates.

5.3 Recommendations for Future Works

Research and development are often required in improving the efficiency of underwater gliders. The following could be considered as recommendations for future improvements:

1. It is possible to improve the efficiency of glider in an uncertain ocean environment by integrating control algorithms such as Artificial Neural Networks (ANNs), Fuzzy Logic Controller (FLC), Auto-tune PID Controller, Homeostatic Controller and U-model Controller to the underwater glider model.
2. It is significant to improve the Simulink model by considering the nonlinear effects on the glider in the water.
3. Numerical investigations are required to determine appropriate control techniques to cope with the influence of wave and ocean currents on controller performance.
4. Use of model updating technology to regulate the inaccuracy of the data prediction with the experimental results.
5. The roll motion could be improved by incorporating water bladders into the glider wings which may eliminate the dedicated hull space.

REFERENCES

- 1) R. Kalvin, J. Taweekun, M. W. Mustafa, F. Ishfaq, and S. Arif, "Design and Fabrication of Under Water Remotely Operated Vehicle," *Journal of Advanced Research in Fluid Mechanics and Thermal Sciences*, vol. 82, pp.133-144, 2021.
- 2) A. A. Yusof, M. K. M. Nor, S. A. Shamsudin, M. R. Alkahari, M. S. M. Aras, M. R. M. Nawawi, M. Z. M. Tumari, M. A. Kasno, "Lessons learned from UTeM Autonomous Underwater Vehicle Competition Initiatives," *Progress in Fluid Power, Mechanisations and Mechatronics*, vol.2, pp.10-26, 2018.
- 3) O. Schofield, J. Kohut, D. Aragon, L. Creed, J. Graver, C. Haldeman, J. Kerfoot, H. Roarty, C. Jones, D. Webb, and S. Glenn, "Slocum gliders: Robust and ready," *Journal of Field Robotics*, vol.24, pp.473-485, 2007.
- 4) D. Joe, R. S. Shankar, R. Vijayakumar, and A. Das, "Concept Design of Autonomus Underwater Glider," *International Journal of Innovative Research and Development*, vol.1, pp.176-189, 2012.
- 5) J. E. Ruiz-Duarte, and A. G. Loukianov, "Higher order sliding mode control for autonomous underwater vehicles in the diving plane". *IFAC-PapersOnLine*, vol.48, pp.49-54, 2015.
- 6) C. Deutsch, J. Kutteneuler, and T. Melin, "Glider performance analysis and intermediate-fidelity modelling of underwater vehicles", *Ocean Engineering*, vol. 210, p.107567, 2020.
- 7) J. Sherman, R. E. Davis, W. B. Owens, and J. Valdes, "The autonomous underwater glider" "Spray", *IEEE Journal of Oceanic Engineering*, vol. 26, 2001, pp.437-446.
- 8) C. C. Eriksen, T. J. Osse, R. D. Light, T. Wen, T. W. Lehman, P. L. Sabin, J. W. Ballard, and A. M. Chiodi, "Seaglider: A long-range autonomous underwater vehicle for oceanographic research," *IEEE Journal of oceanic Engineering*, vol.26, pp.424-436, 2001.
- 9) S. Ziaeeefard, B. R. Page, A. J. Pinar, and N. Mahmoudian, "Effective turning motion control of internally actuated autonomous underwater vehicles," *Journal of Intelligent & Robotic Systems*, vol.89, pp.175-189, 2018.
- 10) M. Y. Javaid, M. Ovinis, T. Nagarajan, and F. B. Hashim, "Underwater gliders: A review," in *MATEC Web of Conferences, EDP Sciences*, 2014, p.02020.

- 11) D. H. Ji, H. S. Choi, J. I. Kang, H. J. Cho, M. G. Joo, and J. H. Lee, "Design and control of hybrid underwater glider," *Advances in Mechanical Engineering*, vol.11, p.1687814019848556, 2019.
- 12) H. Wu, W. Niu, S. Wang, S. Yan, and T. Liu, "Sensitivity analysis of input errors to motion deviations of underwater glider based on optimized response surface methodology," *Ocean Engineering*, vol.209, p.107400, 2020.
- 13) F. Sagala, and R.T. Bambang, "Development of sea glider autonomous underwater vehicle platform for marine exploration and monitoring," *Indian Journal of Geo Marine Sciences*, vol.40, pp. 287-295, 2011.
- 14) N. Mahmoudian, J. Geisbert, and C. Woolsey, "Approximate analytical turning conditions for underwater gliders: Implications for motion control and path planning," *IEEE Journal of Oceanic Engineering*, vol.35, pp.131-143, 2010.
- 15) S. M. Hong, S. Lee, J. W. Hyeon, J. H. Lee, S. Lee, C. Lee, and S. H. Ko, "Optimal design of combined propulsion Underwater Glider for operation of the East Sea of South Korea," *Advances in Mechanical Engineering*, vol.11, p.1687814019856482, 2019.
- 16) Wen-dong, W. Shu-xin, W. Yan-hui, S. Yang, and Z. Ya-qiang, "Stability analysis of hybrid-driven underwater glider," *China Ocean Engineering*, vol. 31, pp.528-538, 2017.
- 17) M.Y. Javaid, M. Ovinis, F. B. Hashim, A. Maimun, and Y. M. Ahmed, and B. Ullah "Pure Heaving and Pure Pitching Motion of an Underwater Glider," *Journal of Computational and Theoretical Nanoscience*, vol.23, pp.1388-1392, 2017.
- 18) Y. Wang, Y. Zhang, M. M. Zhang, Z. Yang, and Z. Wu, "Design and flight performance of hybrid underwater glider with controllable wings," *International Journal of Advanced Robotic Systems*, vol.14,p.1729881417703566, 2017.
- 19) R. Cristi, F. A. Papoulias, and A. J. Healey, "Adaptive sliding mode control of autonomous underwater vehicles in the dive plane," *IEEE journal of Oceanic Engineering*, vol.15, pp.152-160, 1990.
- 20) S. Phoemsapthawee, M. G. L. Boulluec, J. M. Laurens, and F. Deniset, "A potential flow based flight simulator for an underwater glider," *Journal of Marine Science and Application*, vol.12, pp.112-121, 2013.

- 21) A. Honaryar, and M. Ghiasi, "Roll Dynamic Stability of an Autonomous Underwater Vehicle with a Fish-like Hull Shape," *Amirkabir Journal of Mechanical Engineering*, vol.52, pp.2011-2026, 2020.
- 22) K. Isa, and M. R Arshad, "Experimental analysis of homeostatic-inspired motion controller for a hybrid-driven autonomous underwater glider," *Jurnal Teknologi*, vol.74, 2015.
- 23) F. Zhang, O. Ennasr, E. Litchman, and X. Tan, "Autonomous sampling of water columns using gliding robotic fish: Algorithms and harmful-algae-sampling experiments," *IEEE Systems Journal*, vol.10, pp.1271-1281, 2016.
- 24) A. Bender, D. M. Steinberg, A. L. Friedman, and S. B. Williams, "Analysis of an autonomous underwater glider," in *2008 Proceedings of the Australasian conference on robotics and automation*, 2008, pp.1-10.
- 25) F. Zhang, and X. Tan, "Three-dimensional spiral tracking control for gliding robotic fish," In *Decision and Control, 2014 IEEE 53rd Conference on*, 2014, pp. 5340-5345.
- 26) Y. Liu, J. Ma, N. Ma, and Z. Huang, "Experimental and numerical study on hydrodynamic performance of an underwater glider," *Mathematical Problems in Engineering*, 2018.
- 27) E. Y. Hong, H. G. Soon, and M. Chitre, "Depth control of an autonomous underwater vehicle, STARFISH," in *OCEANS'10 IEEE Sydney*, 2010, pp. 1-6.
- 28) E. Y. Hong, and M. Chitre, "Roll control of an autonomous underwater vehicle using an internal rolling mass," In *2015 Field and service robotics*, Springer, 2015, pp. 229-242.
- 29) M. Sangekar, M. Chitre, M. and T. B. Koay, "Hardware architecture for a modular autonomous underwater vehicle STARFISH," In *2008 OCEANS, IEE explore*, 2008 pp. 1-8.
- 30) R. Bachmayer, B. D. Young, C. Williams, C. Bishop, C. Knapp, and J. Foley, "Development and deployment of ocean gliders on the Newfoundland Shelf," In *2006 Proceedings of the Unmanned Vehicle Systems Canada Conference*, 2006.
- 31) Y. Singh, S. K. Bhattacharyya, and V. G. Idichandy, "CFD approach to modelling, hydrodynamic analysis and motion characteristics of a laboratory

- underwater glider with experimental results”, *Journal of Ocean Engineering and Science*, vol.2, pp.90-119, 2017.
- 32) B. Ullah, M. Ovinis, M. B. Baharom, S. S. A. Ali, B. Khan, and M. Y. Javaid, “Effect of waves and current on motion control of underwater gliders,” *Journal of Marine Science and Technology*, vol. 25, pp.549-562, 2020.
 - 33) W. Zihao, L. Ye, W. Aobo, and W. Xiaobing, “Flying wing underwater glider: Design, analysis, and performance prediction,” In *2015 International Conference on Control, Automation and Robotics, 2015*, pp. 74-77.
 - 34) F. Zhang, J. Thon, J, C. Thon, and X. Tan, “Miniature underwater glider: Design and experimental results,” in *2013 IEEE/ASME Transactions on Mechatronics*, 2013, pp.394-399.
 - 35) D. L. Rudnick, R. E. Davis, C. C. Eriksen, D. M. Fratantoni, and M. J. Perry, “Underwater gliders for ocean research,” *Marine Technology Society Journal*, vol.38, pp.73-84, 2004.
 - 36) V. K. Upadhyay, Y. Singh, and V. G. Idichandy, “Modelling and control of an underwater laboratory glider,” In *2015 IEEE Underwater Technology (UT)*, 2015, pp. 1-8.
 - 37) P. Yu, T. Wang, H. Zhou, and C. Shen, “Dynamic modeling and three-dimensional motion simulation of a disk type underwater glider,” *International Journal of Naval Architecture and Ocean Engineering*, vol.10, pp.318-328, 2018.
 - 38) S. Ziaeeefard, G. A. Ribeiro, and N. Mahmoudian, "GUPPIE, underwater 3D printed robot a game changer in control design education," in *2015 American Control Conference (ACC)* , 2015, pp. 2789-2794.
 - 39) N. A. A.Hussain, S. S.A. Ali, M. Ovinis, M. R. Arshad, and U. M. Al-Saggaf, “Underactuated coupled nonlinear adaptive control synthesis using u-model for multivariable unmanned marine robotics,” *IEEE Access*, vol.8, pp.1851-1865, 2019.
 - 40) F. Zhang, “Modeling, design and control of gliding robotic fish,” Ph.D. dissertation, Dept. Elec.Eng., Michigan State Univ., Michigan, USA, 2014.
 - 41) A. Fitriadhy, S. Dewa, N. A. Mansor Adam, C. Y. Ng, and H. S. Kan, “CFD Investigation into Seakeeping Performance of a Training Ship CFD,” *CFD Letters*, vol.13, pp.19-32, 2021.

- 42) B. Claus, R. Bachmayer, and Williams, D. Christopher, “v”. In *2010 IEEE/OES Autonomous Underwater Vehicles*, 2010, pp.1-6.
- 43) F. Tatone, M. Vaccarini, and S. Longhi, “Modeling and attitude control of an autonomous underwater glider,” in *Manoeuvring and Control of Marine Craft, 2009 IFAC 8th International Conference on*, 2009, pp.217-222.
- 44) Y. Liu, S. Xu, S. Tian, H. Zhang, S. Deng, and S. Liu, “A Lab-Scale Underwater Glider With Flexible Camber Trailing Edge Wings,” Research Square, 2021.
- 45) M. Y. Javaid, M. Ovinis, F. B. Hashim, A. Maimun, Y. M. Ahmed, and B. Ullah, “Spiralling motion of an underwater glider: Dynamic modeling,” *ARNP Journal of Engineering and Applied Sciences*, vol.11, 2016.
- 46) R. Hernández-Alvarado, L.G. García-Valdovinos, T. Salgado-Jiménez, A.Gómez-Espinosa, and F. Fonseca-Navarro, “Neural network-based self-tuning PID control for underwater vehicles,” *Sensors*, vol.16, p.1429, 2016.
- 47) E. Petritoli, F. Leccese, and M. Cagnetti, “High accuracy buoyancy for underwater gliders: The uncertainty in the depth control,” *Sensors*, vol.19p.1831, 2019.
- 48) B. Claus, R. Bachmayer, and C. D. Williams, “Development of an auxiliary propulsion module for an autonomous underwater glider,” *Journal of Engineering for the Maritime Environment*, vol.224, pp.255-266, 2010.
- 49) K. Isa, and M. R. Arshad, “Motion simulation for propeller-driven USM underwater glider with controllable wings and rudder,” In *2011 2nd International Conference on Instrumentation Control and Automation, IEEE*, pp.316-321.
- 50) L. Wang, J. Jiang, and L. Zhang, “Model of thermal underwater gliders with PEMFC,” In *IOP Conference Series: Materials Science and Engineering, IOP Publishing*, 2018, p. 052003.
- 51) J. P. Orozco-Muñiz, T. Salgado-Jimenez, and N. A. Rodriguez-Olivares, “Underwater glider propulsion systems VBS part 1: VBS sizing and glider performance analysis,” *Journal of Marine Science and Engineering*, vol.8, p.919,2020.
- 52) S. A Jenkins, and G. D’Spain, “Autonomous underwater gliders,” In *Springer Handbook of Ocean Engineering*, pp. 301-322, 2016.

- 53) S. Abbasi, and M. Zeinali, "Investigation on Nose and Tail Shape Effects on Hydrodynamic Parameters in Autonomous Underwater Vehicles,". *International Journal of Engineering*, vol.31, pp.2102-2108, 2018.
- 54) Barkat Ullah, Design and motion control of an underwater glider in the presence of wave and current disturbances," Ph.D. dissertation, Dept. Mech.Eng., Universiti Teknologi Petronas., Perak, Maalaysia, 2019.
- 55) S. Zhiyu, F. Jing, F. Shunshan, and C. Yufeng, "Study on Hydrodynamic Outline of an Unmanned Underwater Vehicle,". In *2013 Fifth International Conference on Measuring Technology and Mechatronics Automation, IEEE*, 2013, pp. 1056-1059.
- 56) N. H. Tran, Q. T. D. Tran, N. D. Nguyen, and H. S. Choi, 'Study on design, analysis and control an underwater thruster for unmanned underwater vehicle (UUV)," In *2017 International Conference on Advanced Engineering Theory and Applications* ,2017, (pp. 753-764).
- 57) J. G. Graver, "Underwater gliders: Dynamics, control and design," Ph.D. dissertation, Dept. Mech. Eng., Princeton Univ., New Jersey, USA, 2005.
- 58) J. Liu, Z. Wu, J. Yu, and Z. Cao, "Flippers-based turning analysis and implementation of a dolphin robot," In *2017 IEEE International Conference on Robotics and Biomimetics, ROBIO, IEEE*, 2017, pp. 141-146.
- 59) S. K. Jeong, H. S. Choi, J. H. Bae, S. S You, H. S. Kang, S. J. Lee, J.Y. Kim, D. H. Kim, and Y. K. Lee, "Design and control of high speed unmanned underwater glider,". *International Journal of Precision Engineering and Manufacturing-Green Technology*, vol.3, pp.273-279, 2016.
- 60) F. Zhang, and X. Tan, "Passivity-based stabilization of underwater gliders with a control surface," *Journal of Dynamic Systems, Measurement, and Control*, vol.137, p.061006, 2015.
- 61) N. A. A. Hussain, M. R. Arshad, and R. Mohd-Mokhtar, "Modeling and Identification of an Underwater Glider," In *Proceedings of the 2010 International Symposium on Robotics and Intelligent Sensors (IRIS2010)*, Nagoya, Japan, 2010, pp. 8-11.
- 62) K. Isa, and M. R. Arshad, "Buoyancy-driven underwater glider modelling and analysis of motion control," *Indian Journal of Marine Sciences*, vol.41, pp.516-526, 2012.

- 63) N. Mahmoudin and C. Woolsey, "Underwater glider motion control," In *2008 47th IEEE Conference on Decision and Control, IEEE*, 2008, pp.552-557.
- 64) T. Perez, A. Donaire, and F. Valentinis, "Parametric Modelling of Interacting Hydrodynamic Forces in Underwater Vehicles Operating in Close Proximity," *IFAC-Papers OnLine*, vol. 51, pp.92-97, 2018.
- 65) M. Y. Javaid, M. Ovinis, F. M. Hashim, A. Maimun, Y. M. Ahmed, and B. Ullah, "Effect of water current on underwater glider velocity and range," *Jurnal Teknologi*, vol.78, 2016.
- 66) F. Zhang, F. Zhang, and X. Tan, "Steady spiraling motion of gliding robotic fish," In *2012 IEEE/RSJ International Conference on Intelligent Robots and Systems*, 2012, (pp. 1754-1759).
- 67) L. Merckelbach, D. Smeed, and G. Griffiths, "Vertical water velocities from underwater gliders," *Journal of Atmospheric and Oceanic Technology*, vol.27, pp.547-563, 2010.
- 68) M. Y. Javaid, M. Ovinis, N. Thirumalaiswamy, F. Hashim, and B. Ullah, "Study on Wing Aspect Ratio on the Performance of a Gliding Robotic Fish," *Applied Mechanics and Materials* Vol.786, pp. 248-253, 2015.
- 69) K. Alam, T. Ray, and S. G. Anavatti, " Design optimization of an unmanned underwater vehicle using low-and high-fidelity models," *IEEE Transactions on Systems, Man, and Cybernetics: Systems*, vol.47, pp.2794-2808, 2017.
- 70) L. Techy, K. A. Morganseny, and C.A. Woolseyz, "Long-baseline acoustic localization of the Seaglider underwater glider," In *Proceedings of the 2011 American Control Conference, IEEE*, 2011, pp. 3990-3995.
- 71) L. Kan, Y. Zhang, H. Fan, W. Yang, and Z. Chen, " MATLAB-based simulation of buoyancy-driven underwater glider motion," *Journal of Ocean University of China*, vol.7, pp.113-118, 2008.
- 72) B. Ullah, M. Ovinis, M. B. Baharom, J. D. Setiawan, S. S. A. Ali, and M. Y. Javaid, "Motion control strategy of an underwater glider in the presence of external disturbances," *ARNP Journal of Engineering and Applied Sciences*, vol.11, 2016.
- 73) M. Y. Javaid, M. Ovinis, F. B. Hashim, A. Maimun, Y. M. Ahmed, and B. Ullah, "Effect of wing form on the hydrodynamic characteristics and dynamic stability

- of an underwater glider,” *International Journal of Naval Architecture and Ocean Engineering*, vol. 9, pp.382-389, 2017.
- 74) K. Stryczniewicz and P. Drężek, “CFD approach to modelling hydrodynamic characteristics of underwater glider,” *Transactions on Aerospace Research*, vol.4, PP.32-45, 2019.
 - 75) D. R. Blidberg, “The development of autonomous underwater vehicles (AUV); a brief summary,” In *Ieee Icra 2001*, 2001, vol.4, p.1.
 - 76) K. Li, J. Yu, Z. Wu, and M. Tan, “Hydrodynamic analysis of a gliding robotic dolphin based on Computational Fluid Dynamics,” In *2016 35th Chinese Control Conference (CCC), IEEE*, 2016, pp. 6008-6013, 2016.
 - 77) N. A. Ali Hussain, T. M Chung, M. R. Arshad, R. Mohd-Mokhtar, and M. Z. Abdullah, “Design of an underwater glider platform for shallow-water applications,” *International Journal of Intelligent Defence Support Systems*, vol.3, pp.186-206, 2010.
 - 78) M. Y. Javaid, M. Ovinis, and B. Ullah, “Experimental study on hydrodynamic characteristics of underwater glider,” *Indian Journal of Geo-Marine Sciences*, vol. 48, pp. 1091-1097, 2019.
 - 79) F. Zhang, O. Ennasr, and X. Tan, “Gliding robotic fish: an underwater sensing platform and its spiral-based tracking in 3d space,” *Marine Technology Society Journal*, vol.51, pp.71-78, 2017.
 - 80) F. Zhang, F. Zhang, and X. Tan, “Tail-enabled spiraling maneuver for gliding robotic fish,”. *Journal of Dynamic Systems, Measurement, and Control*, vol.136, p.041028, 2014.
 - 81) M. Zhou, “The approach of improving the roll control of a Slocum autonomous underwater glider,” M. S. thesis, Dept. Eng and Applied Science, Memorial Univ., Newfoundland, Canada, 2012.
 - 82) J. Cao, Z. Zeng, and L. Lian, “Dynamics and approximate semi-analytical solution of an underwater glider in spiral motion,” *Indian Journal of Gro-Marine Sciences*, vol.44, pp.2008-2018, 2015.
 - 83) M. Y. Javaid, M. Ovinis, N. Thirumalaiswamy, F. Hashim, A. Maimun, and B. Ullah, “Dynamic motion analysis of a newly developed autonomous underwater glider with rectangular and tapered wing,” *Indian Journal of Geo-Marine Sciences*, vol. 44, pp.1928-1936, 2015.

- 84) E. H. Othman, "A review on current design of unmanned surface vehicles (USVs)," *Journal of Advanced Review on Scientific Research*, vol. 16, pp.12-17, 2015.
- 85) M. G. Joo and Z. Qu, "An autonomous underwater vehicle as an underwater glider and its depth control," *International Journal of Control, Automation and Systems*, vol.13, pp.1212-1220, 2015.
- 86) M. Y. Javaid, M. Ovinis, N. Thirumalaiswamy, F. B. Hashim, A. Maimun, and B. Ullah, "Numerical investigation on the hydrodynamic characteristics of an autonomous underwater glider with different wing layouts," *ARPJ Journal of Engineering and Applied Sciences*, vol.12, 2017.
- 87) A. Lebedev, and V. Filaretov, "Multi-Channel Variable Structure System for the Control of Autonomous Underwater Vehicle," In *2007 International Conference on Mechatronics and Automation, IEEE*, 2007, pp. 221-226.
- 88) P. Jantapremjit, and P.A. Wilson, "Optimal control and guidance for homing and docking tasks using an autonomous underwater vehicle," In *2007 International Conference on Mechatronics and Automation, IEEE*, 2007, pp. 243-248.
- 89) J. G. Graver, R. Bachmayer, N. E. Leonard, and D. M. Fratantoni, "Underwater glider model parameter identification," In *Proc. 13th Int. Symp. on Unmanned Untethered Submersible Technology, UUST*, 2003, pp. 12-13.
- 90) K. Isa, M. R. Arshad, and S. Ishak, "A hybrid-driven underwater glider model, hydrodynamics estimation, and an analysis of the motion control," *Ocean Engineering*, vol.81, pp.111-129, 2019.
- 91) F. Zhang, and X. Tan, "Nonlinear observer design for stabilization of gliding robotic fish," in *2014 American Control Conference, IEE explore*, 2014, pp. 4715-4720.

LIST OF PUBLICATIONS

- 1) K. Panjavarnam, M. Ovinis, and S. Karupanan, “A New Roll and Pitch Control Mechanism for an Underwater Glider,” *Journal of Advanced Research in Fluid Mechanics and Thermal Sciences*, vol.85, pp.143-160,2021, (Q4, Scopus Journal).

APPENDIX A



(a) Balast tank



(b) Linear actuator with movable mass

Figure A.1 : Existing buoyancy engine of the UTP glider



Figure A.2: Setup pitch control module with water bladder in proposed design



Figure A.3: Setup roll control module with water bladder in proposed design



Figure A.4: UTP glider readiness with proposed control mechanism